

Combination therapy in type 1 diabetes

Dissertation
zur Erlangung des Doktorgrades
der Naturwissenschaften

vorgelegt beim Fachbereich 14
der Johann Wolfgang Goethe -Universität
in Frankfurt am Main

von
Stanley Lasch (Stanley.Lasch@t-online.de)
aus Prenzlau

Frankfurt, 2015
(D30)

vom Fachbereich 14 der

Johann Wolfgang Goethe - Universität als Dissertation
angenommen.

Dekan: Prof. Dr. M. Karas

Gutachter : Prof. Dr. D. Steinhilber
Prof. Dr. U. Christen

Datum der Disputation : 03.02.2016

1 Contents

1	Contents	ii
2	Summary	v
3	Zusammenfassung	viii
4	List of figures	xiii
5	List of tables	xv
6	List of abbreviations	xv
7	Introduction	2
7.1	The immune system	2
7.1.1	Innate immune system	2
7.1.2	Adaptive immune system	3
7.1.3	T cells	4
7.2	Autoimmunity	6
7.2.1	Diabetes mellitus	6
7.2.2	Type 1 diabetes	7
7.2.3	Pathogenesis of T1D	9
7.2.4	Mouse models for T1D	11
7.3	Therapy of T1D	14
7.3.1	Immune therapies of T1D	14
7.3.2	aCD3 therapy of T1D	15
7.3.3	Combination therapies with aCD3 in T1D	17
7.4	Chemokines	18
7.4.1	Chemokine overview	18
7.4.2	Cytokines and Chemokines in T1D	20
7.4.3	CXCL10 and its receptor CXCR3 in T1D	21
7.5	Adhesion molecules	23
7.5.1	Function of adhesion molecules	23
7.5.2	Junctional adhesion molecules	25
7.5.3	The role of JAM-C in T1D and other diseases	25
8	Aims	28
9	Results	31
9.1	Anti-CD3 treatment	31
9.1.1	3 µg and 30 µg Anti-CD3 led to half and full inactivation of the T cells	31
9.1.2	aCD3 treatment was more effective at days 10-12 rather than at days 7-9 post-infection	33
9.1.3	aCD3 inactivation predominantly affects specific T cells rather than regulatory T cells	34

Contents

9.1.4	Administration of low dose aCD3 has an intermediate impact on the incidence of T1D	39
9.2	Combination therapy with CXCL10	40
9.2.1	Production of aCXCL10	40
9.2.2	CT significantly reversed T1D in the RIP-LCMV GP mouse model	43
9.2.3	CT reduced the number of infiltrating T cells in the pancreas	45
9.2.4	Frequency and number of islet antigen-specific CD8 T cells were dramatically reduced in CT treated mice	45
9.2.5	The remaining islet antigen-specific T cells in CT and aCD3 treated mice were less active	52
9.2.6	None of the treatments impaired the migration potential	54
9.2.7	CT resulted in a long-lasting remission of T1D	54
9.2.8	The deficiency of CXCL10 reduced severity of T1D and thereby it created the basis to cure the majority of mice	57
9.2.9	CT reverted T1D in diabetic NOD mice	58
9.2.10	CT preserved the β -cell function, but the islets in the pancreas were still covered with infiltrates	59
9.2.11	CT treated mice showed a slight impact on Teff and Treg frequency	62
9.2.12	CT increased the Treg/Teff ratio in both mouse models	66
9.3	Combination therapy with aJAM-C	69
9.3.1	JAM-C was expressed by vascular endothelial cells	69
9.3.2	Production of aJAM-C	71
9.3.3	CT-J slightly improved the T1D remission of the aCD3 monotherapy	72
9.3.4	CT-J and aCD3 treatment reduced the number of infiltrating T cells in the pancreas	74
9.3.5	CT-J treatment diminished the number of islet specific T cells in the pancreas, but it did not significantly improve the aCD3 therapy	76
9.3.6	CT-J slightly influenced the neutrophil infiltration into the pancreas	79
9.3.7	aJAM-C reached the pancreas and was located on vascular endothelial cells in islets and PDLN	80
10	Discussion	85
10.1	aCD3 therapy	86
10.2	Combination therapy with aCXCL10	90
10.3	Combination therapy with aJAM-C	97
10.4	Closing remarks	101
11	Materials and Methods	103
11.1	Materials	103
11.1.1	Molecular weight marker for protein electrophoresis	103

Contents

11.1.2.....Antibodies	104
11.1.3.....Enzymes and proteins.....	106
11.1.4.....Nucleotides and peptides	107
11.1.5.....Kits	107
11.1.6.....Cell lines.....	108
11.1.7.....Virus.....	108
11.1.8.....Mouse Strains	109
11.1.9.....Chemicals	109
11.1.10.....Consumable material and equipment.....	114
11.1.11.....Solutions, buffers and culture media	119
11.2.....Methods.....	124
11.2.1.....Cell biological methods	124
11.2.2.....Molecular biological methods	133
11.2.3.....Experiments with mice	137
11.2.4.....Statistical evaluations.....	140
12..... Literature	142
13..... Appendix.....	161
13.1..... Acknowledgment	161
13.2..... Curriculum vitae.....	162
13.3..... Publications and Presentations	164
13.4..... Declaration of academic honesty.....	165

2 Summary

Type 1 Diabetes (T1D) is an autoimmune disorder in which the own immune system attacks the insulin producing β -cells in the pancreas. Therapy of T1D with anti-CD3 antibodies (aCD3) leads to a blockade of the autoimmune process in animal models and patients resulting in reduced insulin need. Unfortunately, this effect is only temporal and the insulin need increases after a few years. In the first approach, I aimed at a blockade of the cellular re-entry into the islets of Langerhans after aCD3 treatment by neutralising the key chemokine CXCL10, which is important for the T cell migration. In the second approach I tried to block the transmigration of leukocytes through the endothelial layer into inflamed tissue with an anti-JAM-C antibody (aJAM-C) after aCD3 treatment.

I used the well-established RIP-LCMV-GP mouse model of T1D. As target autoantigen in the β -cells, such mice express the glycoprotein (GP) of the lymphocytic choriomeningitis virus (LCMV) under control of the rat insulin promoter (RIP). These mice develop T1D within 10 to 14 days only after LCMV-infection. In the first combination therapy (CT) I treated diabetic RIP-LCMV-GP mice with 3 μ g aCD3 per mouse (3 injections in 3 days) followed by administration of a neutralising anti-CXCL10 monoclonal antibody (8 injections of 100 μ g aCXCL10 per mouse over 2.5 weeks).

CT reverted T1D in RIP-LCMV-GP mice significantly (CT: 67 % reversion; control: 16 % reversion) and with superior efficacy to monotherapies with aCD3 (38 % reversion) and aCXCL10 (36 % reversion).

The CD8 T cells in the spleen have fully regenerated at day 31 after infection. However, the frequency of islet antigen (GP)-specific CD8 T-cells was significantly reduced by 73 % in the spleen after CT compared to isotype control treated mice. In contrast, in aCD3 treated mice the T cells were only reduced by 56 % of the frequency of isotype control treated mice. Flow cytometry and immunohistological examinations demonstrated a marked reduction of CD8 T cells in the pancreas of CT treated mice. Importantly, the number of islet antigen (GP)-specific CD8 T cells was reduced dramatically by 78 % in the

Summary

pancreas of CT treated mice, whereas aCD3 treatment led to a less pronounced reduction of the islet antigen-specific CD8 T cell number (23 %). This reduction of infiltration was long lasting since in the pancreas of CT treated mice the β -cells produce insulin and there were almost no infiltrating T cells present at day 182 post-infection. aCD3 treated mice also showed many insulin producing cells after 182 days post-infection. Nevertheless, their pancreas displayed also some infiltrates around the islets.

In order to confirm my data I treated non-obese diabetic (NOD) mice with CT. In contrast to RIP-LCMV-GP mice, NOD mice develop spontaneous T1D within 15 to 30 weeks after birth, due to polymorphisms in the Idd3 locus, which is linked to IL-2 production, and a mutation in the CTLA-4 gene. Strikingly CT cured 55 % of diabetic NOD mice, whereas only 30 % showed T1D reversion with aCD3 alone and none reverted after isotype control administration.

The impact of CT on aggressive islet antigen-specific T cells (Teff) was stronger in the RIP-LCMV-GP than in the NOD model. In contrast, regulatory T cells (Tregs) were induced predominantly in NOD mice rather than in RIP-LCMV-GP mice. However, looking at the Treg/Teff ratio and compared to isotype control antibody treated mice, I found a significant 4-fold increase in the pancreas of CT treated RIP-LCMV-GP mice and a 17-fold increase in the PDLN of CT treated NOD mice. In addition, a tendency for an increase in Treg/Teff ratio was obtained in the spleen of CT-treated RIP-LCMV-GP as well as NOD mice compared to aCD3 and isotype control antibody treated mice.

In the second combination therapy with neutralising anti-JAM-C monoclonal antibody (CT-J) I again treated diabetic RIP-LCMV-GP mice with 3 μ g aCD3 per mouse (3 injections in 3 days) followed by administration of an anti-JAM-C antibody (8 injections of 100 μ g aJAM-C per mouse over 2.5 weeks).

CT-J (51 % reversion) slightly improved the aCD3 therapy (41 % reversion). However, there was no significant difference between CT-J and aCD3 administration in terms of total CD8 and islet antigen-specific CD8 T cells.

JAM-C also interacts with the integrin receptor macrophage-1 antigen (MAC-1), which is among others expressed by neutrophils. Accordingly, JAM-C could be involved in neutrophil transmigration to the pancreas. Indeed, I found a

Summary

significant reduction for the infiltrating neutrophils into the pancreas of mice after CT-J compared to aCD3 monotherapy.

In summary the addition of aJAM-C to aCD3 monotherapy showed a small improvement, which was associated with a reduced neutrophil migration into the pancreas. However, JAM-C seemed to play only a minor role in T1D development and some other adhesion molecules might be more important. Nevertheless, the combination of aCD3 and aCXCL10 resulted in a significant and long lasting reduction of aggressive T cells in the pancreas in two independent mouse models. Furthermore a protective immune balance was obtained. Since both antibodies are available for as well as tested in humans and the therapy is only for a short period of time after autoimmune diabetes onset, this combination therapy might kick-start a novel therapy for T1D.

3 Zusammenfassung

Typ 1 Diabetes (T1D) ist eine autoimmune Erkrankung, bei der die Insulin produzierenden β -Zellen vom eigenen Immunsystem angegriffen werden. Umweltfaktoren, wie virale oder bakterielle Infektionen, sowie β -Zell Tod führen zur Präsentation von Inselzellantigenen, wie zum Beispiel Insulin, durch dendritische Zellen und deswegen zu einer erhöhten Aktivierung von T-Zellen. Ohne regulatorische Mechanismen können aktivierte autoreaktive T-Zellen selektiv die β -Zellen im Pankreas zerstören. Dies führt zu einer verminderten Produktion von Insulin und dadurch zur Entwicklung von T1D.

Das Ziel des Projekts ist es T1D mit einer Kombinationstherapie zu behandeln. Es wird eine temporäre anti-CD3 Antikörper (aCD3) Therapie verwendet, um T-Zellen kurzzeitig zu inaktivieren. Dann sollen die wieder regenerierenden T-Zellen mit einer zweiten Therapie daran gehindert erneut in den Pankreas einzuwandern und die β -Zellen anzugreifen. Dazu werden zwei verschiedene Ansätze getestet. Erstens die Blockade des Chemokins CXCL10, welches T-Zellen zu den Stellen der Entzündung (β -Zellen) lockt. Zweitens Blockade von JAM-C, welches unter anderem eine Rolle bei der Transmigration von Leukozyten durch die Endothelschicht (Blutgefäß zum Pankreas) spielt.

Es wird das RIP-LCMV Mausmodell für T1D verwendet. Dabei wird ein spezifisches Antigen des lymphozytären Choriomeningitis Virus (LCMV) unter Kontrolle des Ratten Insulin Promotors (RIP) in den β -Zellen des Pankreas der Mäuse exprimiert. Nach LCMV-Infektion richtet sich die Immunantwort gegen das Virus und die Antigen-exprimierenden β -Zellen, wodurch diese zerstört werden. Dadurch entwickeln die Mäuse einen autoimmunen Diabetes.

Ich hatte gefunden, dass eine Verabreichung von 30 μ g und 3 μ g aCD3 pro Maus zur vollen und halben Inaktivierung der T-Zellen im Blut führte. Die Inaktivierung erreichte aber auch Pankreas, pankreatischen Lymphknoten und Milz, jedoch waren CD4 stärker als CD8 T-Zellen von der Inaktivierung betroffen. Nichtsdestotrotz schienen die FoxP3⁺ CD4 T-Zellen resistenter gegenüber der aCD3 Behandlung zu sein als die CD4 T-Zellen im Allgemeinen, wodurch deren Frequenz anstieg. Währenddessen wurden die Insel-Antigen spezifischen CD8 T-Zellen stärker inaktiviert als die CD8 im Allgemeinen, wodurch deren

Zusammenfassung

Frequenz sank. Beide Dosen zeigten eine bessere Wirkung mit einer Behandlung von Tag 10-12 nach Infektion, dem Beginn der β -Zell Zerstörung, gegenüber Tag 7-9 nach Infektion, dem Zeitpunkt der maximalen T-Zell Frequenz. Für die Kombinationstherapie hatte ich 3 μ g aCD3 pro Maus verwendet, um erstens den Effekt der Zweittherapie besser zu sehen und zweitens die Nebeneffekte der Immunsuppression zu verringern. Da die T-Zellen sehr schnell regenerieren ist das Fenster für eine Zweittherapie sehr klein.

Zuerst wurde T1D durch eine LCMV-Infektion induziert. An Tag 10 nach der Infektion, wenn die meisten Mäuse schon diabetisch sind, wurde an drei aufeinanderfolgenden Tagen 3 μ g des anti-CD3 Antikörpers pro Maus gegeben. Der anti-CXCL10 Antikörper (aCXCL10) wurde ab Tag 13 jeden zweiten Tag zwei Wochen lang verabreicht (8 Injektionen).

Hier hatte ich gefunden, dass die Kombination von aCD3 mit aCXCL10 (CT) den Effekt der Monotherapien mit aCD3, aCXCL10 oder Isotyp-Kontroll-Antikörper übertrifft. In der CT behandelten Gruppe blieben nur 33 % der Mäuse diabetisch, während dessen es 62 % nach Gabe von aCD3 und 84 % nach Isotyp-Kontroll-Antikörper Behandlung blieben. Die aCD3 Monotherapie hatte anfangs einen ähnlichen Effekt wie CT, allerdings wurden die Mäuse teilweise nach ca. 25 Tagen wieder diabetisch. In Gegensatz dazu blieb der therapeutische Effekt nach CT langfristig erhalten. Dieses bestätigte sich auch durch die Untersuchung von CT behandelten Mäusen nach 20 und 31 Tagen. An Tag 20 hatte sich die generelle CD4 und CD8 Frequenz aller Therapiegruppen wieder auf den Level von Isotyp-Kontrolle behandelten Mäusen normalisiert, welches auf ein wiederhergestelltes Immunsystem schließen lässt. Hingegen war zu diesem Zeitpunkt die Frequenz der Insel-Antigen spezifischen CD8 T-Zellen in der Milz und auch die absolute Anzahl im Pankreas nach CT und aCD3 Therapie signifikant niedriger als bei Isotyp-Kontrolle behandelten Mäusen. Im Pankreas war auch die absolute Anzahl aller CD4 und CD8 T-Zellen nach CT und aCD3 Behandlung viel geringer im Vergleich zu Isotyp-Kontrolle behandelten diabetischen Mäusen. Zudem war die Migrationsfähigkeit der verbleibenden Insel-Antigen spezifischen CD8 T-Zellen und CD8 T-Zellen im Allgemeinen in allen Mäusen gleich. Für die regulatorischen T-Zellen (FoxP3⁺) war nur ein

Zusammenfassung

leichter nicht signifikanter Anstieg durch CT im Vergleich zur aCD3 Therapie sichtbar.

An Tag 31 nach Infektion war die Frequenz der Insel-Antigen spezifischen CD8 T-Zellen in der Milz und auch deren absolute Anzahl im Pankreas nach CT interessanterweise ähnlich zu Tag 20 nach Infektion. Währenddessen stieg deren Frequenz und Anzahl bei aCD3 behandelten Mäusen in Richtung des Niveaus von unbehandelten diabetischen Mäusen an.

Um den Einfluss, sowie die Wichtigkeit von CXCL10 in der Pathogenese von T1D genauer zu untersuchen wurde eine RIP-LCMV-GP x CXCL10 KO Kreuzung gezüchtet und mit LCMV infiziert. RIP-LCMV-GP x CXCL10 KO Mäuse hatten dabei eine geringere und verzögerte T1D Inzidenz als normale RIP-LCMV-GP Mäuse. Statt an Tag 10 waren 70 % der Mäuse erst an Tag 14 nach Infektion diabetisch. Zudem hat sich der T1D bei der Hälfte der Mäuse wieder zurück gebildet. Dadurch zeigt sich auf der einen Seite das CXCL10 in der initialen Phase, der T-Zell Einwanderung, noch durch andere Faktoren kompensiert werden kann. Jedoch auf der anderen Seite scheint CXCL10 in der chronischen Phase entscheidend zu sein, um die T-Zellen am Ort der Entzündung zu halten.

Des Weiteren wurden die RIP-LCMV-GP x CXCL10 KO Mäuse mit 3 µg aCD3 pro Maus von Tag 10-12 behandelt, um auch hier die Wirksamkeit einer Kombination aus T-Zell-Inaktivierung und Migrationsblockierung zu demonstrieren. Dabei zeigte die aCD3 Therapie nicht nur eine signifikante Verbesserung gegenüber unbehandelten Mäusen, es konnten sogar alle diabetischen Mäuse geheilt werden.

Als zweites Model wurde das NOD Mausmodel verwendet, da es einen anderen Mechanismus der T1D Entstehung besitzt. Hier werden die Mäuse aufgrund eines Immundefekts nach 15-30 Wochen spontan diabetisch. Auch in diesem Model zeigte sich, dass die Kombination von aCD3 mit dem aCXCL10 den Effekt der Monotherapie mit aCD3 allein übertrifft und 55 % statt 30 % der diabetischen Mäuse geheilt wurden. Der Mechanismus vom RIP-LCMV-GP Model ließ sich nicht genau reproduzieren, da NOD Mäuse keinen so homogenen Krankheitsverlauf haben wie RIP-LCMV-GP Mäuse. Wobei auch hier eine starke Tendenz vorhanden war, dass die Frequenz der Insel-Antigen

Zusammenfassung

spezifischen CD8 T-Zellen in der Milz und auch deren absolute Anzahl im Pankreas nach CT niedriger war als bei Isotyp-Kontrolle-Antikörper oder aCD3 behandelten Mäusen. Jedoch hatte ich einen viel ausgeprägteren Effekt für die Induzierung von regulatorische T-Zellen durch CT im Vergleich zur aCD3 und der Isotyp-Kontroll-Therapie gefunden. Dabei wurden hauptsächlich regulatorische CD4 T-Zellen gefunden, jedoch wurden auch regulatorische CD8 T-Zellen entdeckt, welche noch stärker als die CD4 Tregs induziert wurden. Dadurch hatte sich im NOD Model, wie auch im RIP-LCMV Model, das Immungleichgewicht in Richtung eines regulatorischen Milieus verschoben. Dieses regulatorische Milieu könnte die Ursache für den Langzeit-Effekt von CT darstellen.

In einem zweiten Ansatz der Kombinationstherapie wurde wieder von Tag 10-12 nach LCMV dreimal 3 µg aCD3 pro Maus gegeben. Daraufhin wurde ein anti-JAM-C Antikörper (aJAM-C) ab Tag 13 jeden zweiten Tag zwei Wochen lang verabreicht (8 Injektionen). Die Kombinationstherapie mit aJAM-C (CT-J) hatte nur eine leichte Verbesserung von 10 % mehr geheilten Mäusen gegenüber der aCD3 Monotherapie mit 41 % geheilten Mäusen zur Folge. An Tag 31 war auch hier die Frequenz der Insel-Antigen spezifischen CD8 T-Zellen in der Milz und auch deren absolute Anzahl im Pankreas nach Kombinationstherapie und aCD3 Therapie signifikant niedriger als bei der Isotyp-Kontrolle, jedoch konnte kein Unterschied zwischen CT-J und aCD3 Monotherapie festgestellt werden. Da auch beschrieben ist das JAM-C mit MAC-1, welcher unter anderem von Neutrophilen exprimiert wird, interagiert, wurde die Neutrophilen-Einwanderung genauer untersucht. Im Gegensatz zu den T-Zellen waren signifikant weniger Neutrophile, welche bei der initialen Immunantwort eine Rolle spielen, im Pankreas von CT-J behandelten Mäusen im Vergleich zur aCD3 Monotherapie zu finden. Im der Milz war dagegen eine höhere Frequenz von Neutrophile nach CT-J im Vergleich zu aCD3 und Isotyp-Kontroll-Antikörper behandelten Mäusen vorhanden. Deswegen scheint es so, als ob die Neutrophilen in der Milz festgehalten werden und nicht in den Pankreas einwandern können. Dies könnte der Grund für den leichten Unterschied in der Inzidenz darstellen.

Zusammenfassung

Zusammengefasst hat eine Kombination von aCD3 und aJAM-C nur einen minimalen zusätzlichen Effekt bewirkt. Deswegen wäre es sinnvoll ein weiteres Adhensionsmolekül, welches eine größere Rolle in der T-Zell-Migration spielt zu blockieren oder sogar drei Antikörper, wie aCD3, aCXCL10 und aJAM-C zu kombinieren. Im Gegensatz dazu revertiert eine Kombinationstherapie von aCD3 und aCXCL10 den T1D durch eine zusätzliche Blockade der CXCL10-abhängigen T-Zell-Migration sowohl stärker als auch für einen längeren Zeitraum. Eine erneute Einwanderung regenerierter T-Zellen in die Langerhans'schen Inseln wird verhindert und damit die Immunpathogenese gestoppt. Zusätzlich wird vor allem in NOD Mäuse das Gleichgewicht der Immunzellen in Richtung regulierender Zellen verschoben. Es ist wichtig nochmals hervorzuheben, dass die Mäuse zu Beginn der Behandlung schon diabetisch waren. Mein Ansatz stellt also eine eigentliche Therapie und keine bloße Prävention des T1D dar. Die aCD3 Monotherapie befindet sich schon in klinischen Studien, jedoch wird dort die Autoimmunreaktivität des T1D nur verzögert. Somit könnte mein Ansatz der Kombinationstherapie auch im Menschen den Effekt der aCD3 Monotherapie deutlich verbessern.

4 List of figures

Figure 1:	Environmental factors might initiate T1D development.	10
Figure 2:	The development of T1D in the RIP-LCMV mouse model is based on viral infection.....	12
Figure 3:	RIP-LCMV-GP and RIP-LCMV-NP mice develop T1D in a different way.....	13
Figure 4:	aCD3 treatment resulting in an inactivation of T cells.....	16
Figure 5:	Many chemokine receptors possess more than one ligand.....	20
Figure 6:	Rolling, adhesion and transmigration is influenced by CAMs.....	24
Figure 7:	Overview of the presumable antibody effect.	28
Figure 8:	3 µg and 30 µg aCD3 led to half and full inactivation of the T cells in the blood.	32
Figure 9:	The aCD3 therapy had a better effect at days 10-12 than at days 7-9.	35
Figure 10:	aCD3 treatment was more effective for Teff than Tregs.....	36
Figure 11:	Immunohistochemistry revealed that an aCD3 dose of 3 µg had only a minor impact on T cell infiltration in the pancreas.....	38
Figure 12:	BG levels showed that the low aCD3 dose had only an intermediate effect.....	39
Figure 13:	aCXCL10 was of high purity and it reduced the migration of T cells.....	41
Figure 14:	The injected aCXCL10 went to the infiltrates in the pancreas.	42
Figure 15:	CT led to a remission in more mice than the monotherapies.	44
Figure 16:	Immunohistochemistry sections of the pancreas revealed that the infiltration was strongly decreased in CT treated mice.....	46
Figure 17:	Flow cytometry analysis showed that the frequency and number of islet antigen-specific T cells was significantly decreased in CT treated mice.	48
Figure 18:	aCD3 administration led to less experienced CD8 T cells indicated by a lower TNFα production.....	50
Figure 19:	CT reduced the islet specific cytotoxic potential.....	51
Figure 20:	A reduced activity of remaining T cells was shown after aCD3 treatment.....	53
Figure 21:	The T cells of CT, aCD3 aCXCL10 and isotype control treated mice were undistinguishable in their migration potential.....	55
Figure 22:	CT increased the Treg / Teff ratio in the pancreas of RIP-LCMV-GP mice.	57
Figure 23:	aCD3 cured all mice in the absence of CXCL10.	58
Figure 24:	CT exceeded the effect of aCD3 treatment in NOD mice.....	60

List of figures

Figure 25:	Immunohistochemistry revealed a preserved insulin production after CT and aCD3 administration in NOD mice.....	61
Figure 26:	Less experienced CD8 T cells were present after aCD3 administration in NOD mice indicated by a lower TNF α production.	63
Figure 27:	Flow cytometry analysis of NOD mice revealed a slight reduction of islet antigen-specific T cells as well as a slight increased Treg frequency after CT.....	65
Figure 28:	CT and aCD3 treatment increased the CD4 and CD8 Treg number evaluated by fluorescence staining.	67
Figure 29:	CT significantly elevated the Treg/Teff ratio in NOD and RIP-LCMV-GP mice.	68
Figure 30:	JAM-C was only expressed on CD31 ⁺ vascular endothelial cells.....	70
Figure 31:	aJAM-C was of high purity.	71
Figure 32:	CT-J administration slightly improved the T1D reversion in RIP-LCMV-GP mice compared to aCD3 treated mice.....	73
Figure 33:	Immunohistochemistry of the pancreas of mice showed a reduced infiltration after CT-J.	75
Figure 34:	CTJ did not significantly improve the aCD3 effect in terms of T cell infiltration.	77
Figure 35:	aCD3 as well as CT-J treatment reduced the cytotoxicity in RIP-LCMV-GP mice.	79
Figure 36:	CT-J reduced the neutrophil infiltration into the pancreas compared to aCD3 therapy.	81
Figure 37:	aJAM-C bound specifically to vascular endothelial cells in the pancreas and it formed a thin layer around islets.....	82
Figure 38:	aJAM-C bound specifically to vascular endothelial cells in spleen and PDLN.	83
Figure 39:	Overview of the CT effect.....	92
Figure 40:	Overview of the CT-J effect.....	100
Figure 41:	Banding pattern of the prestained protein marker.	103

5 List of tables

Table 1:	Proteins of the molecular weight marker.	103
Table 2:	Antibodies for flow cytometry.	104
Table 3:	Antibodies for immunohistochemistry.....	105
Table 4:	Antibodies for treatment.	106
Table 5:	Enzymes and proteins.....	106
Table 6:	Nucleotides and peptides.	107
Table 7:	Kits.	107
Table 8:	List of used chemicals.	109
Table 9:	List of consumable material and equipment.	114
Table 10:	List of used buffers and solutions.	119
Table 11:	The components of the PCR reaction.	134
Table 12:	Cycling.	135
Table 13:	Lower SDS-gel.	136
Table 14:	Upper SDS gel.	136

6 List of abbreviations

AIRE	- Autoimmune regulator
APC	- Antigen presenting cell
APS	- Ammonium persulfate
BSA	- Bovine serum albumin
Ca ²⁺	- Calcium ions
CaCl ₂	- Calcium chloride
CCL	- C-C motif chemokine ligand
CCR	- C-C motif chemokine receptor
CD	- Cluster of differentiation
CSFE	- Carboxyfluorescein succinimidyl ester
CT	- Combination therapy of anti-CD3 and anti-CXCL10 antibody
CT-J	- Combination therapy of anti-CD3 and anti-JAM-C antibody
CTLA	- T lymphocyte-associated antigen
CXCL	- C-X-C motif chemokine ligand
CXCR	- C-X-C motif chemokine receptor
Da	- Dalton (g/mol)
DC	- Dendritic cell
dist.	- Distilled
dl	- decilitre

List of abbreviations

DMSO	- Dimethyl sulfoxide
DTT	- Dithiothreitol
EDTA	- Ethylenediaminetetraacetic acid
FACS	- Fluorescence-activated cell sorting
FBS	- Fetal bovine sera
FoxP3	- Forkhead box P3
g	- Gram
GAD	- Glutamic acid decarboxylase
GFAP	- Glial fibrillary acidic protein
GFP	- Green fluorescent protein
GP	- Glycoprotein
h	- Hours
HEPES	- 2-(4-(2-Hydroxyethyl)- 1-piperazinyl)-ethansulfonsäure
ICCS	- Intra cellular cell staining
IFN	- Interferon
Ig	- Immunoglobulin
IL	- Interleukin
i.p.	- Intraperitoneal
i.v.	- Intravenous
JAM	- Junctional adhesion molecule
KCl	- Potassium chloride
kDa	- Kilo Dalton (kg/mol)
KH ₂ PO ₄	- Monopotassium phosphate
LCMV	- Lymphocytic Choriomeningitis Virus
Mac	- Macrophage antigen
Mg	- Microgram
µl	- Microlitre
mg	- Milligram
MHC	- Major histocompatibility complex
ml	- Millilitre
min	- Minute
mol	- Amount of substance
MTP	- Microtiter plate
NaCl	- Sodium chloride
Na ₂ HPO ₄	- Disodium phosphate
NaH ₂ CO ₃	- Monosodium carbonate
NaN ₃	- Sodium azide
NEAA	- Non essential amino acids
Nm	- Nanometre
NOD	- Non-obese diabetic mouse
NP	- Nucleoprotein

List of abbreviations

PDLN	- Pancreatic draining lymph nodes
Pen/Strep	- Penicillin / Streptomycin
PFU	- Plaque forming units
Podo	- Podoplanin
PTPN22	- Protein tyrosine phosphatase, non-receptor type 22
RIP	- Rat insulin promotor
Rpm	- Rounds per minute
RT	- Room temperature
SDS-PAGE	- Sodium dodecyl sulphate - Polyacrylamide gel electrophoresis
sec	- Second
t	- Time
T1D	- Type 1 diabetes
T2D	- Type 2 diabetes
Tris	- Tris(hydroxymethyl)aminomethane
TCR	- T cell receptor
Tf	- Transcription factor
TGF	- Transforming growth factor
T _H cell	- T helper cell
TLR	- Toll-like receptor
TNF	- Tumour necrosis factor
Tregs	- Regulatory T cells
Teff	- Effector T cells
U	- Rounds
°C	- Degree Celsius
%	- Percent

Introduction

7 Introduction

7.1 The immune system

The human body is permanently exposed to a broad spectrum of bacteria, viruses, fungi and parasites. Most of them are able to proliferate as well as live inside the body and may also kill the infected human. The skin is the first barrier against pathogens and temperature as well as different pH values also prevent pathogens from nesting in humans. However, if pathogens escape these barriers, the immune cells fight them inside the body. In the course of time a very complex and effective immune system has developed, consisting of two main parts: the innate and the adaptive immune system. The innate immune system recognises structures of pathogens in a non-antigen specific way and responds immediately to intruders. In contrast, the adaptive immune system reacts antigen-specifically, but requires more time to evolve its power (1).

7.1.1 Innate immune system

The innate immune system represents the first line of defence against pathogens inside the body and it is a very old defence mechanism, indicated by a presence in different shapes in almost all plants and animals. Monocytes, neutrophils, natural killer (NK) cells as well as macrophages belong to that group and they identify specific structures of pathogens. An important mechanism to recognise specific structures are the Toll-like receptors (TLRs). These TLRs are located in the cell membrane to detect bacteria and fungi, but also even in the membrane of intracellular compartments to identify viruses. Binding of a protein to TLRs leads to a signal transduction and in the end it activates specific transcription factors.

Most of the innate immune cells are also able to secrete inflammatory factors like cytokines and chemokines. These molecules activate or attract further

immune cells from the adaptive immune system (1). Especially neutrophils are able to phagocytose pathogens as well as release granules for degranulation of pathogens. In addition, neutrophils also release chromatin to form a neutrophil extracellular trap (NET) which engulfs pathogens (2).

7.1.2 Adaptive immune system

As mentioned before, the adaptive immune response is antigen-specific and it consists of two systems acting in parallel: the humoral and the cell-mediated immune response. Immunoglobulins (Ig) belong to the humoral system and are secreted by B cells.

Besides B cells, further important cell groups of the adaptive immune system include T cells and antigen presenting cells (APC) such as dendritic cells. The cytotoxic T cells recognise specific antigens and kill infected cells. Moreover, the development of memory antigen specific cells allows the adaptive immune system to respond very fast and effective to a second attack with the same pathogen. The antigen specificity enables the adaptive immune system to fight against a broad spectrum of pathogens without attacking the own cells. Importantly, the recognition of antigens is accomplished by the major histocompatibility complex (MHC), which is known in humans as human leukocyte antigen (HLA). To this end, peptides of pathogens are digested into fragments, which bind to MHC molecules. Subsequently, the peptide fragments are presented on the surface of the cells, offering them to T cells for recognition by antigen-specific receptors.

The diversity of the antigen-specificity is a result of a strong variation in genetic recombination. Thereby a variety of 10^{12} different T cell receptors and 10^8 different immunoglobulins is achieved. To avoid an attack of self-antigens, several barriers and steps such as the thymic selection as well as regulatory cells exist. Importantly, failure of this system may lead to an immune response to self-antigens, resulting in the development of autoimmune diseases (1; 3).

7.1.3 T cells

Initially, pluripotent hematopoietic stem cells from the bone marrow are cluster of differentiation 4 (CD4) as well as CD8 negative and some of them migrate to the thymus. In the thymus these cells first express both transmembrane receptors and they have to pass positive as well as negative selection processes. In the positive selection the T cells are tested for functionality. To this end, the correct conformation of the β chain of the T cell receptor (TCR) and the ability to interact with the MHC has to be verified. Consequently, cells that are unable to react to MHC molecules undergo programmed cell death.

In contrast, in the negative selection T cells, binding to self-antigens, are inactivated to avoid an immune reaction against own structures. Approximately 2 % of all T cells withstand this positive and negative selection. After that selection the T cells differentiate into either CD4 or CD8 T cells and migrate to the periphery.

Naïve CD8 T cells only interact with peptides presented by MHC class I molecules. After that activation, CD8 T cells release the cytotoxins perforin, granzymes, and granulysin. Subsequently, perforin forms pores into the membrane of the target cell and granzymes enter the cytoplasm initiating programmed cell death. Moreover, CD8 T cells produce interferon γ (IFN γ), which directly activates macrophages.

In contrast, the naïve CD4 T cells, called T-helper cells (T_H), are activated by peptide presentation of MHC class II molecules that are expressed on B cells, dendritic cells and macrophages. Upon activation the CD4 T cells produce a large variety of cytokines and that cytokine profile as well as the function differs from subtype to subtype. The main classes of T_H cells are T_H1, T_H2, T_H17 and regulatory T cells (Tregs). Naïve CD4 T cells differentiate in response to interleukin 12 (IL-12) and IFN γ to T_H1 cells which typically produce IFN γ , tumour necrosis factor α (TNF α) as well as IL-2. They are critical for the clearance of intracellular microorganisms such as viruses. In contrast, T_H2 cells, which mature in response to IL-4, are important in the immune response to extracellular parasites. To this end, this subtype generally produces IL-4, IL-5 as well as IL-13. Another subtype, the T_H17 cells, develops in response to

Introduction

transforming growth factor β (TGF- β) as well as IL-6 and secretes IL-6, IL-17 as well as IL-22.

Despite of thymic selection some potential autoreactive T cells escape central tolerance and find its way into circulation. Due to the immunosuppressive power of Tregs these autoreactive T cells do not implicitly result in the development of autoimmunity. Tregs can be categorised into two subgroups: inducible and naturally occurring Tregs. In the periphery non-regulatory T cells can differentiate into inducible Tregs in the presence of IL-4, IL-10 as well as TGF- β and due to this they are a potential target for therapeutic strategies. Nevertheless, under healthy conditions naturally occurring Tregs (nTregs), which are CD4⁺ as well as CD25⁺, are more important. These nTregs mature in the presence of IL-2 and IL-28. In addition, both Treg types express the transcription factor forkhead box P3 (FoxP3). However, the regulatory mechanism of Tregs is still poorly understood, but it is assumed that a cell-cell interaction leads to the inhibition of the IL-2 production as well as the proliferation of T cells. Besides, the cytotoxic T-lymphocyte-associated protein 4 (CTLA-4), which is a negative regulator of T cell activation, might be involved in this process (1; 3).

7.2 Autoimmunity

A failure of central or peripheral tolerance results in autoimmune disorders and leads to a damage of either a specific organ such as in autoimmune hepatitis, multiple sclerosis as well as T1D or it concerns the whole system such as in rheumatoid arthritis, systemic sclerosis or systemic lupus erythematosus. Autoimmunity is mediated by a B cells/antibody and/or T cell response against self-antigens. Many factors are involved in the development of autoimmune diseases, such as genetic predisposition, environmental factors and vaccination. In most autoimmune diseases genetic susceptibility predominantly depends on the MHC haplotype. Other alleles, that are associated with the development of an autoimmune disorder, contain the autoimmune regulator (AIRE), CTLA-4 as well as the protein tyrosine phosphatase non-receptor type 22 (PTPN22). CTLA-4 and PTPN22 are both involved in the negative control of the T cells activation (4).

For the reason that an incongruity was found in homozygotic twins also environmental factors are supposed to be involved in the loss of self-tolerance. The most prominent environmental factors are viral infections, which disbalance the immune system. However, despite of the confirmed role of genetic and environmental factors their specific contribution to the disease progression is still poorly understood (3).

7.2.1 Diabetes mellitus

Diabetes mellitus is characterised by chronic hyperglycaemia due to a reduced insulin secretion or function. Exogenous insulin administration still leads to late complications like nephropathy, retinopathy and severe hypoglycaemia, which may reduce the life expectancy by 10-15 years (5). Insulin (A-chain peptide, B-chain peptide) originates from the cleavage of the C-peptide from its precursor proinsulin by several proteases. Importantly, β -cells produce insulin and are located in the islets of Langerhans (islets) in the pancreas. These islets

were discovered in 1869 by Paul Langerhans and they represent 1-2 % of the mass of a human pancreas. Four main cell types were found in islets: α , β , δ and PP cells. α cells are the counterpart to β -cell and secrete glucagon. Subsequently, glucagon induces the release of glucose into the blood stream. In contrast, the insulin, which is produced by β -cells, promotes the glucose uptake and reduces the blood glucose (BG) level. Moreover, a very small number of PP cells exist in the islets. They produce the pancreatic polypeptide, which results in an inhibition of intestinal motility and stimulates gastric leader cells. In addition, the fourth class, namely δ cells, may inhibit all three secreted hormones by producing somatostatin.

In the 1950s a clear distinction was made between type 1 (T1D) and type 2 diabetes (T2D). In T2D the insulin deficiency resulted from a decreased function of insulin on target cells (6). Due to this insulin resistance the β -cells try to compensate and release more insulin. Therefore, the β -cells get exhausted which in the end leads to a lack of insulin. T2D is mainly caused by excessive body weight as well as insufficient exercise and it predominantly appears in adults.

In contrast, T1D is a real autoimmune disease where the insulin secreting β -cells are destroyed due to a specific immune reaction. In some adults with initially classified T2D a slowly progressing form of T1D was observed, named latent autoimmune diabetes of the adult (LADA) (7).

7.2.2 Type 1 diabetes

T1D mostly starts during childhood and in contrast to other autoimmune diseases it occurs independently of the gender. The prevalence of T1D is 10 % of all diabetes cases and it is assumed that approx. 80,000 children develop T1D each year (8). Similar to other autoimmune diseases various factors cause T1D such as genetic susceptibility, environmental factors and drugs.

Half of the regions associated with a genetic predisposition contain MHC (HLA) genes (9). The HLA haplotypes DQA1*0501 DQB1*0201 and DQA1*0301 DQB1*0302 are associated with the highest risk for the

Introduction

development of T1D and it is assumed that they can act in a synergistic fashion (3). In contrast, Greenbaum et al. found a connection between the haplotype DQA1*0102 DQB1*0602 and a protective effect (10). Interestingly, the sequence analysis of DQ and DR molecules with a predisposition to T1D revealed an importance of the aspartic acid residue in position 57 of the DQ β chain, which is critical for peptide binding (11).

Non-MHC genes play a minor role in T1D, since the relative T1D risk is very low. Nevertheless, it was shown that genes encoding CTLA-4, insulin, IL-2 and PTPN22 are susceptibility factors (3; 4; 12).

However, the fact that only 35-50 % of monozygotic twins develop the disease (9) reveals that there is a gene susceptibility, but other factors might also be important. This hypothesis is consistent with the observation that the migration of humans from low to high T1D incidence countries resulted in an acquirement of the T1D incidence similar to the adopted country (13). Interestingly, a geographical north to south gradient of T1D development exists, which suggested a role of vitamin D₃. It was shown that active vitamin D₃ modified dendritic cells to a semi-mature phenotype, resulting in the ability of these dendritic cells to induce Tregs (14). Moreover, the maternal intake of vitamin D₃ during pregnancy protected T1D development (15). However, trials in humans revealed no clear benefit from exogenous Vitamin D₃ administration in recent-onset diabetes patients (16). Beside climatic influences, T1D has a higher prevalence in industrialised countries. This supports the “hygiene hypothesis” according to which a reduced exposure to antigens is responsible for an idle immune system. Due to that also the regulatory mechanism might be rudimentary, which could result in an autoimmune response.

There is evidence that virus infections play also a role in the etiology of T1D. The most prominent ones are the Coxsackie B1 (17; 18) and Coxsackie B4 virus (19). Interestingly, there is a homology between a β -cell antigen and the virus protein VP1. Therefore, there is a potential cross-reactivity of virus VP1-specific T cells to that β -cell antigen. Such a molecular mimicry is suggested to be responsible for the autoimmune reaction (19).

Nevertheless, it is difficult to identify a responsible diabetogenic virus, since the virus infection is cleared years before clinical onset of T1D. In addition, virus

infections might also be helpful by stimulation of Tregs or hyperactivation of aggressive T cells (20).

7.2.3 Pathogenesis of T1D

β -cell specific autoantibodies are often found in diabetic patients. The four main autoantibodies are directed to insulin, glutamic acid decarboxylase (GAD65), insulinoma antigen-2(IA-2) and islet-specific glucose 6 phosphatase catalytic subunit related protein (IGRP). Interestingly, they are present in some individuals for decades prior T1D diagnosis and are associated with a high risk to develop T1D. However, there is no evidence that islet-specific autoantibodies play a role in the disease pathogenesis (3). Nevertheless, B cells might be involved as antigen presenting cells (APC) indicated by an absence of T1D in B cell deficient NOD mice (21).

These B cells present the autoantigen to T cells, which are of crucial importance in the immune pathogenesis. Macrophages and B cells are present in islets, but the inflammation is predominantly composed of CD8 T cells (22). In addition, transfer of CD4 as well as CD8 T cells resulted in a development of T1D in healthy mice (23; 24). Moreover, the progression of T1D is connected with increased IFN γ , which is produced by T cells, in the islets (25) and a lack of IFN γ reduced the incidence of T1D in the RIP-LCMV mouse model dramatically (26). Furthermore, diabetes was prevented by adoptive transfer of Tregs into NOD mice (27-30).

Thus, it is assumed that T1D primarily requires a genetic predisposition. Initially a local event such as viral or bacterial infection results in β -cells death via molecular mimicry or bystander activation of specific T cells due to general inflammation of the pancreas (Figure 1A). Subsequently, APCs such as dendritic cells or B cells present the antigen to T cells in the PDLN (Figure 1B). Consequently, the T cells are activated and migrate to the pancreas (Figure 1C). Activated autoreactive T cells selectively destroy the β -cells in the pancreas, which results in a decreased production of insulin and therefore in a development of chronic hyperglycemia as well as T1D (Figure 1D). Regulatory

Introduction

T cells are also activated (Figure 1E) and in an appropriate number they may inhibit these islet-specific autoreactive T cells resulting in a prevention of T1D (Figure 1F) (3).

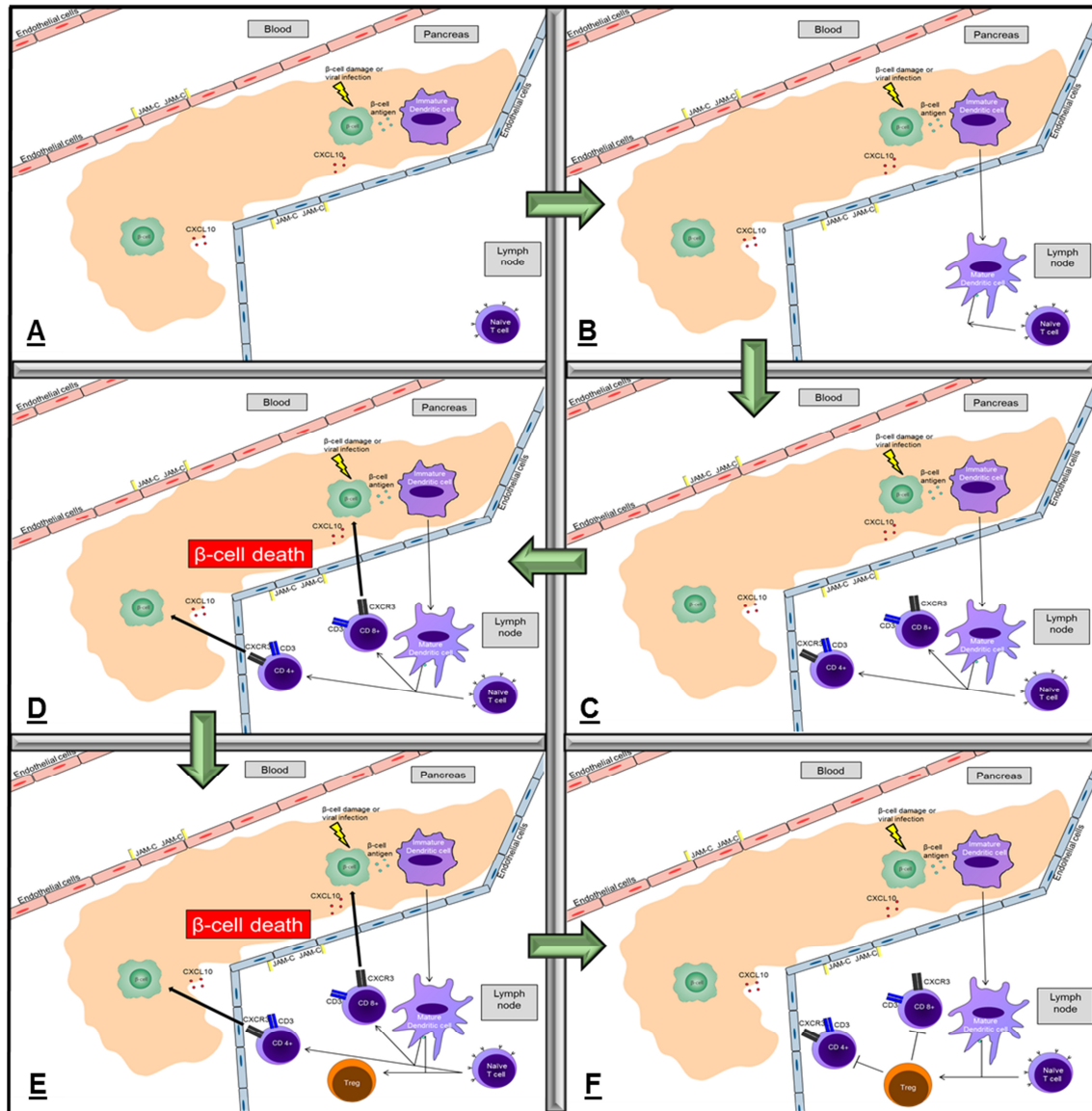


Figure 1: Environmental factors might initiate T1D development.

(A) Environmental factors like viral as well as bacterial infection or β -cell death may lead to an increased antigen uptake of dendritic cells. (B) In the PDLN the antigen is presented by dendritic cells to T cells. (C) Due to this, cross-reactive T cells are potentially activated by specific antigens. (D) Without regulatory mechanism, activated autoreactive T cells selectively destroy β -cells in the pancreas, which results in a decreased production of insulin and consequently in a development of chronic hyperglycaemia and T1D. (E) Under normal conditions antigen specific regulatory T cells are also activated in an appropriate number. (F) They may inhibit these autoreactive T cells and prevent T1D.

7.2.4 Mouse models for T1D

To investigate the origin and therapy of T1D, two major mouse models are generally used: The spontaneously non-obese diabetic (NOD) and the lymphocytic choriomeningitis virus (LCMV) inducible rat insulin promoted (RIP) mouse model.

7.2.4.1 NOD mouse model

The spontaneous NOD mouse model was one of the first animal models for T1D. In 1980 Makino et al. found a mouse strain that spontaneously developed T1D (31). These NOD mice showed polymorphisms in the Idd3 locus, which is linked to IL-2 production. Interestingly, the IL-2 action depends on the concentration and it was shown that low amounts of IL-2 promoted survival of Tregs in mice (32). However, a loss of IL-2 production can contribute to the development of autoimmunity (33). Moreover, a mutation in exon 2 of the CTLA-4 gene is present in NOD mice, leading to its incorrect splicing. CTLA-4 is of importance in the suppression of the T cell immune response. Consequently, an incorrect splicing of CTLA-4 resulted in the development of T1D in NOD mice (4). In addition, the incidence of T1D is more common in females than in males. Importantly, in both genders the frequency of T1D development strongly depends on the sanitary conditions (3).

7.2.4.2 RIP-LCMV mouse model

In RIP-LCMV mice a specific antigen of the LCMV is expressed by the β -cells in the pancreas. The immune system of the mice is tolerant to this “self-antigen”. After infection with LCMV the immune system recruits antigen-specific T cells to clear the virus. Subsequently, these T cells also attack the antigen presenting β -cells and destroy them. Therefore, mice only develop autoimmune diabetes after virus infection (Figure 2) (34).

Introduction

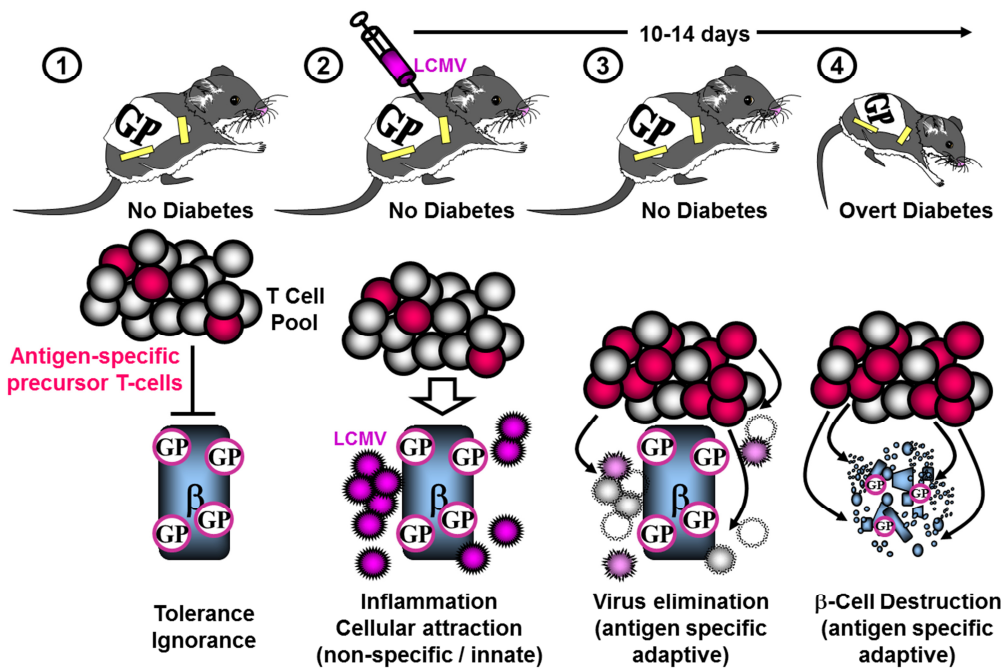


Figure 2: The development of T1D in the RIP-LCMV mouse model is based on viral infection.

This figure shows the mechanistic hypothesis to explain the RIP-LCMV mouse model. A specific antigen of the LCMV is expressed by β -cells in the pancreas of the mice. After infection with LCMV the immune system recruits specific T cells to clear the virus. These T cells also attack the antigen presenting β -cells and destroy them. Therefore the mice develop autoimmune diabetes. Figure adapted from Urs Christen.

Based on the viral target antigen, the RIP-LCMV model can be divided into two different types: the nuclear protein (NP) is used in the RIP-LCMV-NP and the glycoprotein (GP) in the RIP-LCMV-GP model. RIP-LCMV-NP mice express the antigen in the pancreas as well as in the thymus, which results in the inactivation of the high-avidity NP-specific CD8 T cells. For that reason in RIP-LCMV-NP mice the assistance of CD4 T cells is required to induce T1D. In contrast, in the RIP-LCMV-GP model the antigen is exclusively expressed in the pancreas of mice. Due to this the LCMV-GP-specific T cells are not negatively selected in the thymus and CD8 T cells with a high avidity are able to migrate into the pancreas, resulting in a CD4 T cell independent destructive process. Consequently, the onset of T1D after LCMV infection differs in the RIP-LCMV-NP and the RIP-LCMV-GP model and the mice develop T1D within 1-6 months or 10-14 days, respectively (35).

Introduction

The RIP-LCMV mouse model has several advantages to the NOD model. It allows to follow the precise kinetic of disease, due to the homologous T1D development after infection. Moreover, the antigen is well known, which leads to the opportunity to detect antigen-specific T cells by flow cytometry or on quick frozen sections.

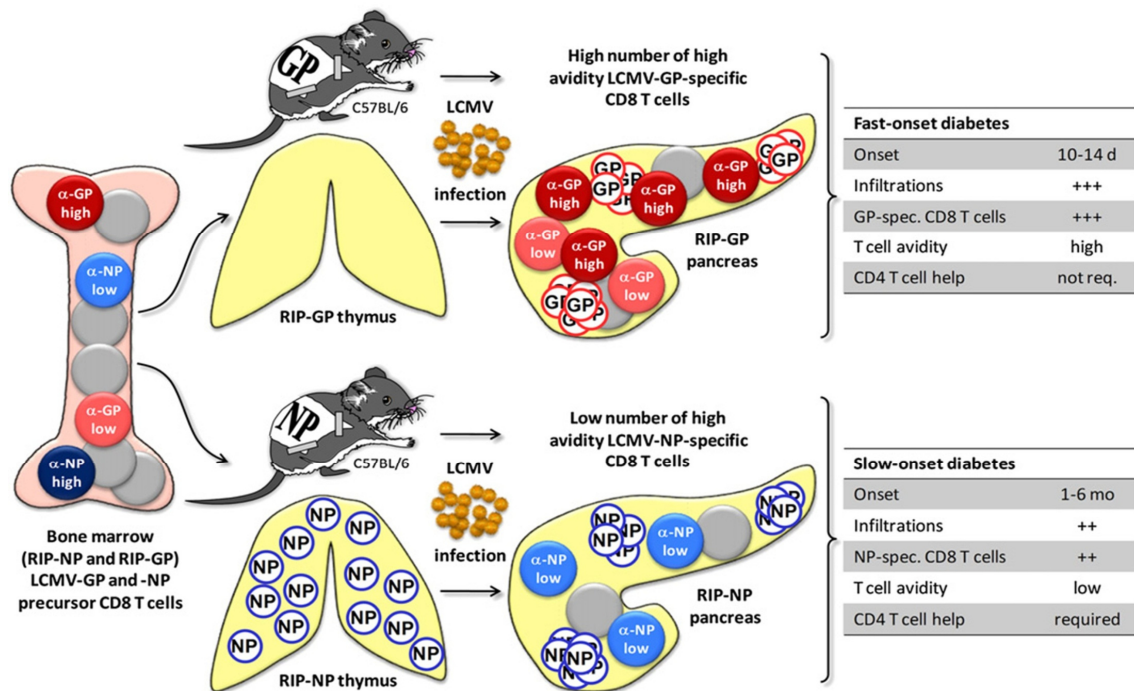


Figure 3: RIP-LCMV-GP and RIP-LCMV-NP mice develop T1D in a different way.

There are two different types of the RIP-LCMV model: the RIP-LCMV-NP and the RIP-LCMV-GP model. In the RIP-LCMV-GP model the antigen is exclusively expressed in the pancreas of RIP-LCMV-GP mice. In contrast, in RIP-LCMV-NP mice the antigen is also expressed in the thymus. This results in the inactivation of the high avidity NP-antigen-specific CD8 T cells. The high avidity GP-antigen-specific CD8 T cells in the RIP-LCMV-GP model are not excluded and they migrate to the pancreas. For that reason the onset of T1D after LCMV-infection of RIP-LCMV-NP mice is very slow compared to RIP-LCMV-GP mice. In addition, RIP-LCMV-GP mice develop T1D CD4 T cell independently, whereas RIP-NP mice require help of CD4 T cells. Figure adapted from Urs Christen.

7.3 Therapy of T1D

Exogenous insulin administration cannot avoid the late complications of T1D like nephropathy, retinopathy and severe hypoglycaemia, which may reduce the life expectancy by 10-15 years (5). Due to that, there is a need for a therapy of T1D. At diagnose of T1D most of the β -cell mass is already destroyed (36) and therefore many therapies failed. In order to identify pre-diabetic patients the biomarkers have to be more precise. Measurement of autoantibodies and genetics as well as knowledge of the relative background may identify people at high risk to develop T1D (37), however, it is impossible to predict the exact moment the autoimmune process is going to start. Chee et al. investigated a new approach to measure antigen-specific T cells (38), which reflect the severity of insulinitis, but this method has to be further established. Nevertheless, there are some promising approaches with antigen-specific therapies or antibodies against immune cells to treat new onset diabetic patients.

7.3.1 Immune therapies of T1D

Several general immune suppressive drugs like cyclosporine (39) showed a beneficial outcome. However, this success in T1D therapy was at the cost of many adverse side effects (40). Later, monoclonal antibodies against T cells or B cells, which are more specific interventions, have been tested in clinical trials and demonstrated strong effects (41; 42). The anti-CD20 antibody rituximab against B cells partially preserved the β -cell function, but after three months the C-peptide release declines again (41). One further therapy of T1D might be the T cell inactivation by anti-CD3 (aCD3) treatment, which is described in more detail in the next paragraph. However, both immunosuppressive drugs cause many adverse events. In order to reduce the side effects caused by aCD3 or anti-CD20 antibody non-immunosuppressive approaches such as antigen-specific therapies have also been investigated. However, the phase 3 trial with GAD65-alum (43) failed to meet its primary endpoints. Do to this,

antigen-specific therapies might not be useful as intervention therapies. However, a prevention trial with oral insulin in humans with high titers of insulin autoantibodies demonstrated a four year delay in the onset of T1D (44). In contrast, in a study from Finland nasal insulin showed no prevention in high-risk children (45). Thus, it seems that antigen-specific therapies alone are not effective enough in humans.

7.3.2 aCD3 therapy of T1D

It is suggested that in lymph nodes, the effector T cells are activated by islet autoantigens presented by antigen presenting cells (APC). These pathogenic T cells are resistant to Foxp3⁺ regulatory T cells and therefore they actively proliferate. This might lead to an imbalance between pathogenic and regulatory T cells resulting in an autoimmune response (Figure 4 top row). One promising therapy of T1D is the aCD3 treatment. The administration of aCD3 induces a significant inactivation of T cells in lymphoid organs and in the infiltrated tissues. This inactivation essentially involves activated effector T cells rather than regulatory T cells. (Figure 4 second row). Subsequently, the immune system produces new T cells and regenerates. Dendritic cells that present specific autoantigens express less co-stimulatory molecules but deliver more inhibitory signals for autoantigen-specific pathogenic T cells. In addition, in the presence of such tolerogenic dendritic cells, naive autoreactive CD4 T cells can be converted into regulatory T cells. Moreover, TGF- β also induces regulatory T cells. Therefore the balance shifts from effector T cells to regulatory T cells and this induces self-tolerance (Figure 4 third row) (46).

Introduction

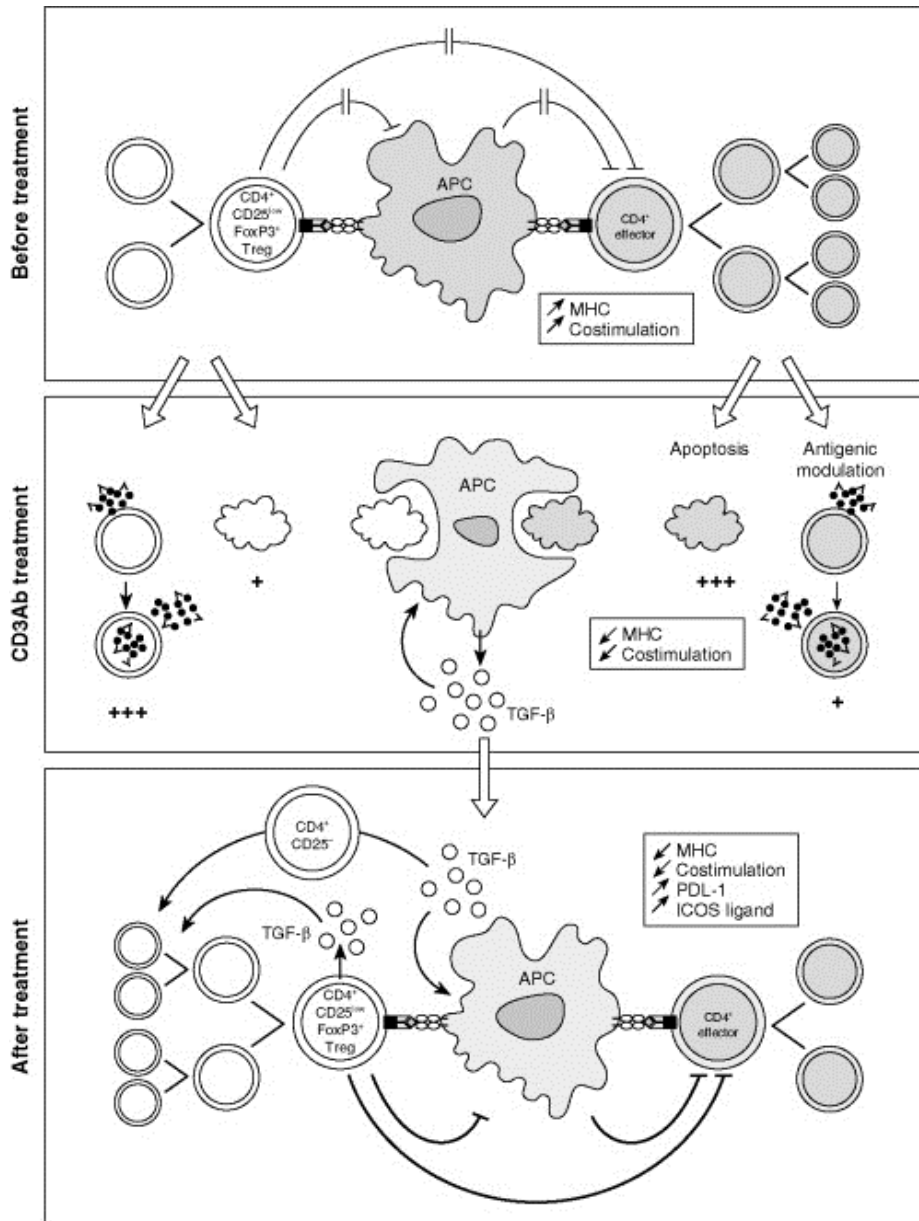


Figure 4: aCD3 treatment resulting in an inactivation of T cells.

This figure shows the mechanistic hypothesis to explain the tolerogenic effect of aCD3. (1) Effector T cells are activated by their autoantigens presented by antigen presenting cells (APCs) in pancreatic draining lymph nodes (PDLN). These pathogenic T cells are resistant to Foxp3⁺ regulatory T cells and they actively proliferate, resulting in an autoimmune response. (2) Administration of aCD3 induces a significant inactivation of T cells and this essentially involves activated effector T cells rather than regulatory T cells. (3) Dendritic cells that present specific autoantigens express less co-stimulatory molecules but deliver more inhibitory signals. These dendritic cells can inhibit autoantigen-specific pathogenic T cells and promote the expansion of regulatory T cells. In addition, in the presence of such tolerogenic dendritic cells, naïve autoreactive CD4⁺ CD25^{hi} T cells can be converted into adaptive Tregs. This results in a long term immune regulation after a short term aCD3 administration. Figure adapted from You et al. (46).

The aCD3 showed a strong effect in several mouse models such as the NOD (47; 48) as well as the RIP-LCMV model (49) and it was already used in clinical trials as monotherapy. Due to severe side effects of the regular antibody in some clinical trials with the aCD3 OKT3 (50) the Fc-part, that was responsible for FcR-binding of the antibody, was separated. In the past, two F(ab)₂-fragments of aCD3 were used in clinical trial: the oteelixumab (ChAglyCD3) in Europe (Defend-1-study (42; 51; 52)) and teplizumab (hOKT3 γ 1(Ala-Ala)) in America (protégé study (53; 54)). aCD3 demonstrated a decreased insulin need with a strong effect in younger patients in an early phase of the β -cell destruction. Unfortunately, after one year the insulin need increased again. 75 % of the patients develop anti-idiotypic antibodies directed against aCD3 after the first treatment (51; 55; 56). Consequently, a repeated treatment was ineffective in most individuals (57). In addition, the treatment with those aCD3 F(ab)₂-fragments still resulted in some side effects like cytokine release, fever and headache. In order to further reduce the side effects the dose was reduced 16-fold in a phase 3 study with oteelixumab (52) compared to its preceding Phase 2 trial (42; 51; 52). Unfortunately, the reduced side effects came along with a loss in efficacy. Thus, there is need for an alternative approach, such as an aCD3 combination therapy.

7.3.3 Combination therapies with aCD3 in T1D

Several combinations of aCD3 and secondary treatments were attempted and they often improved the effect of the aCD3 monotherapy. The first approaches to combine aCD3 with ciclosporin or rapamycin failed and both abolished the aCD3 mediated effect (48; 58). However, there were also some effective studies such as the T cell inactivation (aCD3) combined with B cell inactivation (anti-CD20 antibody (59)). The remission of T1D was increased and also the insulinitis was reduced in the combination therapy compared to an isotype control treatment. Unfortunately, the benefit in infiltration was lost after three months. The combination of aCD3 with immunising agents like proinsulin (60), *Lactococcus Lactis* secreting proinsulin and IL-10 (61) or GAD65 (62) as well as

a β -cell protection approach with the Vitamin D3 analogue TX527 (27) expanded the FoxP3⁺ Treg population, resulting in an enhanced remission of the disease. It was suggested that the induction of Tregs restored a protective immune balance and that this is the basis for a long term effect. Other groups focused on the enhancement of β -cell proliferation after aCD3 therapy. Treatment with exendin-4 (63) and dipeptidyl peptidase-4 inhibitor MK626 (64) demonstrated an increased insulin content by enhancing the recovery of residual islets.

It has to be investigated, if these strategies are also effective in humans. However, it seems that the T cells re-infiltrated the pancreas after aCD3 and also after some of the conducted combination therapies (59). Nevertheless, only a few groups tried to block the re-infiltration of recovered T cells.

7.4 Chemokines

Important factors for the migration of T cells are chemokines. Interestingly, they are involved in several autoimmune diseases such as Graves' disease (65), rheumatoid arthritis (66), systemic lupus erythematosus (67), multiple sclerosis (68), and also T1D.

7.4.1 Chemokine overview

Chemokines are small proteins with a molecular mass between 8 and 15 kDa and beside their chemotaxis activity they are also involved in the modulation of the functional properties of several leukocytes. Monocytes, splenocytes endothelial cells, fibroblasts and keratinocytes are influenced by cytokines to produce these chemokines. Presently more than 50 different chemokines are identified in humans (69; 70).

The chemokine superfamily is grouped into five classes according to the number and space between two conserved cysteines at the N-terminus: the

Introduction

C-X-C, C-C, C-X-3-C, X-C, X-C and C-X motif (71). The C-C motif is the largest group and it possesses four cysteines, whereby two of them are close together at the N-terminus. In contrast, the C-X-C and the C-X-3-C motifs have one or three amino acids between the N-terminal cysteines (71). The two other chemokine family members are different. The X-C motif only consists of two instead of four cysteines (72) and the new identified C-X motif lacks one of the first two N-terminal cysteines (73).

According to their function, chemokines can also be divided into two major groups: the homeostatic and the inflammatory chemokines (74). Homeostatic chemokines are also expressed in healthy tissue and are involved in the re-localisation of leukocytes. In contrast, inflammatory chemokines are predominantly expressed under inflammatory conditions and mediate the migration of leukocytes to inflamed tissue.

Chemokines bind to their specific GTP-binding coupled chemokine receptors (75). The receptors possess a seven-transmembrane structure and are expressed by a variety of leukocytes (76). In addition, the nomenclature follows that of chemokines (CCR, CXCR, CX3CR and XCR) (75). Importantly, the chemokines and their receptors form a complex network, because on the one hand most of the 22 chemokine receptors have more than one ligand (Figure 5). On the other hand many chemokines can bind to more than one chemokine receptor (74; 75). Thus, it is difficult to block only one specific pathway.

Introduction

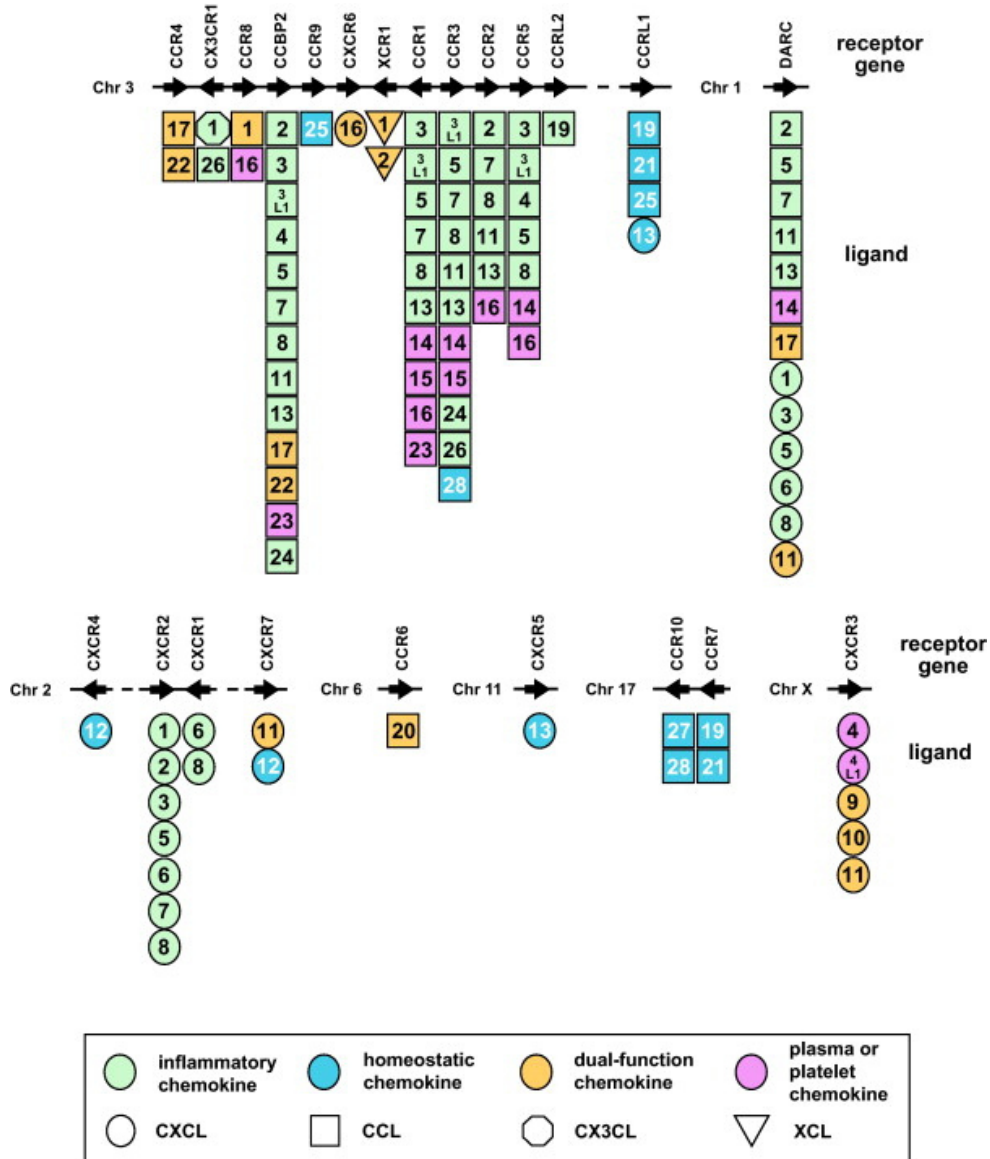


Figure 5: Many chemokine receptors possess more than one ligand.

Genomic organisation of the human chemokine receptors is displayed. Arrows indicate the chemokine receptor genes and their transcriptional orientation. The chemokine ligands CXCL (circles), CCL (square), CX3CL (hexagon) and XCL (triangle) recognised by each receptor are also shown below the receptor genes. The inflammatory (green), homeostatic (blue), dual (yellow) or plasma (purple) function is indicated by different colours. Figure adapted from Nomiya et al. (74).

7.4.2 Cytokines and Chemokines in T1D

The immune response in T1D depends on pro inflammatory cytokines like IFN γ , TNF α or IL-2 and anti-inflammatory cytokines such as IL-4, IL-5, IL-10 and TGF- β , which were mainly secreted by regulatory T cells (77; 78).

The influence of IFN γ and TNF α was investigated by several studies and a lack of IFN γ dramatically reduced the incidence of T1D in the RIP-LCMV mouse model (26). In terms of TNF α the effect depends very much on the progression of the disease. On the one hand the early expression of TNF α increased the T1D incidence and on the other hand late expression led to a remission of the autoimmune destruction in the RIP-LCMV mouse model (79).

In T1D chemokines are not as extensively described as cytokines. A study by Lohmann et al. showed a tendency for an increased peripheral blood mononuclear cell expression of chemokine receptors CXCR3 and CCR5 in long standing diabetic patients (80). In addition, the chemokine level of CCL3 is upregulated in recent onset diabetic patients (80). Importantly, a variety of clinical trials demonstrated higher serum CXCL10 levels in patients with T1D (81-83).

Since the ligands CXCL9, 10 and 11 for CXCR3 are all IFN γ inducible chemokines and CXCR3 as well as CXCL10 are both elevated in patients with T1D, this axis seems to be of crucial importance in T1D.

7.4.3 CXCL10 and its receptor CXCR3 in T1D

CXCL9, 10 and 11 demonstrate many similar properties. For example the three chemokines show a structural homology (84) and are produced by keratinocytes, macrophages, fibroblasts as well as endothelial cells after stimulation with IFN γ (85; 86). Due to the IFN γ dependent immune response to viruses, CXCL10 was often upregulated after virus infection (87-89). Moreover, CXCL9, 10 and 11 also behave as antagonists for CCL3 (90) and they play a role in several inflammatory diseases such as hepatitis B (91), ischemia (92), insulinitis (93), autoimmune encephalomyelitis (94) and T1D (95). In addition, the binding affinity to their only receptor CXCR3 is different for all of them (96-99).

Similar to the other chemokine receptors CXCR3 is a G protein-coupled seven-membrane-spanning glycoprotein. CXCR3 is internalised in consequence of the binding of CXCL9, 10 or 11, leading to an intracellular activation signalling cascade. Subsequently, this results in cytoskeleton rearrangement and cell

movement. CXCR3 is predominantly found on activated T cells, natural killer cells, B cells and dendritic cells (98; 100). In addition, three splice variants of CXCR3 are described in human: CXCR3-A, CXCR3-B, and CXCR3-alt. Beside the classical binding to CXCR3-A, CXCL9, CXCL10, and CXCL11 interact with the CXCR3-alt isoform, which mediates chemotaxis (101). Moreover, binding of CXCL9, CXCL10, and CXCL11 to CXCR3-B impairs endothelial cell growth (102).

Despite of this homogeneity, only the CXCL10 chemokine forms dimers with a molecular weight of 20 kDa (103). Moreover, it was also shown that CXCL10 was involved in the suppression of angiogenesis (104; 105). Furthermore, of this subfamily CXCL10 seems to be the important chemokine in T1D indicated by the findings that the blockade of CXCL10 and not CXCL9 resulted in a lower T1D incidence (95). In addition, in several clinical trials patients with T1D demonstrated higher serum CXCL10 levels (81-83) and also NOD mice showed a higher level of CXCL10 at T1D onset (106). Moreover, it was also shown that β -cells themselves produced CXCL10 in response to inflammatory stress (93; 107) and consequently formed an islet antigen-specific T cell gradient around the islets (34).

It has been suggested that a high local expression of CXCL10 outside the infiltrated tissue attracted the T cells away from the side of inflammation, resulting in an abrogation of the autoimmune process. The high local expression of CXCL10 in the NOD and RIP-LCMV mouse model was achieved by an infection with a virus, which predominantly accumulates in the pancreatic lymph nodes (PDLN). The T cells migrate to the PDLN and were strongly activated, resulting in apoptosis (108). Consistently, it was also shown that overexpression of CXCL10 in the islets of Langerhans attracted T cells without any infection in transgenic mice (109). This demonstrated that CXCL10 may strongly influence the T cell migration.

7.5 Adhesion molecules

One important factor in the leukocyte migration is the rolling, adhesion and transmigration through the cell layers. Cell adhesion molecules (CAMs) such as selectins, integrins and the immunoglobulin superfamily are mainly involved in this process (110; 111).

7.5.1 Function of adhesion molecules

The first step of the migration cascade is the rolling, where leukocytes are captured out of the blood flow to the luminal endothelial layer (Figure 6). This is mediated by the heterophilic selectin family that binds to glycosylated ligands such as P-selectin glycoprotein ligand 1 (PSGL1) on leukocytes (112). Three different types of selectins exist and two of them, P- and E-selectin, are expressed by endothelial cells during inflammation. In contrast, L-selectin is found on most leukocytes and can bind to the endothelial cell surface glycoprotein CD34 (110; 111). There is evidence that these selectins are important in T1D. In the NOD model preventive neutralisation of L-selectin resulted in a reduced infiltration of T cells and the treatment of diabetic mice delayed the disease progression (113; 114).

Integrins such as leukocyte function-associated antigen 1 (LFA-1) or very late antigen 4 (VLA-4) are expressed by almost all leukocytes. In contrast, macrophage-1 antigen (Mac-1) is only expressed by monocytes, neutrophils, macrophages, and natural killer cells. However, all three are heterodimers of α and β subunits and they interact with the immunoglobulin superfamily members on endothelial cells (Figure 6) (112). For instance the immunoglobulin superfamily member intercellular adhesion molecule 1 (ICAM-1) binds to LFA-1 and MAC-1, whereas vascular-cell adhesion molecule 1 (VCAM-1) binds to VLA-1. In addition, the homophilic PCAM-1 is predominantly found on leukocytes, platelets, as well as endothelial cells. Binding of integrins to these members of the immunoglobulin superfamily contributes to the slow down

Introduction

process of leukocytes and leads to a firm adhesion (Figure 6) (110; 111). Interestingly, the inhibition of the interaction between the integrin VLA-4 and its partner VCAM-1 resulted in a reduction of T1D (113; 115). In contrast, an interference with PCAM-1 or ICAM-1 interactions only showed a marginal effect (110; 115). For instance blocking of the homophilic PCAM-1 interaction only resulted in a decreased migration of monocytes and neutrophils, but showed no influence in T1D incidence (116). In addition, the immunoglobulin superfamily plays a role in the transmigration of cells (Figure 6).

The junctional adhesion molecule (JAM) family is another immunoglobulin superfamily member, which is expressed in tight junctions of epithelial and endothelial cell contacts as well as by leukocytes and platelets (117). Importantly, it is suggested that the JAMs are involved in the transmigration of leukocyte (118).

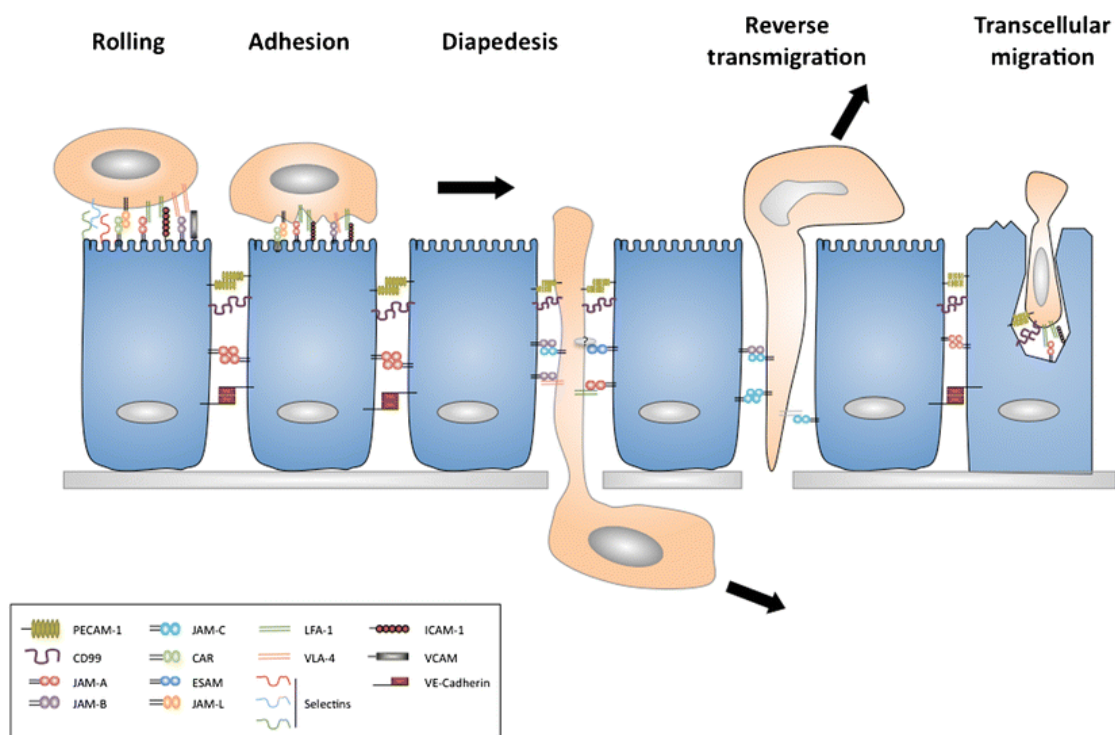


Figure 6: Rolling, adhesion and transmigration is influenced by CAMs.

Migration of leukocytes through endothelial cells can be separated into different steps: rolling, adhesion, transmigration and reverse transmigration. Under inflammatory conditions, JAMs are localised on the luminal surfaces of the endothelium and are able to interact with integrins expressed by leukocytes. JAM-A, PECAM-1 and CD99 contribute to the migration of leukocytes through endothelial cells. The leukocytes can exit the abluminal side by reverse transmigration, which is regulated by JAM-C. Another route for leukocytes is to pass the endothelial cell layer using a transcellular mechanism. This process is regulated by CD99, PECAM-1, ICAM-1 and JAM-A. Figure adapted from Garrido-Urbani et al. (117).

7.5.2 Junctional adhesion molecules

The JAM family is composed of seven members: the three classical members JAM-A, JAM-B as well as JAM-C and the four related proteins JAM-4, JAM-L, CAR as well as ESAM (117). JAMs are type 1 transmembrane glycoproteins which consist of one transmembrane domain and one cytoplasmic tail. The cytoplasmic tail is of variable length and has phosphorylation sites that may interact with PKA, PKC or Casein Kinase II. In addition, this tail contains a PDZ domain which includes the post-synaptic density protein and a zonula occludens protein (ZO-1) binding motif (119; 120).

JAMs are able to bind in a homophilic as well as heterophilic manner in trans- and cis-configurations. They are mostly found in endothelial tight junctions. However, the members of the JAM family have different expression patterns in various organs indicating a potential tissue-specific function. For instance, JAM-A is found on endothelial as well as epithelial cells and it forms heterophilic interaction with LFA-1 (121). Interestingly, on the blood-brain-barrier JAM-A is highly enriched (122). In contrast, JAM-B is predominantly expressed in high endothelial venules and on lymphatic endothelial cells, where the JAM-A expression is less dominant (122). However, the blood-brain-barrier requires a very low permeability, whereas vascular endothelial cells support trafficking of lymphocytes. Due to that it might be that JAM-B and JAM-C are more involved in leukocytes migration than JAM-A. In addition, JAM-B can bind to JAM-C and this heterophilic binding is even stronger than the homophilic or the JAM-B/VLA-4 interaction (123; 124). The JAM-C interactions are described in more detail in the next chapter.

7.5.3 The role of JAM-C in T1D and other diseases

JAM-C expression in mice is restricted to endothelial cells as well as platelets and it is assumed that JAM-C is important for the transmigration of leukocytes (125), due to its interaction with JAM-B or MAC-1 (124; 126). Furthermore, JAM-C binds homophilic, but in contrast to the heterophilic interactions, that

occurs with rapid dynamics, resulting in a weak binding (127). Intriguingly, human JAM-C was also expressed by lymphocytes and it was shown that JAM-C was increased on activated human T cells (124; 128). Due to that, the influence of JAM-C on several diseases was investigated *in vitro* and *in vivo*. For instance JAM-C was upregulated in a cerulein-induced pancreatitis mouse model (129). Administration of a neutralising antibody against JAM-C decreased the leukocyte infiltration. In contrast, overexpression of JAM-C in the same mouse model led to an accumulation of leukocytes at the site of inflammation (129). Moreover, Christen et al. showed that blocking of JAM-C resulted in a decrease of T1D incidence in RIP-LCMV-GP as well as NP mice (130). For that reason JAM-C might be important in T1D. In addition, recent investigations revealed a role of JAM-C in reverse transmigration of monocytes (131). Bradfield et al. demonstrated that after aJAM-C treatment the monocyte number in the lung was indeed reduced. However, this reduction was not a consequence of a lower transmigration, to a greater degree it was due to increased reverse transmigration over the endothelial cell barrier. Besides JAM-C can be processed by “A Disintegrin And Metalloproteinase 10” (ADAM-10) or ADAM-17 which resulted in a shedding from the endothelial surface (132). This soluble JAM-C showed an important influence on angiogenesis and tumour growth in mice (132; 133).

Aims

8 Aims

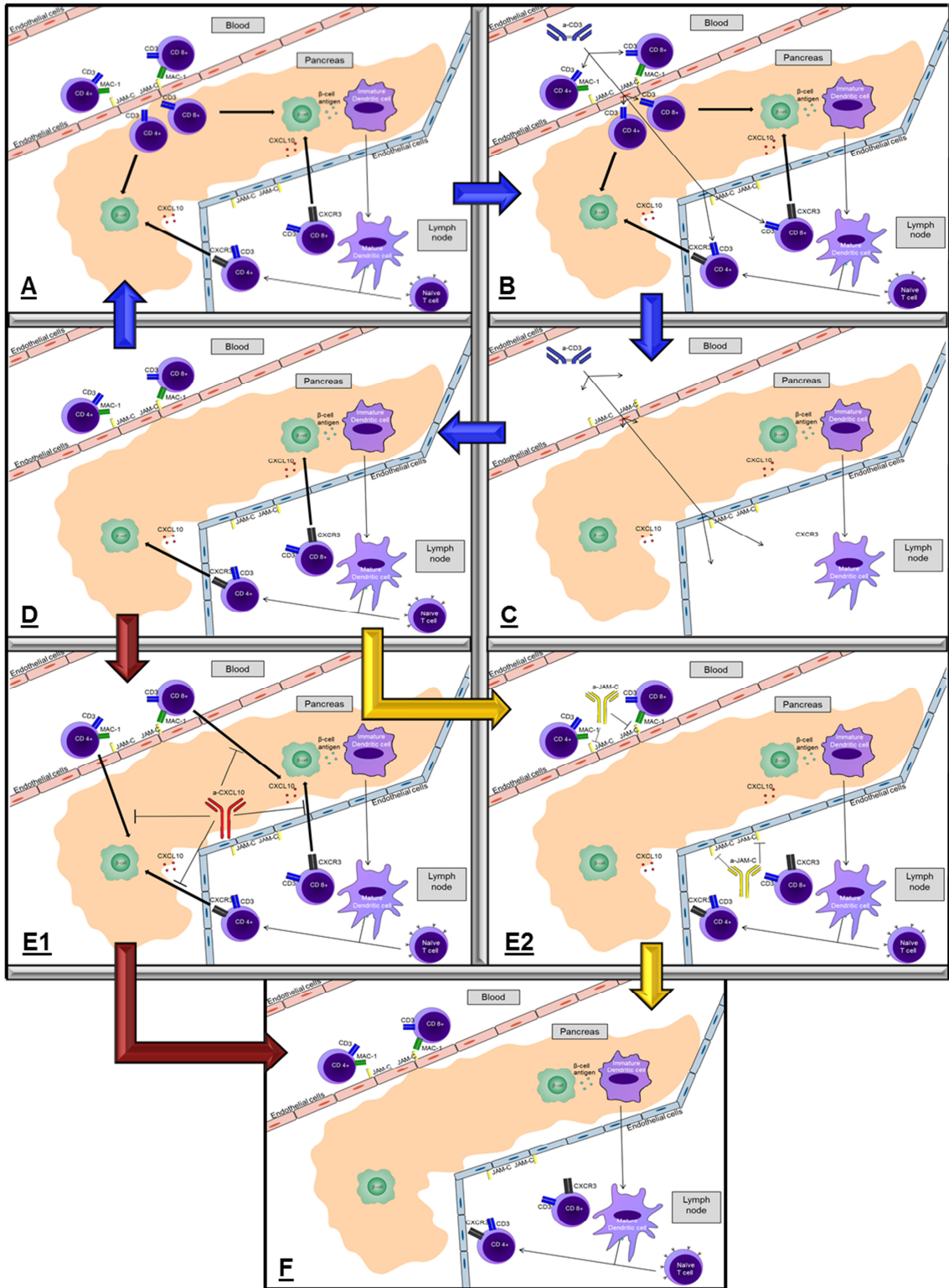
In the present work I investigated an immunotherapy for T1D. The anti-CD3 antibody (aCD3) therapy has a beneficial effect in patients with T1D. However, in most patients the autoimmune response recrudesced after two years and for that reason I tried a combination of a T cell inactivating aCD3 therapy and a treatment with a second antibody which blocks the re-infiltration of aggressive T cells into the pancreas. The administration of aCD3 induces a significant inactivation of T cells in lymphoid organs and in the infiltrated tissues. Soon after, the immune system regenerates and new T cells are produced. Unfortunately, without a second therapy these recovered T cells migrate into the pancreas over a CXCL10 and JAM-C mediated mechanism. Consequently, the T cells attack yet again the antigen-expressing β cells in the pancreatic islets of Langerhans (Figure 7A-D; Blue arrows).

Aim1: In the first approach I wanted to stop the re-infiltration of recovered T cells with an antibody against the chemotactic chemokine CXCL10 (aCXCL10), which is important for the T cell migration to the islets of Langerhans (Figure 7E1+F; Red arrows).

Aim2: In the second approach I wanted to block the JAM-C mediated transmigration of leukocytes through the endothelial layer into the pancreas with a neutralising antibody against the adhesion molecule JAM-C (aJAM-C) (Figure 7E2+F; Yellow arrows).

Figure 7: Overview of the presumable antibody effect.

Figure is displayed on the next page. (A) Environmental and genetic factors may lead to an increased antigen uptake of dendritic cells in the pancreas. In the PDLN the antigen is presented by matured dendritic cells to T cells. Accordingly, there might be a potential activation of cross-reactive T cells by specific antigens. These aggressive T cells migrate through a JAM-C/MAC-1 and CXCL10/CXCR3 mediated mechanism into the pancreas. Subsequently, these T cells attack the antigen presenting β -cells in the pancreas. (B+C) The administration of aCD3 induces a significant inactivation of T cells in lymphoid organs and in the infiltrated tissues. (D) Soon after, the immune system regenerates and new T cells are produced. (D→A) Unfortunately, without a second therapy these recovered T cells migrate into the pancreas and they attack yet again the β cells in the pancreas (pathway marked with blue arrows). (E1) Treatment with aCXCL10 blocks the re-infiltration of recovered T cells (pathway marked with red arrows). (E2) Administration of aJAM-C blocks the transmigration of leukocytes (pathway marked with yellow arrows) and both results in an abrogation of the autoimmune response (F).



Results

9 Results

In the present work I evaluated two combination therapies for T1D. In particular I studied the effect of an anti-CXCL10 (aCXCL10) or anti-JAM-C (aJAM-C) antibody treatment as follow-up therapies to the already established anti-CD3 antibody (aCD3) treatment. Therefore, I divided this dissertation into three main parts. The first part deals with the aCD3 monotherapy, the second with the combination therapy of aCD3 and aCXCL10 (CT) and the last with the combination therapy of aCD3 and aJAM-C (CT-J).

9.1 Anti-CD3 treatment

First I determined the concentration and treatment window of the aCD3 administration and the ideal starting time for the second therapy. From experiments in the past and from data of other groups we knew that it was appropriate to inject aCD3 three times.

9.1.1 3 µg and 30 µg Anti-CD3 led to half and full inactivation of the T cells

At first I analysed different aCD3 concentrations. For one I wanted to find an aCD3 dose with a maximal effect. In addition, in order to lower the side effects caused by immunosuppressive drugs and to achieve a stronger impact of the second therapy I wanted to find a dose with a moderate (half-maximal) effect. Thus, uninfected C57BL/6 mice were treated for three days with aCD3 concentrations ranging from 0.3 to 30 µg per mouse. The blood was collected one and five days after the last antibody dose was injected as described in 11.2.3.1. Lymphocytes were isolated (11.2.1.9) and analysed by flow cytometry (11.2.1.10).

Results

30 μg aCD3 led to full inactivation of the T cells (87 %; $p=0.008$) and 3 μg aCD3 led to half inactivation of the T cells (45 %; $p=0.0165$ / Figure 8A and B). Thus, I chose these two concentrations for my further studies. For the reason that T cells had almost fully recovered already five days after the last aCD3 dose (Figure 8A), the time frame for starting with the second therapy is small and the mice need to be treated immediately after aCD3 administration.

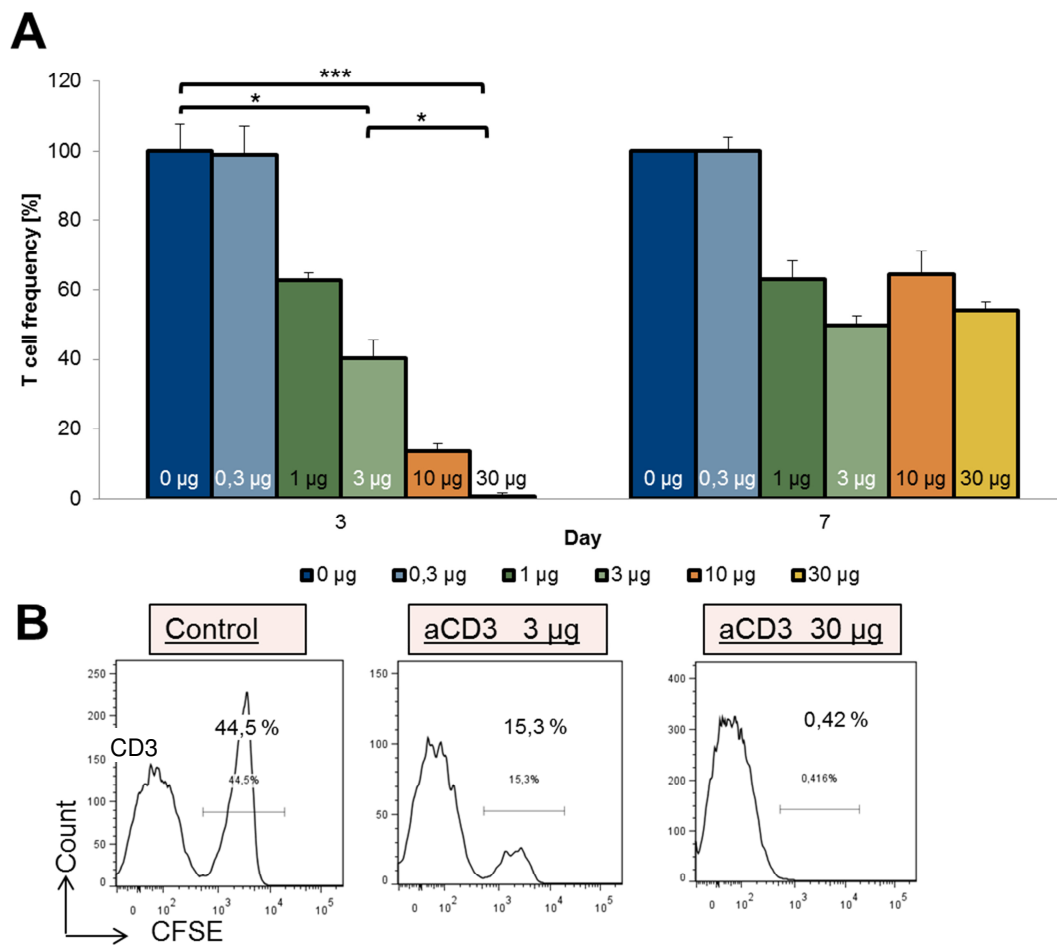


Figure 8: 3 μg and 30 μg aCD3 led to half and full inactivation of the T cells in the blood.

(A) The administration of different concentrations aCD3 (from 0.3 to 30 μg per mouse) resulted in an inactivation of T cells in the blood of uninfected C57BL/6 mice in a dose dependent manner. Relative T cell frequencies of CD3 T cells were measured by flow cytometry. (B) Representative dot blots of blood lymphocytes from flow cytometry at day 3 after first aCD3 injection. Data are mean values \pm SD ($n=3$). Significant differences are indicated as follows: $p < 0.05$ (*); $p < 0.01$ (**); $p < 0.001$ (***)

9.1.2 aCD3 treatment was more effective at days 10-12 rather than at days 7-9 post-infection

In the RIP-LCMV-GP mouse model some crucial points are known. The first step is the virus elimination (days 0-7 after virus infection), where the immune system expands and recruits specific T cells to clear the virus. After viral clearance, the specific T cells peak in numbers and begin to infiltrate into the pancreas where the β -cells carrying the viral antigen are located (days 8-10). Initially the T cell infiltration seems to impair the insulin production by the β -cells through induction of cellular stress without actually killing them. Nevertheless, from day 10 on the β -cells are destroyed by LCMV-GP-specific T cells and most of them have been eliminated by day 20 post-infection. It has been shown previously that aCD3 has no effect when given before the autoimmune process has started (48). In the RIP-LCMV model, the aCD3 treatment might also interfere with the virus elimination between day 0 and 6 and thereby influence the initiation of the autoimmune destruction process. Similarly, it seems not useful to treat the mice very late, where most of the β -cells are already destroyed, since the chances of a remission would then be low. Therefore, the infected RIP-LCMV-GP mice received three daily intravenous injections of either 3 μ g or 30 μ g aCD3 from days 7-9, the time of the T cell peak, or from days 10-12, the beginning of the β -cells destruction. The lymphocytes from blood, spleen, PDLN and pancreas were isolated one day after the last antibody dose (11.2.1.6-11.2.1.9) and analysed by flow cytometry (11.2.1.10).

The high dose of aCD3 inactivates most of the T cells in all analysed organs at both times analysed (Figure 9A-D). The effect of the treatment was stronger on CD4 T cells, whereas the reduction of CD8 T cells was much less pronounced with both doses of aCD3. Thus, our findings confirm the recent observation that the differential expression of the CD3 receptor on T cell subsets influences the aCD3-induced T cell inactivation (134). Importantly, the low dose of aCD3 showed a significant reduction of 40-60 % of T cells when treated at days 10-12 post-infection (Figure 9A+C). In contrast, there was no significant reduction of T cells when treated at days 7-9 post-infection (Figure 9A+B). One reason for this observation would be the high number of T cells at this point of time. Of high

importance for our study was that we reached the pancreas with both doses of aCD3 reducing the frequency of CD4 and CD8 T cells significantly (Figure 9).

For the reason that the low dose showed a better efficacy if given at the start of the β -cell destruction, I treated the mice at days 10–12 in all following experiments. Another advantage of treating the mice starting at day 10 after infection is that mice show already clear clinical signs of T1D, namely a strong hyperglycaemia. Thus, the treatment constitutes a real therapy and not a mere prevention.

9.1.3 aCD3 inactivation predominantly affects specific T cells rather than regulatory T cells

In the next experiment I investigated the inactivation of additional subgroups of T cells, because there was a clear difference between CD4 and CD8 T cell inactivation (Figure 9A-D). The most important subsets in T1D are regulatory T cells (Tregs) and islet antigen-specific effector T cells (Teff), which were identified by the transcription factor FoxP3 or the cytokine IFN γ produced upon stimulation with the immunodominant LCMV-GP peptide, respectively. RIP-LCMV-GP mice were treated for three days with 3 or 30 μ g aCD3 at days 10-12 after LCMV infection. Then the lymphocytes from blood, spleen, pancreatic lymph node and pancreas were isolated one day after the last antibody dose (11.2.1.6-11.2.1.9) and analysed by flow cytometry after stimulation with islet (LCMV-GP)-specific peptides (11.2.1.11). Alternatively, pancreas, PDLN and spleen were embedded in OCT and cut into 7 μ m sections (11.2.1.13).

In line with the last experiment the high dose of aCD3 had an effect on CD4 T cells in blood, spleen, PDLN and pancreas. The CD4 T cell frequency in spleen and blood was reduced to approx. 50 % with 3 μ g aCD3 compared to untreated mice and it was further reduced to approx. 10 % ($p=0,0013$) with 30 μ g aCD3 (Figure 10A+B). In the PDLN and pancreas the aCD3 treatment was less effective and 30 μ g aCD3 reduced both the frequency and absolute CD4 T cell number to only approx. 50 % (Figure 10C+D). Again the reduction of CD8 T cells was much less pronounced in all organs (Figure 10A+D).

Results

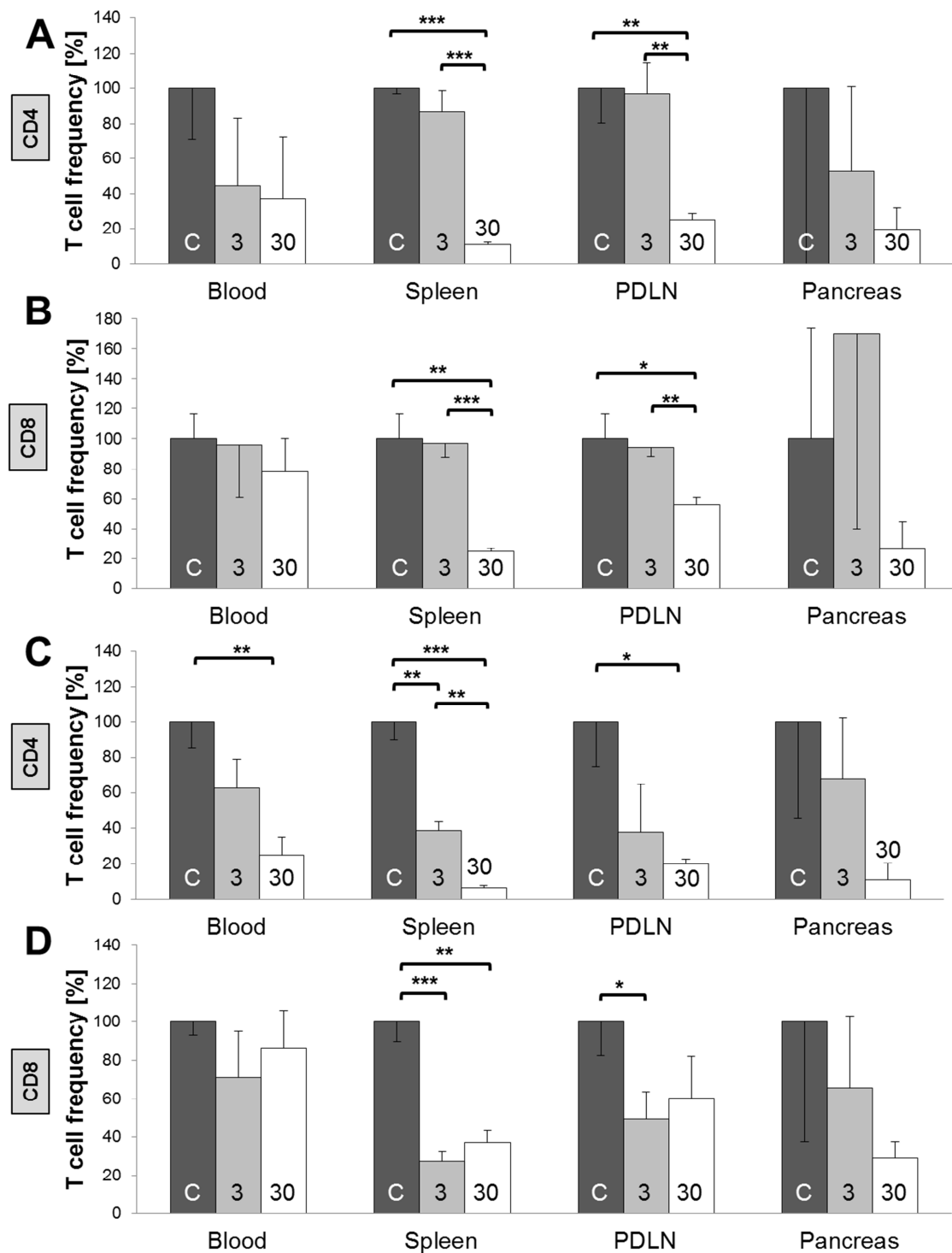


Figure 9: The aCD3 therapy had a better effect at days 10-12 than at days 7-9.

Lymphocytes were isolated from blood, spleen, PDLN and pancreas of untreated control RIP-*LCMV-GP* mice (dark grey) or mice after three daily injections of 3 µg aCD3 (light grey) or 30 µg aCD3 (white) and analysed by flow cytometry one day after the last aCD3 injection. Relative CD4 and CD8 T cells frequencies of RIP-*LCMV-GP* mice treated with aCD3 at day 7-9 (A) and 10-12 (B) post-infection are displayed. Data are mean values \pm SD (n=3). Significant differences are indicated as follows: $p < 0.05$ (*); $p < 0.01$ (**); $p < 0.001$ (***)

Results

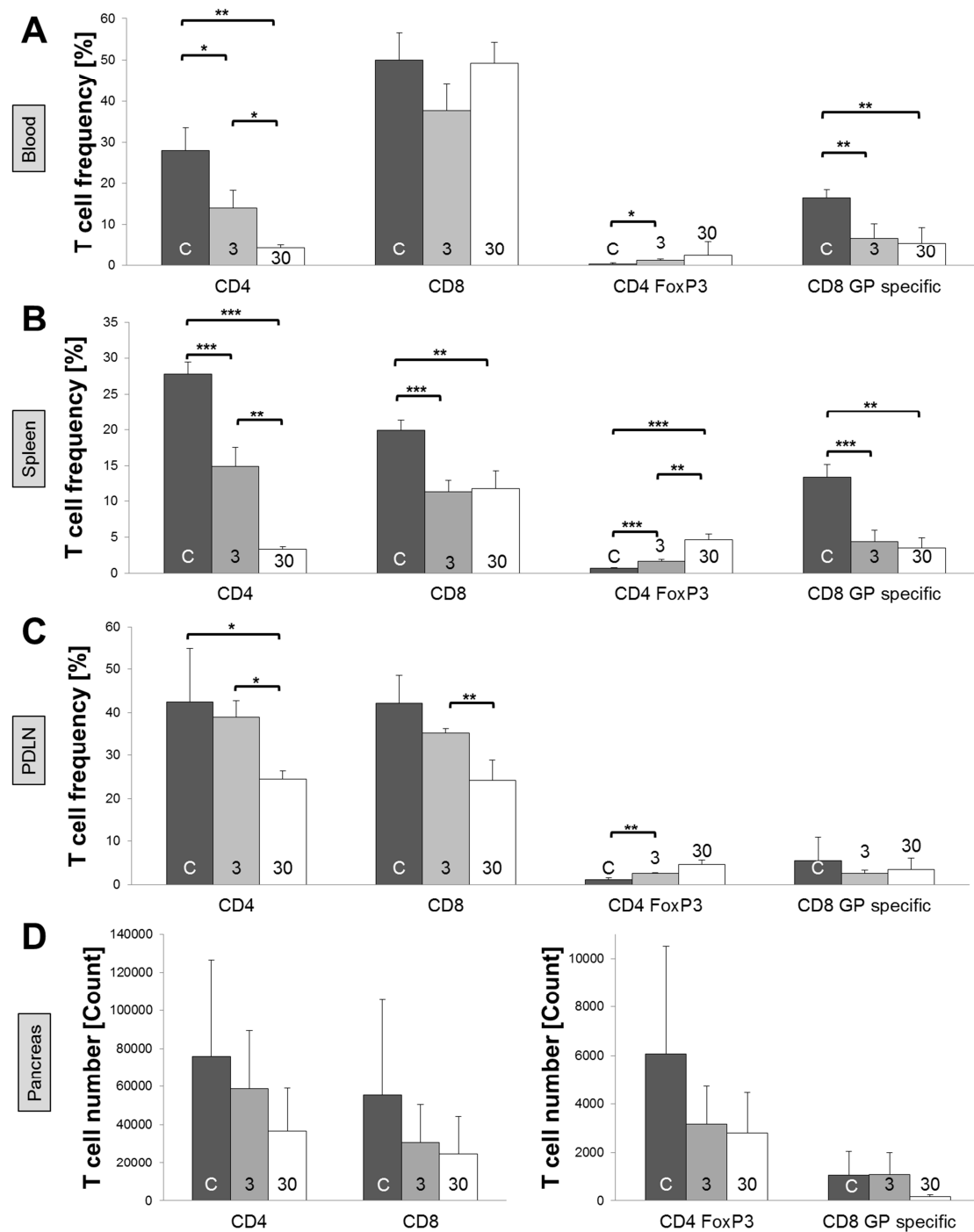


Figure 10: aCD3 treatment was more effective for Teff than Tregs.

Flow cytometry of lymphocytes isolated from blood (A), spleen (B), PDLN (C) and pancreas (D) was performed at day 13 of RIP-LCMV-GP mice that were either untreated (dark grey) or received three daily injections of 3 μ g aCD3 (light grey) or 30 μ g aCD3 (white) at days 10-12 post-infection. Frequencies of total CD4 T cells, total CD8 T cells and FoxP3⁺ CD4 T cells in blood, spleen and PDLN and their absolute number in the pancreas are displayed. Frequencies of islet antigen (LCMV-GP33)-specific CD8 T cells in blood, spleen and PDLN and their absolute number in the pancreas were obtained by stimulation of isolated lymphocytes with LCMV-GP33 followed by intracellular IFN γ staining and flow cytometry. Data are mean values \pm SD (n=4). Significant differences are indicated as follows: p < 0.05 (*); p < 0.01 (**); p < 0.001 (***).

Results

Immunohistochemistry staining of the pancreas confirmed the reduction of infiltration after aCD3 treatment at day 13 post-infection (Figure 11A). The pancreas of aCD3 treated mice showed much more intact islets producing insulin than the pancreas of untreated control mice indicated by the brown staining on the pancreas overview (Figure 11A). Also the overall insulinitis was reduced with the administration of both 3 μ g and 30 μ g aCD3 (Figure 11B). Almost 50 % of the islets of mice that were treated with the high dose of aCD3 showed no infiltrations and also 34 % of the islets present in 3 μ g aCD3 treated mice had no infiltration (Figure 11A+B). It is important to keep in mind that the pancreatic β -cell mass that is needed to ensure normal glycaemia is approx. 20-30 % in human (135) and 10 % in mice (136).

Although the frequency of CD4 T cells in general was reduced, aCD3 treatment significantly increased the frequency of FoxP3⁺ CD4 T cells in blood (eight-fold), spleen (seven-fold) and PDLN (five-fold) (Figure 10A+C). In the pancreas, I found a tendency towards a lower absolute number of FoxP3⁺ CD4 T cells after aCD3 administration. However, this was more likely a result of a lower degree of insulinitis (Figure 10D). Importantly, the frequency of islet antigen-specific CD8 T cells of total CD8 T cells was significantly decreased in all organs although the frequency of total CD8 T cells was not reduced in this manner (Figure 10A+C). In spleen and blood the high dose of aCD3 inactivated 74 % or 67 % of islet antigen-specific CD8 T cells, respectively. Similarly, the low aCD3 dose inactivated 67 % or 59 % in spleen and blood, respectively. The effect was weaker in the PDLN with both doses of aCD3 and inactivated 47 % (3 μ g) or 52 % (30 μ g) of islet antigen-specific CD8 T cells. Importantly, in the pancreas the absolute number of islet antigen-specific CD8 T cells decreased to 16 % of the number obtained in untreated control mice with 30 μ g aCD3 (Figure 10D).

Thus, we could demonstrate that aCD3 treatment indeed inactivated islet antigen-specific CD8 T cells, the main driver of the T1D development in the RIP-LCMV model, locally in the pancreas.

Results

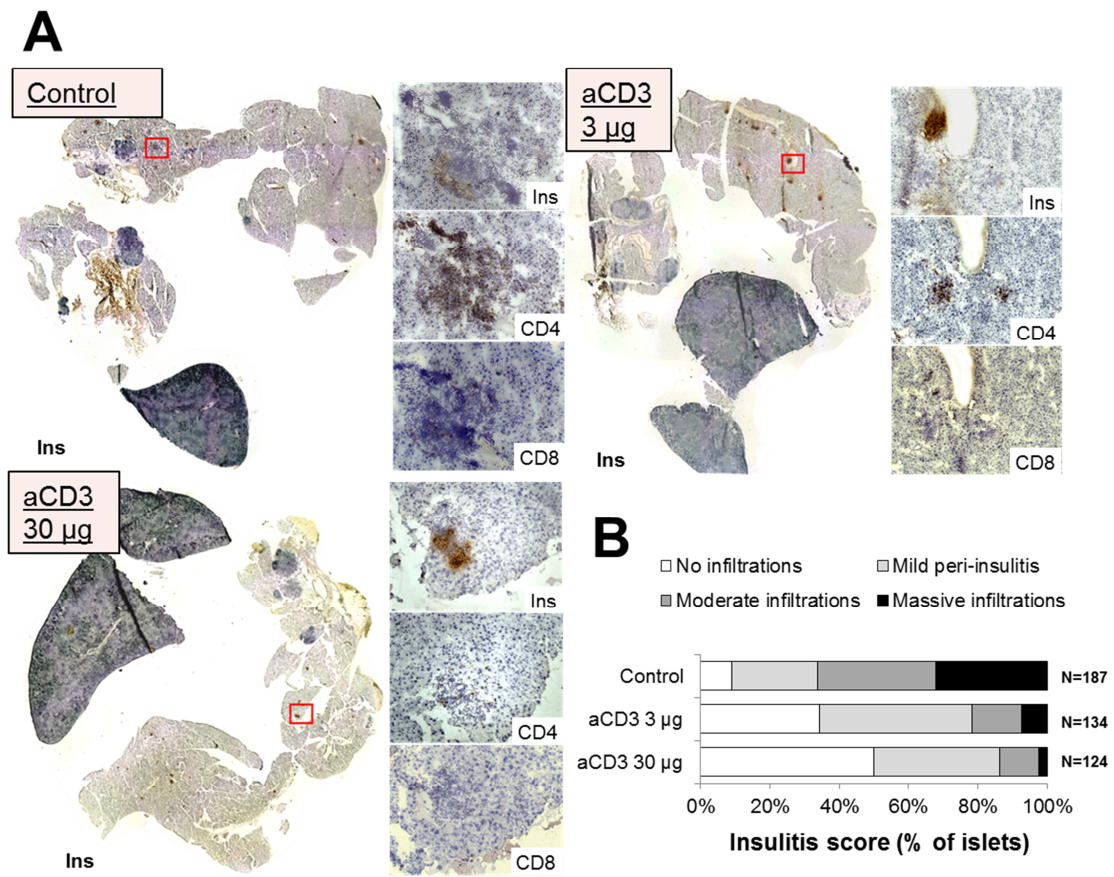


Figure 11: Immunohistochemistry revealed that an aCD3 dose of 3 µg had only a minor impact on T cell infiltration in the pancreas.

(A) At day 13 after infection immunohistochemistry of pancreas tissue sections from RIP-LCMV-GP mice was performed. The mice were treated with three daily injections of 3 or 30 µg aCD3 at days 10-12 post-infection. Consecutive sections were stained for insulin (Ins), CD4 and CD8 T cells. Positive staining is indicated by a brown colour. Representative pancreas section overviews were reassembled from pictures taken at a low magnification (4x) and blow ups were taken at a higher magnification (20x). (B) Insulitis of more than 100 individual islets from pancreas sections of three mice per group was calculated by semi-quantitative analysis. Islets were categorised into no infiltrations (white), mild peri-insulitis (<20 %, light grey), moderate infiltrations (<50 %, dark grey) and massive infiltrations (>50 %, black). Data are mean values +/- SD (n=3).

9.1.4 Administration of low dose aCD3 has an intermediate impact on the incidence of T1D

To investigate the influence of 3 μ g and 30 μ g aCD3 on T1D reversion I treated RIP-LCMV-GP mice at days 10-12 post-infection with aCD3 and measured the blood glucose (BG) level for 196 days.

Most of the infected mice in the untreated control group develop severe T1D with BG levels above 600 mg/dl within 20 days (Figure 11C). Administration of a high aCD3 dose (30 μ g) showed a strong effect and most of the mice were cured shortly after therapy begin with BG levels below 300 mg/dl (Figure 11C). In contrast, mice treated with a low dose aCD3 (3 μ g) took longer to reach a non-diabetic BG level (< 300 mg/dl) and their BG level fluctuated extensively (Figure 11C).

Due to the fact that the low aCD3 dose showed an intermediate effect on the T1D remission in RIP-LCMV-GP mice, I proceed with a low aCD3 dose for the following combination therapies to avoid a massive general immune suppression and to be able to investigate the influence of the second therapy.

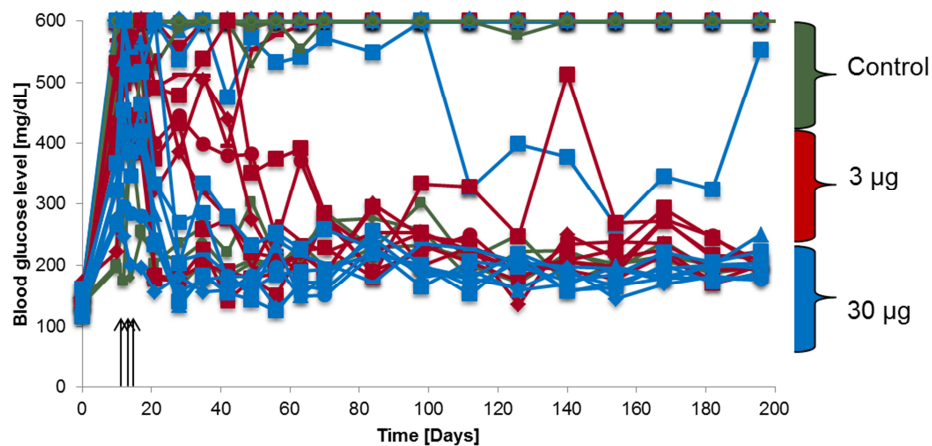


Figure 12: BG levels showed that the low aCD3 dose had only an intermediate effect.

The BG level of untreated mice (green) or of mice treated with three doses 3 μ g (red) as well as 30 μ g (blue) aCD3 at days 10-12 post-infection is displayed. Arrows indicate the point of time of aCD3 administration and BG levels were determined until day 196 after infection.

9.2 Combination therapy with CXCL10

Several human trials revealed that the aCD3 effect was not long-lasting (42; 51; 57) and the disease recurred within one or two years probably due to a re-infiltration of lymphocytes. Accordingly, I wanted to block the re-entry of recovered T cells with an antibody against the chemotactic chemokine CXCL10 after inactivation with aCD3. CXCL10 has an important role in the T cell migration and it is also produced by β -cells under inflammatory stress.

9.2.1 Production of aCXCL10

First the anti-CXCL10 antibody (aCXCL10) had to be produced. The aCXCL10 producing hybridoma cells obtained from Andrew Luster were cultured (11.2.1.1) and the supernatant was purified by using a Protein G column and FPLC (11.2.1.12) (Figure 13A). The purity and function was tested by SDS-PAGE (11.2.2.4) and in a migration assay (11.2.1.5), respectively.

The elution profile of aCXCL10 showed one clear peak (blue line) shortly after the elution was initiated (green line; Figure 13A). The fractions (red) were evaluated in a Bradford assay and fractions containing a concentration above 1 mg/ml aCXCL10 were pooled (Figure 13B). Following this, the concentration of the pooled fractions (red) of each batch was determined in a Bradford assay (Figure 13C). SDS-PAGE of the batches revealed a pure antibody with a light chain (25 KDa) as well as a heavy chain (50 KDa) similar to the control IgG antibody (Figure 13E). In the migration assay without CXCL10 only a few T cells migrate through the membrane. The addition of CXCL10 led to a strong migration of T cells through the membrane, demonstrating the importance of this chemokine for the T cell migration. Indeed, the CXCL10 induced T cell migration was inhibited with all batches of aCXCL10 to approx. 40 % of the control IgG.

To ensure that aCXCL10 reached the pancreas, the distribution of the injected hamster derived aCXCL10 was investigated by in situ staining of 7 μ m RIP-

Results

LCMV-GP pancreas sections (11.2.1.13) with a second antibody against hamster antibodies three days after the last of eight antibody doses. The staining clearly showed that aCXCL10 reached the pancreas, spleen and PDLN after aCXCL10 monotherapy or CT treatment of mice (Figure 14A). Examination of the sections at higher magnification revealed that the injected aCXCL10 was located directly in the infiltrates (Figure 14B). After the end of the observation (day 182 post-infection) aCXCL10 was not detectable anymore (Figure 14C). Thus, the pure aCXCL10 was able to inhibit T cell migration. It reached the pancreas and went directly into the infiltrates.

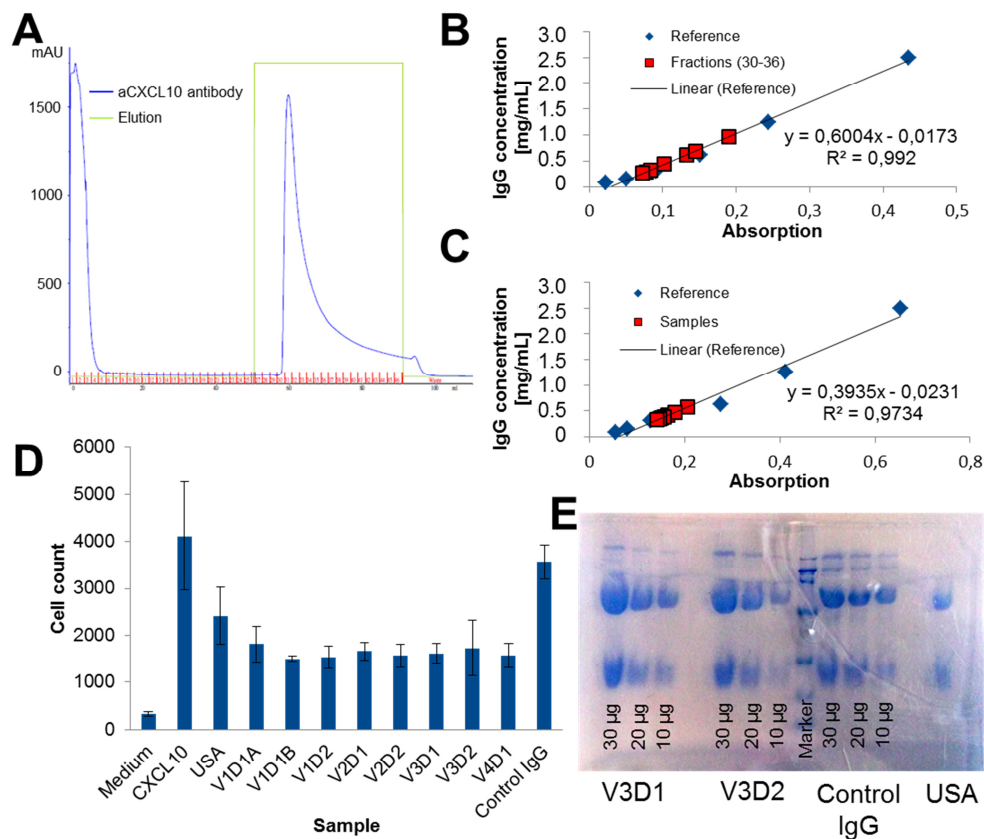


Figure 13: aCXCL10 was of high purity and it reduced the migration of T cells.

(A) A representative elution diagram of aCXCL10 purification by protein G FPLC chromatography is shown. The concentration of the fractions (red) (B) and whole pooled batches (red) (C) were determined by Bradford assay by using a serial dilution of a standard control antibody (blue) and linear regression. (D) The function of aCXCL10 was tested by a migration assay. The negative control contains only medium without CXCL10. The positive controls include medium with CXCL10 and medium with CXCL10 as well as isotype control antibody. Data are mean values \pm SD ($n=3$). (E) SDS-PAGE of two representative batches of aCXCL10 and a standard control antibody at three different amounts (30, 20 and 10 μ g) showed two bands. One band was present at 50 kDa (heavy chain) and the other one at 25 kDa (light chain), indicating a purified antibody.

Results

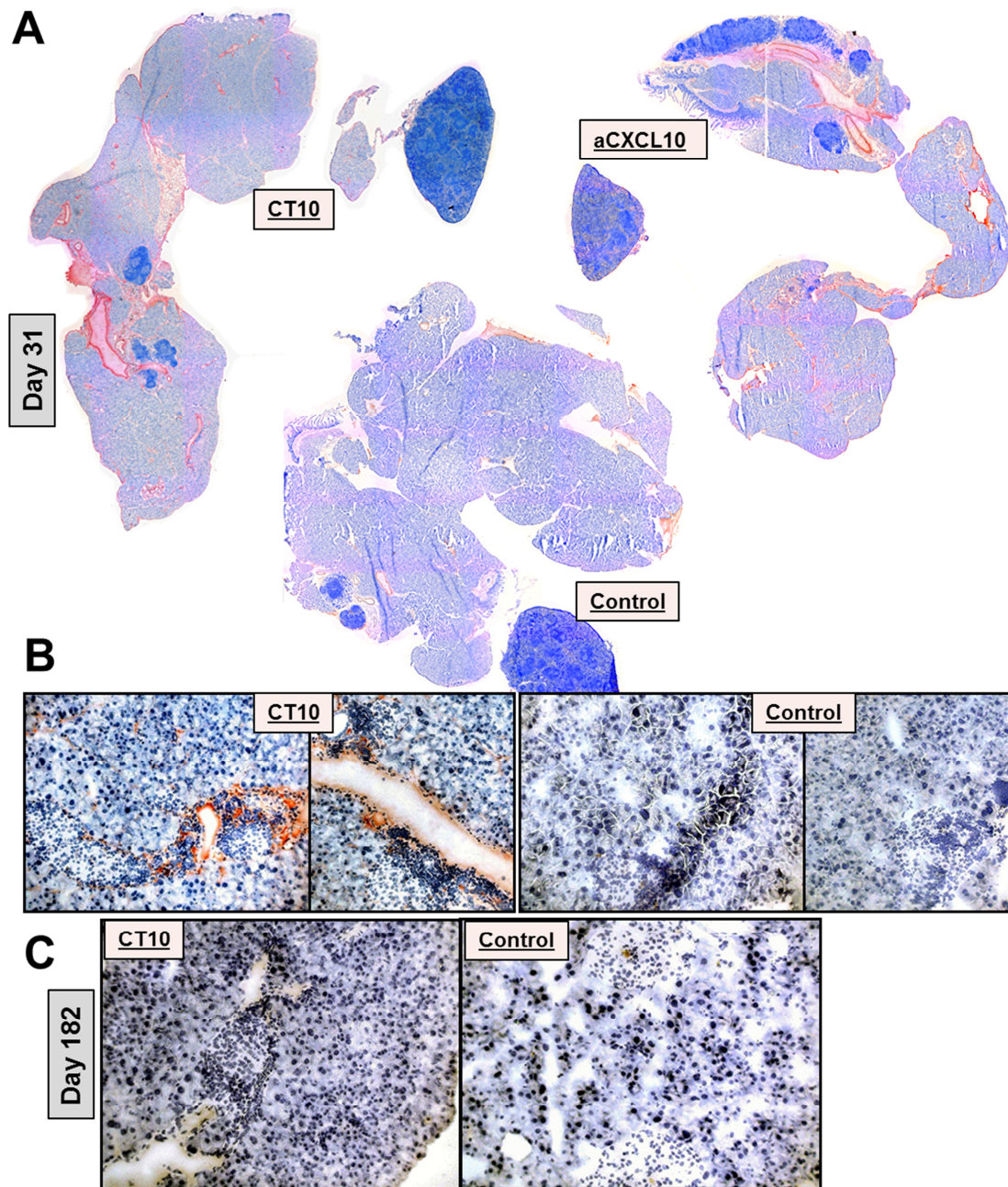


Figure 14: The injected aCXCL10 went to the infiltrates in the pancreas.

(A) Immunohistochemistry of 7 μm pancreas tissue sections from RIP-LCMV-GP mice was performed at day 31 after infection. The mice were treated with three daily injections of 3 μg aCD3 at days 10-12 post-infection and 8 injections of 100 μg aCXCL10 or isotype control from day 13-28 post-infection. Sections were stained for the injected aCXCL10 and positive staining is indicated by red-brown colour. Representative pancreas section overviews were reassembled from pictures taken at a low magnification (4x). Blow ups were taken at a higher magnification (20x) at day 31 post-infection (B) and day 182 post-infection (C).

9.2.2 CT significantly reversed T1D in the RIP-LCMV GP mouse model

Based on the previous results we designed CT as follows: RIP-LCMV-GP mice were infected with LCMV and 3 µg aCD3 were injected intravenously for three days (10-12 post-infection). Upon the next day I treated the mice eight times with 100 µg aCXCL10 or isotype control (three intraperitoneal injections/week). The last aCXCL10 injection was given at day 28 after LCMV infection (Figure 15A).

At the initiation of the therapy (day 10 after infection) most of the mice were diabetic and CT resulted in a reversion of T1D in 67 % of the mice (Figure 15B). Indeed, this effect was significantly better than the remission of T1D after the monotherapies with either aCD3 (38 %) or aCXCL10 (36 %) (Figure 15B). This reversion of T1D was long-lasting since no relapse occurred in any of the cured mice treated with CT (Figure 15B). Interestingly, before day 17 post-infection the average BG was similar between the aCD3 treated and the CT group. However, the isotype control treatment of aCD3 treated mice showed an increase in BG level after day 20, whereas CT treatment led to a steady decrease (Figure 15C). The comparison between the BG levels on day 12 (last aCD3 injection) and day 35 post-infection (one week after the last aCXCL10 dose) demonstrated that the BG levels in 70 % of CT treated mice decreased and also some highly diabetic mice (BG >500 mg/dl) returned to normoglycaemia (BG <200 mg/dl) (Figure 15D). In contrast, most of the isotype control treated mice (68 %) and aCXCL10 single therapy treated mice (71 %) displayed a massive increase in BG levels in this period of time (Figure 15D). The administration of aCD3 demonstrated a patchy result. The same frequency of mice increased (47 %) and decreased (47 %) in their BG level (Figure 15D).

Results

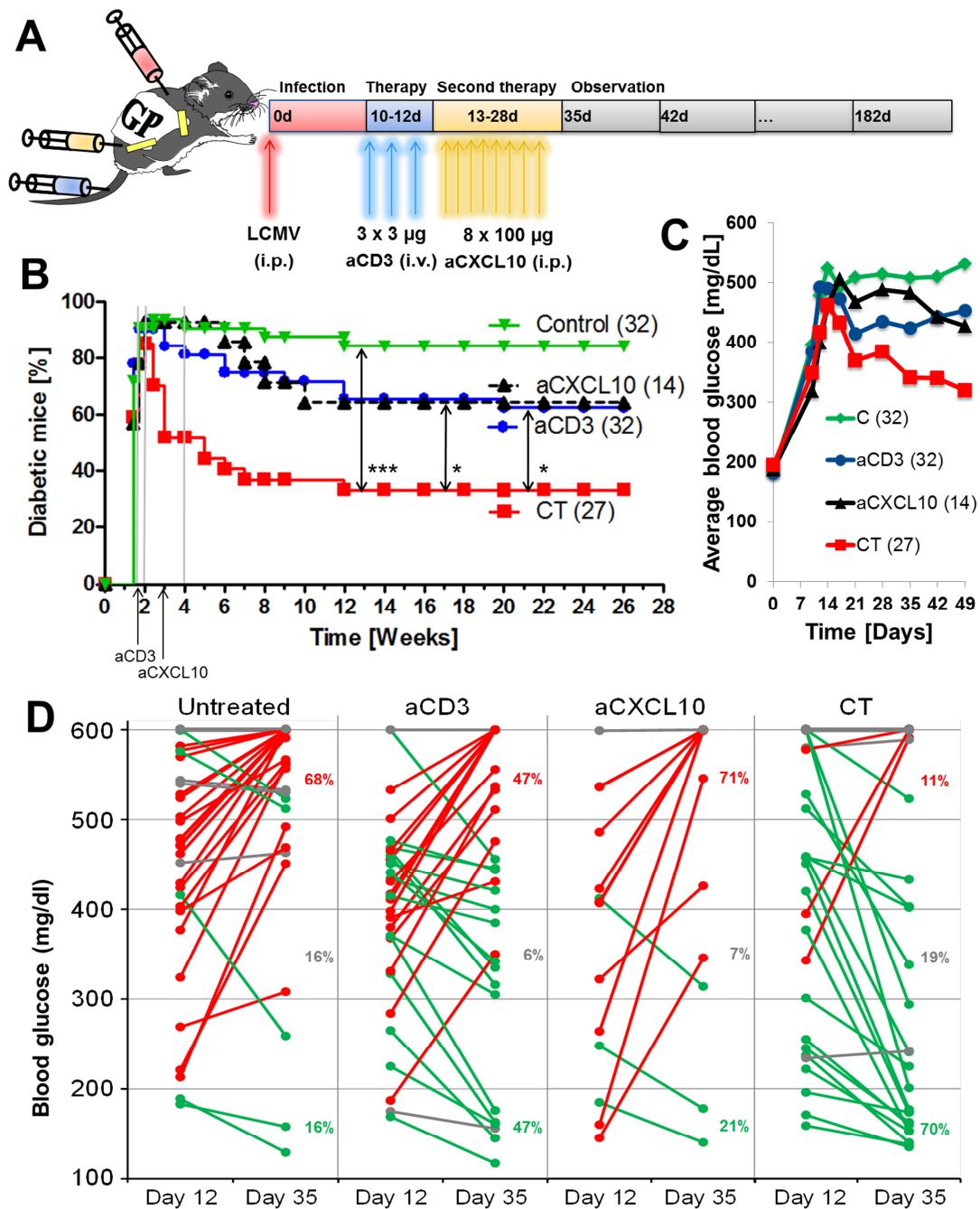


Figure 15: CT led to a remission in more mice than the monotherapies.

(A) RIP-LCMV-GP mice were infected with LCMV, treated with three daily injections of 3 μ g aCD3 at days 10-12 post-infection and 8 injections of 100 μ g aCXCL10 or isotype control from day 13-28 post-infection. (B) BG levels were determined until week 26 after infection. Mice with BG levels >300 mg/dl were considered to be diabetic and mice with a stable BG level <300 mg/dl reverted T1D. The number of mice analysed in each group is indicated in brackets. Significant differences are indicated as follows: $p < 0.05$ (*); $p < 0.01$ (**); $p < 0.001$ (***). (C) Average BG levels of each group of the first 50 days after infection are shown. (D) A comparison of BG levels was performed between day 12 (end of aCD3 treatment) and day 35 (one week after last injection) after infection. Mice that at day 35 post-infection displayed an increase in BG of >20 mg/dl are shown in red. Mice that decreased in their BG level (>20 mg/dl) or mice that showed almost the same BG level (\pm 20 mg/dl) are indicated in green or grey, respectively.

9.2.3 CT reduced the number of infiltrating T cells in the pancreas

The progression of T1D can be followed by analysing the integrity of the islets of Langerhans and their infiltration by immune cells. For that reason 7 μ m pancreas section of RIP-LCMV-GP mice treated with isotype control, aCXCL10, aCD3 or CT were stained by immunohistochemistry (11.2.1.13) for insulin, CD4 and CD8 on day 31 after infection (three days after the last aCXCL10 injection). The previous experiments revealed that less T cells were present in aCD3 treated compared to untreated mice one day after the last dose of aCD3 (day 13 post-infection) (Figure 11A). At day 31 after infection, the pancreas of mice that received the isotype control antibody showed almost no insulin producing β -cells, indicated by an absence of brown staining in the pancreas overview. Thus, the antigen presenting β -cells were destroyed and consequently the T cell had been migrated out of the pancreas (Figure 16A). Unlike isotype control treated mice, the pancreas of aCXCL10 treated mice revealed on the one hand slightly more insulin production. On the other hand a massive infiltration of T cells was present in the islets (Figure 16A). Exclusively aCD3 and CT treated mice demonstrated a marked insulin production in combination with a strongly reduced T cell infiltration (Figure 16A+B). It is important to note that only CT administration was able to protect the pancreas against the re-entry of T cells in some mice (Figure 16A).

9.2.4 Frequency and number of islet antigen-specific CD8 T cells were dramatically reduced in CT treated mice

In the RIP-LCMV-GP mouse model, the progression of the disease is predominantly mediated by a CD8 T cell response (35; 137). Thus, the isolated lymphocytes from blood, spleen, pancreatic lymph node and pancreas (11.2.1.6-11.2.1.9) of isotype control, aCXCL10, aCD3 and CT treated RIP-LCMV-GP mice were analysed at day 20 and 31 post-infection by flow cytometry after stimulation with islet (LCMV-GP)-specific peptides (11.2.1.11).

Results

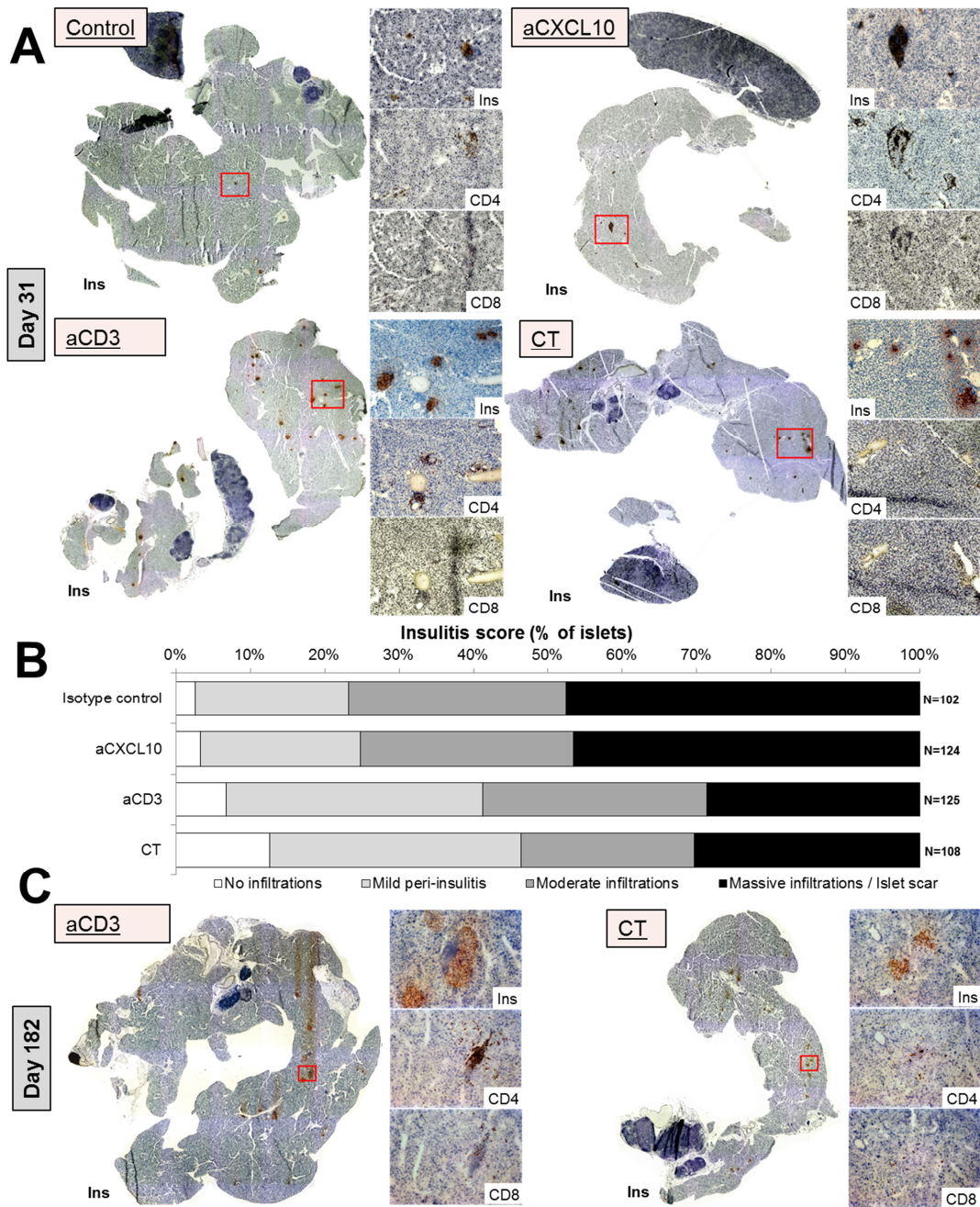


Figure 16: Immunohistochemistry sections of the pancreas revealed that the infiltration was strongly decreased in CT treated mice.

(A) Immunohistochemistry of 7 μ m pancreas tissue sections from RIP-LCMV-GP mice was performed at day 31 after infection. The mice were treated with isotype control, aCXCL10, aCD3 or CT as described above. Consecutive sections were stained for insulin (Ins), CD4 and CD8 T cells and positive staining is indicated by brown colour. Representative pancreas section overviews were reassembled from insulin pictures taken at a low magnification (4x) and blow ups were taken at a higher magnification (20x). (B) Semi-quantitative analysis of insulinitis of more than 100 individual islets from pancreas sections of four mice per group was performed. Islets were categorised into no infiltrations (white), mild peri-insulitis (<20 %, light grey), moderate infiltrations (<50 %, dark grey) and massive infiltrations (>50 %, black). Data are mean values \pm SD (n=4). (C) Immunohistochemistry of pancreas tissue sections from RIP-LCMV-GP mice at day 182 after infection is displayed.

Results

After completion of CT (day 31 after infection; 3 days after last aCXCL10 dose) the T cells were fully recovered in blood, spleen and PDLN (Figure 17A+B). In contrast to day 31, at day 20 post-infection (4 of 8 injections of aCXCL10) the frequency of CD8 T cells in blood and PDLN as well as the frequency of CD4 T cells in the spleen were still decreased (approx. 30 %) (Figure 17C). Importantly, we discovered that the frequency of islet antigen (LCMV-GP33)-specific CD8 T cells was significantly reduced by 65 % in the spleen of CT treated mice compared to the isotype control treated mice at day 20 after infection. The aCD3 monotherapy reduced the frequency of islet antigen-specific CD8 T cells by only 55 % and the treatment with aCXCL10 did not influence the T cell frequencies (Figure 17C). At day 31 after infection a comparison between the different treatment groups revealed that in aCD3 treated mice the T cells still were decreased by only 56 % compared to the frequency of isotype control treated mice (Figure 17B). In contrast, CT expanded the reduction of islet antigen-specific CD8 T cells to 73 % of isotype control treated mice in the spleen (Figure 17B), resulting a significant lower frequency of islet antigen-specific CD8 T cells compared to aCD3 administration. Moreover, in the blood and PDLN aCD3 as well as CT treatment demonstrated a similar impact on T cells (Figure 17A-C). Interestingly, except for CT, none of the treatments did significantly influence the Treg frequency either at day 20 or at day 31. After CT we detected a significant increase in the FoxP3⁺ Tregs frequency in the PDLN compared to the mice that received the isotype control at day 31 (Figure 17A+B).

In the pancreas the total number of infiltrating T cells, rather than their relative frequency, is crucial. Importantly both, aCD3 and CT treatment results in a reduced total number of CD4 and CD8 T cells at day 20 and 31. The total number of islet antigen-specific CD8 T cells was significantly diminished by 81 % in the pancreas of CT treated mice compared to isotype control treated mice at day 20. The aCD3 and aCXCL10 monotherapies reduced the frequency of islet antigen-specific CD8 T cells by only 66 % and 49 %, respectively (Figure 17C). Importantly, at day 31 after infection the total number of islet antigen-specific CD8 T cells was diminished after aCD3 administration by just 23 % of the number obtained from isotype control treated mice (Figure 17B).

Results

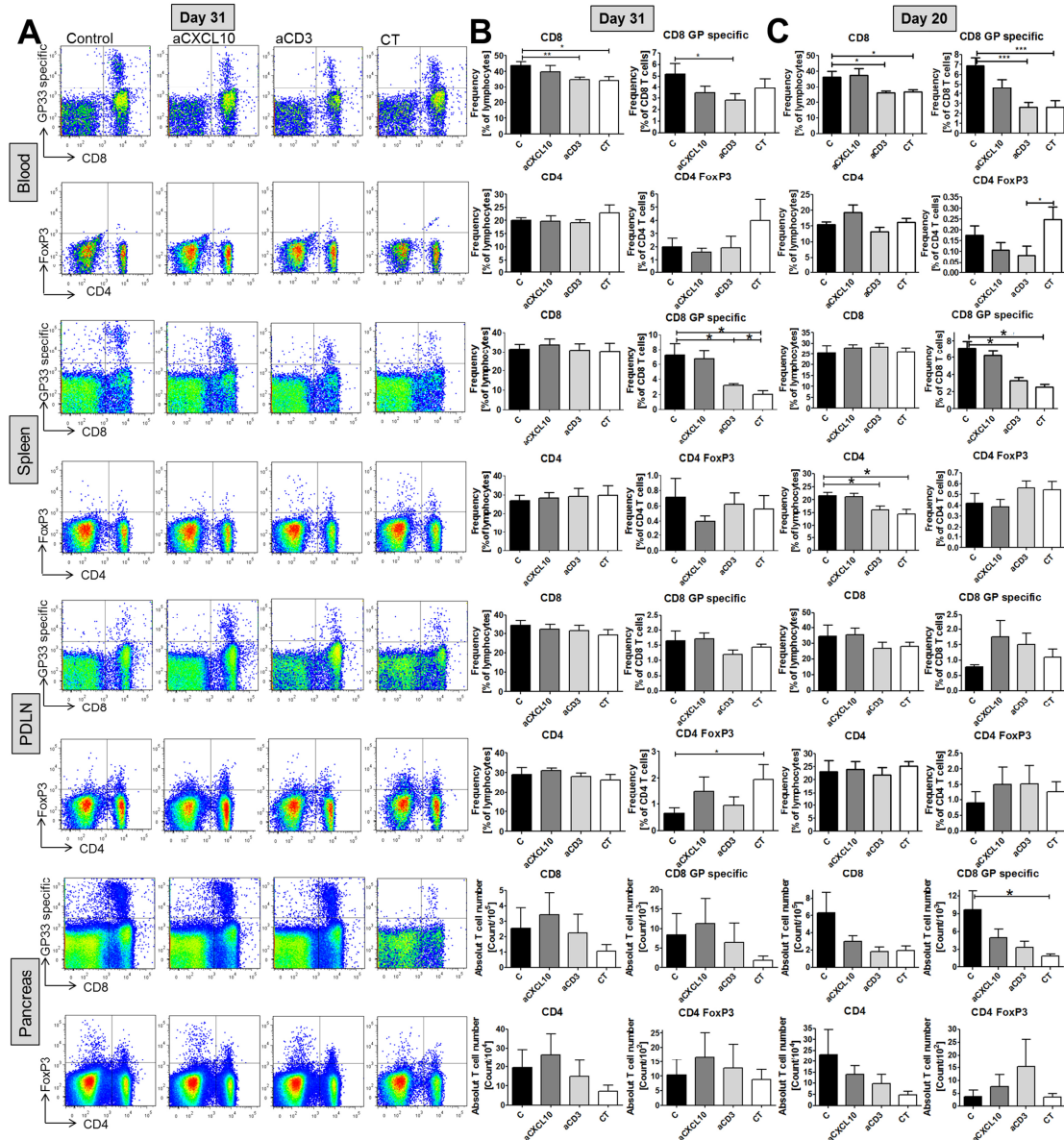


Figure 17: Flow cytometry analysis showed that the frequency and number of islet antigen-specific T cells was significantly decreased in CT treated mice.

The mice were treated with isotype control, aCXCL10, aCD3 or CT and samples of blood, spleen, PDLN and pancreas were removed at day 20 and 31 after infection. After lymphocyte isolation, the frequency of CD4 T cells, CD8 T cells, FoxP3⁺ CD4 T cells and antigen (LCMV-GP33)-specific CD8 T cells were analysed by flow cytometry. In the pancreas the absolute T cell number of infiltrating cells was more important. Frequencies of islet antigen (LCMV-GP33)-specific CD8 T cells in blood, spleen and PDLN and their absolute number in the pancreas were obtained by stimulation of isolated lymphocytes with LCMV-GP33 followed by intracellular IFN γ staining and flow cytometry. (A) Representative dot blots from flow cytometry of lymphocytes harvested at day 31 post-infection are shown. At day 31 (B) and 20 (C) after infection, the frequencies and absolute number of CD4 T cells, CD8 T cells, FoxP3⁺ CD4 T cells and RIP-LCMV-GP33-specific CD8 T cells are displayed. Data are mean values \pm SD (day 31: n=6-13; day 20: n=10). Significant differences are indicated as follows: p < 0.05 (*); p < 0.01 (**); p < 0.001 (***)

Results

Thus, it seemed that in monotherapy treated mice the T cells re-entered the pancreas. Strikingly at day 31 after infection the T cells did not recover after CT in the pancreas and still 78 % of islet antigen-specific CD8 T cells were inactivated (Figure 17B).

IFN γ is one of the first cytokines produced by T cells after stimulation, whereas TNF α is produced later. Accordingly, experienced CD8 T cells express both IFN γ and TNF α (79; 138; 139). At day 20 post-infection most of the IFN γ producing islet antigen-specific T cells produce also TNF α (77 %) after stimulation with the immunodominant LCMV epitope GP33 in the spleen (Figure 18A+B). Similar results were obtained in blood (86 % double positive (dp) T cells) and PDLN (53 % dp T cells). Unlike aCD3 treatment, CT demonstrated a small significant reduction of approx. 20 % of double positive T cells in the spleen, blood and PDLN (59 %, 65 % or 34 % dp T cells, respectively) (Figure 18A+B). In contrast, in the pancreas only 33 % of IFN γ producing T cells also generated TNF α in isotype control treated mice. However, this frequency was dramatically reduced to 6 % in the pancreas of CT treated mice (Figure 18A+B). Such a low frequency of TNF α -producing T cells indicates that most of the islet antigen-specific T cells have been only recently activated and therefore might originate from a T cell pool that has regenerated after aCD3 treatment.

At day 31 after infection an *in vivo* cytotoxicity assay was performed. We assumed that this cytotoxicity assay would show a reduced killing of islet peptide loaded splenocytes in CT treated mice due to less cytotoxic T cells. The splenocytes were isolated from C57BL/6 mice, split into two equal aliquots and labelled with either a high carboxyfluorescein succinimidyl ester (CFSE^{hi}) concentration or a low CFSE (CFSE^{lo}) concentration. Islet antigen GP33 loaded CFSE^{lo} splenocytes and an equal amount of unloaded CFSE^{hi} splenocytes were transferred into LCMV-infected mice that had been treated with CT, aCD3, aCXCL10 or isotype control (11.2.3.4). The ratio of CFSE^{lo} and CFSE^{hi} splenocytes was calculated at several points of time (Figure 19A+B).

The mice that received the isotype control antibody or aCXCL10 revealed a marked reduction of islet antigen loaded target cells after 6 h (43 %; 51 %

Results

respectively) and after 24 h only almost all target cells were destroyed (10 %; 8 % respectively) (Figure 19A+B). In contrast, CT and aCD3 therapy prolonged the survival of injected target cells. Almost no target cells were killed in CT treated mice after 6 h and a notable number survived more than 24 h (19 % of target cells) (Figure 19A+B). This indicated a reduced islet antigen-specific cytotoxicity after CT. Looking at the half-life of antigen loaded target cells, it becomes clear that indeed CT had a strong impact on the islet specific immune response and the half-life was significantly increased (13 h half-life) compared to the half-life in the isotype control treated mice (6 h half-life) (Figure 19C). The treatment with aCD3 alone had an intermediate impact and prolonged the half-life of injected target cells to 9 h.

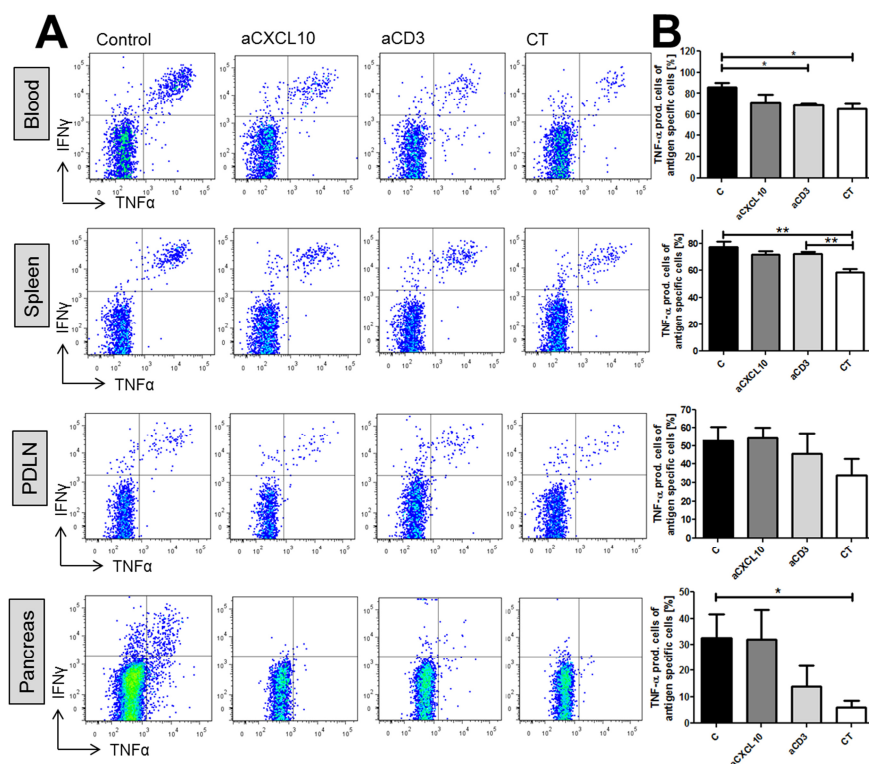


Figure 18: aCD3 administration led to less experienced CD8 T cells indicated by a lower TNF α production.

RIP-LCMV-GP mice were treated with isotype control, aCXCL10, aCD3 or CT and samples of blood, spleen, PDLN and pancreas were removed at day 20 post-infection. Frequencies of islet antigen (LCMV-GP33)-specific CD8 T cells in blood, spleen and PDLN were obtained by stimulation of isolated lymphocytes with LCMV-GP33 followed by intracellular IFN γ staining and flow cytometry. (A) Representative dot plots from flow cytometry of lymphocytes harvested at day 20 after infection are shown. (B) The ratio of GP33-specific TNF α ⁺ CD8 T cells was calculated. Data are mean values \pm SD (n=5). Significant differences are indicated as follows: p < 0.05 (*); p < 0.01 (**); p < 0.001 (***)

Results

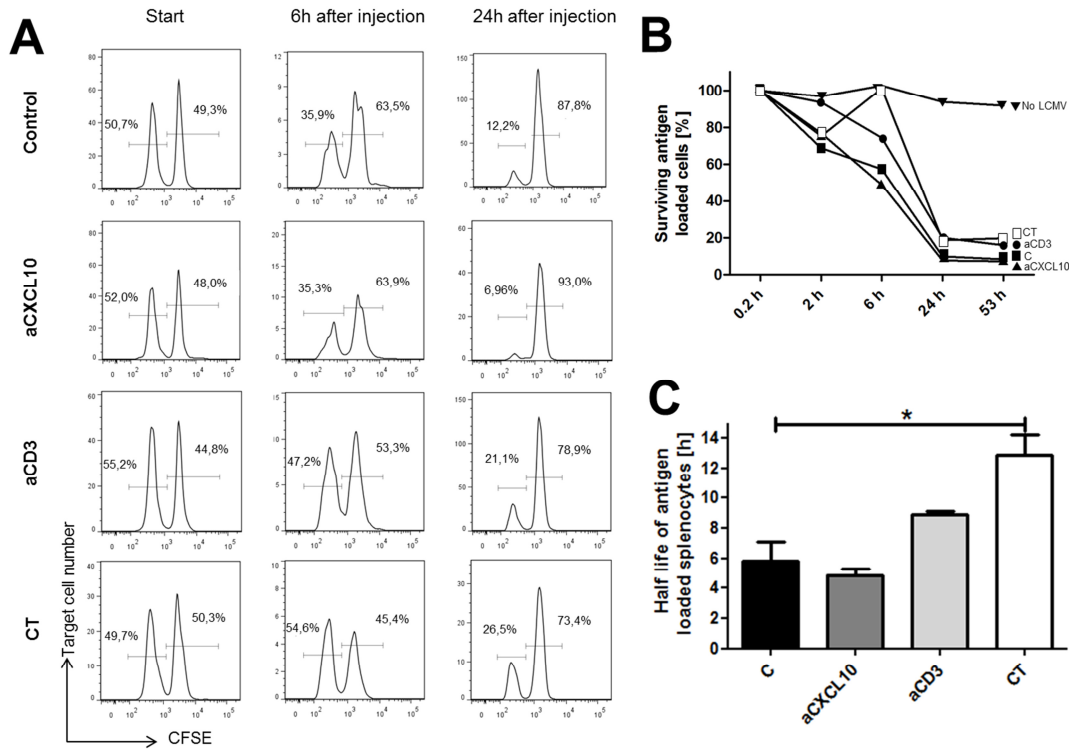


Figure 19: CT reduced the islet specific cytotoxic potential.

Splenocytes from uninfected C57BL/6 mice were isolated and loaded with the immunodominant CD8 peptide GP33 or left unloaded and labelled either with a low (CFSE^{lo}; peptide loaded) or high (CFSE^{hi}; unloaded) concentration CFSE. These two populations were mixed at a 1:1 ratio and injected into isotype control, aCXCL10, aCD3 or CT treated RIP-LCMV-GP mice at day 31 after infection. Blood samples were taken after 10 min, 2h, 6h, 24h and 48h after injection and the isolated lymphocytes were analysed by flow cytometry. (A) Representative histograms from flow cytometry are displayed. (B) The ratio of CFSE^{lo}/CFSE^{hi} was calculated and normalised to the ratio at the injection of target cells (10 min post-injection). (C) The half-life of target cells after injection is displayed. Data are mean values \pm SD (n=2-4). Significant differences are indicated as follows: $p < 0.05$ (*); $p < 0.01$ (**); $p < 0.001$ (***)

In summary after completion of CT the overall T cell frequency was similar in all groups, which indicated a restored immune response after aCD3-mediated inactivation. However, CT treated mice had a lower frequency of islet antigen-specific T cells in blood, spleen as well as PDLN and the general infiltration in the pancreas was dramatically reduced in contrast to monotherapies and isotype control treated mice. Indeed, when comparing the total number islet antigen-specific T cells in the pancreas, it becomes clear that a re-entry of islet antigen-specific CD8 T cells was only prevented with CT.

9.2.5 The remaining islet antigen-specific T cells in CT and aCD3 treated mice were less active.

CT treated mice showed a reduced cytotoxicity, due to a systemic lower number of islet antigen-specific T cell. However, it might be that the activity of islet antigen-specific T cells was also diminished. Therefore, the flow cytometry data at day 13, 20 and 31 post-infection from Figure 10 and Figure 17 was re-analysed. The IFN γ producing T cells were divided into two groups and the ratio of highly IFN γ producing (intensity over 10^4) and low IFN γ producing (intensity below 10^4) T cells was calculated.

One day after aCD3 challenge most of the highly active T cells were inactivated in the spleen, PDLN and pancreas, indicated by a reduced IFN γ high to IFN γ low ratio (Figure 20A). This effect continued till day 20 after infection in aCD3 as well as CT treated mice (Figure 20A). However, at day 31 post-infection the ratio of IFN γ high to IFN γ low CD8 T cells in the PDLN and pancreas was similar to the ratio in isotype control treated mice. Merely, in the spleen a significant reduction of the IFN γ high to IFN γ low ratio in the aCD3 and CT treated mice was observed (Figure 20A). Nevertheless, there was no difference at any point of time in the ratio of IFN γ high to IFN γ low CD8 T cells between CT and aCD3 administration indicating aCD3 dependent effect.

Moreover, I found that the aCD3 action was not confined to the depletion of T cells, it also inactivated T cells in our mouse model. After stimulation of T cells with the islet antigen GP33, the IFN γ production indicated active islet antigen-specific T cells and the tetramer also labelled islet antigen-specific T cells that did not produce IFN γ , due to an aCD3 mediated inactivation. 29 % of the islet antigen (LCMV-GP33)-specific T cells were depleted with 3 μ g aCD3. In contrast, 39 % were only inactivated one day after the last aCD3 dose (Figure 20B). The high dose of aCD3 resulted in a similar inactivation and depletion (38 % and 36 % respectively) of the islet antigen-specific T cells (Figure 20B). Seven days later (day 20 post-infection) the frequency of activated islet antigen-specific T cells increased to 42 % in mice treated with 3 μ g aCD3 (Figure 20B), which indicated a regeneration of T cells. Interestingly, the addition of aCXCL10 halted the increase of activated islet antigen-specific T cells (33 %).

Results

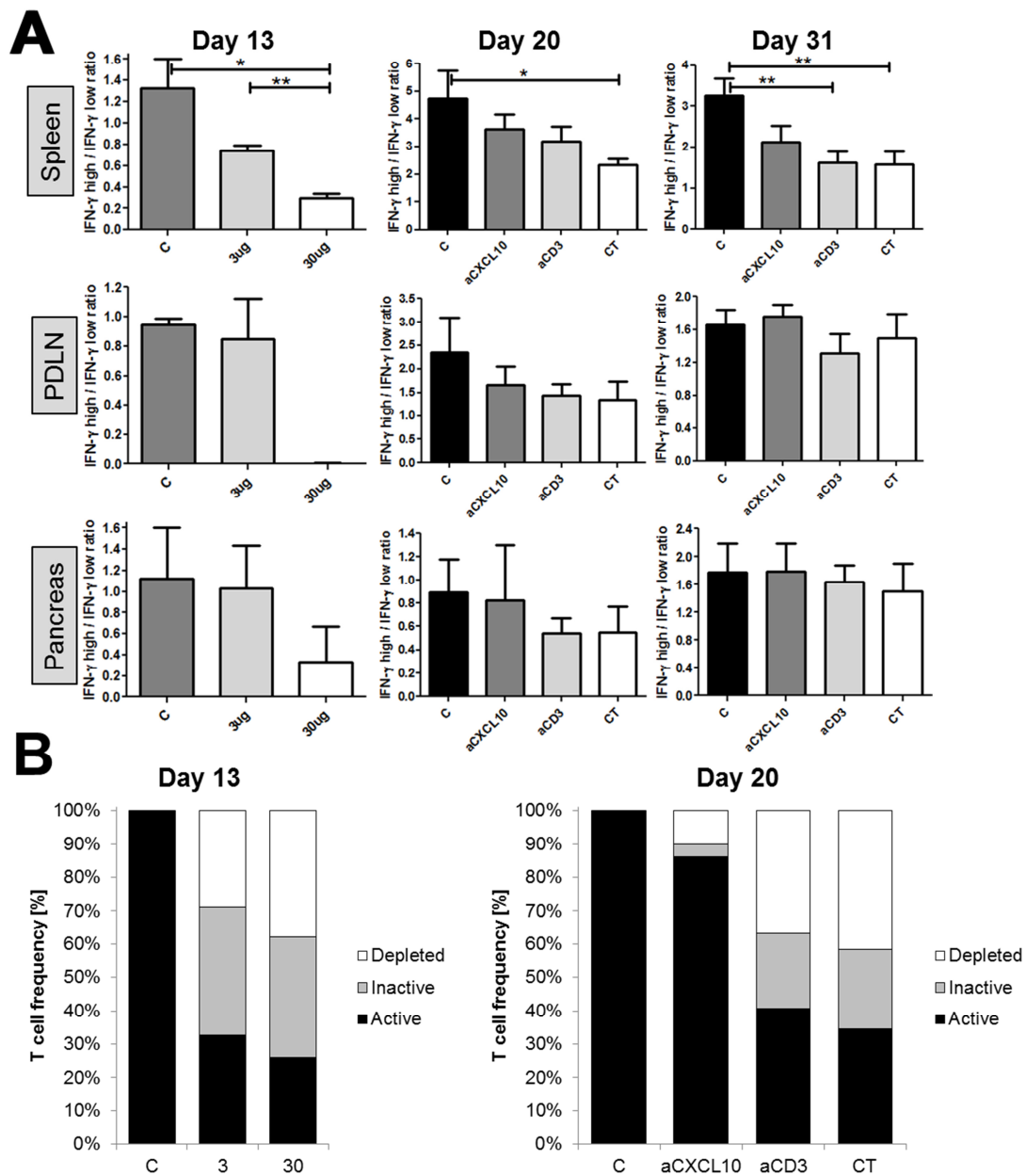


Figure 20: A reduced activity of remaining T cells was shown after aCD3 treatment.

(A) RIP-LCMV-GP mice were treated with isotype control, aCXCL10, aCD3 or CT and samples of blood, spleen, PDLN and pancreas were removed at day 13, 20 and 31 after infection. Frequencies of islet antigen (LCMV-GP33)-specific CD8 T cells in blood, spleen and PDLN and pancreas were obtained by stimulation of isolated lymphocytes with LCMV-GP33 followed by intracellular IFN γ staining and analysing by flow cytometry. The ratio of high active (IFN γ high; intensity over 10^4) and less active (IFN γ low; intensity below 10^4) islet antigen (LCMV-GP33)-specific CD8 T cells was calculated. Data are mean values \pm SD (day 31: n=6-13; day 20: n=10). Significant differences are indicated as follows: p < 0.05 (*); p < 0.01 (**); p < 0.001 (***). (B) At day 13 and 20 the frequency of depleted (white; 100 % - tetramer specific), inactive (grey; tetramer specific - IFN γ^+) and active (black; IFN γ^+) T cells was determined.

9.2.6 None of the treatments impaired the migration potential

We assumed that the reduced migration into the pancreas is not dependent on a diminished inherent migration potency of T cells. To confirm this I isolated splenocytes from mice treated with CT, aCD3, aCXCL10 or isotype control and performed a migration assay along a CXCL10 gradient at day 20 post-infection (11.2.1.5). 0 mM, 20 mM, 40 mM CXCL10 were used in the lower chamber and the frequencies of migrated T cells were analysed by flow cytometry before and after the migration assay.

The CD8 T cell migration was more influenced by the CXCL10 gradient than CD4 T cell migration (Figure 21A+B). However, the migration of both CD4 and CD8 T cells was CXCL10 dependent. Importantly, the migration potential of the various treatment groups was undistinguishable indicated by a similar 1.5-fold increase of the CD8 T cell frequency using 40 mM CXCL10 in all groups (Figure 21A+B). In addition, the frequency of islet antigen-specific T cells of total CD8 T cells did not change with different CXCL10 concentrations in all treatment groups. Consequently, the migration potential of the islet antigen-specific T cell was similar to general CD8 T cells and the treatment with aCD3 and/or CXCL10 did not influence it (Figure 21C).

9.2.7 CT resulted in a long-lasting remission of T1D

The remission of T1D was long-lasting since many insulin producing islets were detectable in the pancreas of both CT and aCD3 treated mice after 182 days (Figure 16C). However, immunohistochemistry revealed that a re-infiltration of T cells was only blocked in after CT indicated by infiltrates around the islets of aCD3 treated mice (Figure 16C).

Due to less insulin production the isotype control treated mice had to be sacrificed before reaching day 182 post-infection. For that reason only the T cell frequencies in blood, spleen, PDLN and the absolute number in the pancreas of cured aCD3 and CT treated mice were analysed by flow cytometry at day 182 post-infection. I found no significant difference in T cell frequencies and number

Results

beside a slightly lower frequency of CD8 T cells in the blood after CT (Figure 22A+B). Importantly, CT treatment resulted in a protective milieu in the pancreas indicated by a 4 fold increased Treg / Teff ratio compared to aCD3 treated mice (Figure 22C).

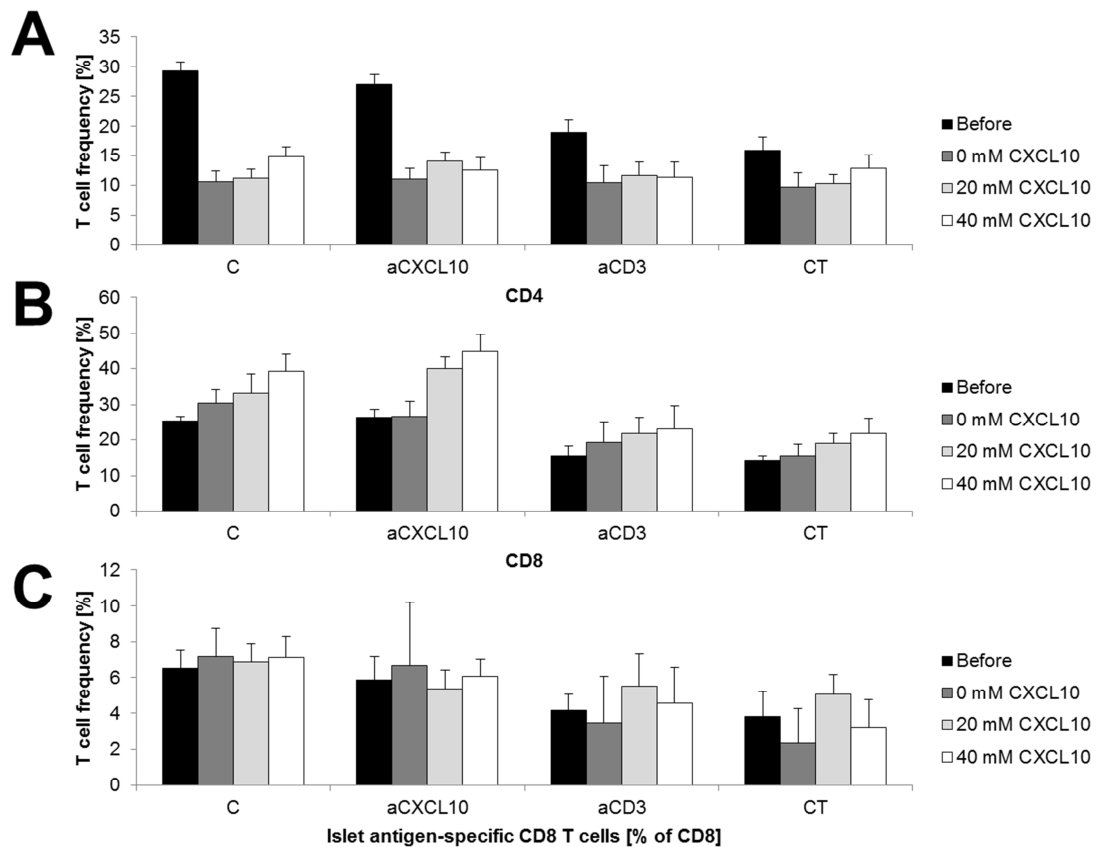


Figure 21: The T cells of CT, aCD3 aCXCL10 and isotype control treated mice were undistinguishable in their migration potential.

RIP-LCMV-GP mice were treated with isotype control, aCXCL10, aCD3 or CT and the spleen was removed at day 20 after infection. After splenocytes isolation, a migration assay was performed with 20 mM (light grey) or 40 mM (white) CXCL10 gradient or without CXCL10 (dark grey). Before (black) and after the migration assay, the frequency of CD4 T cells (A), CD8 T cells (B) and RIP-LCMV-GP33-specific CD8 T cells (C) were analysed by flow cytometry. Data are mean values \pm SD (n=5).

Results

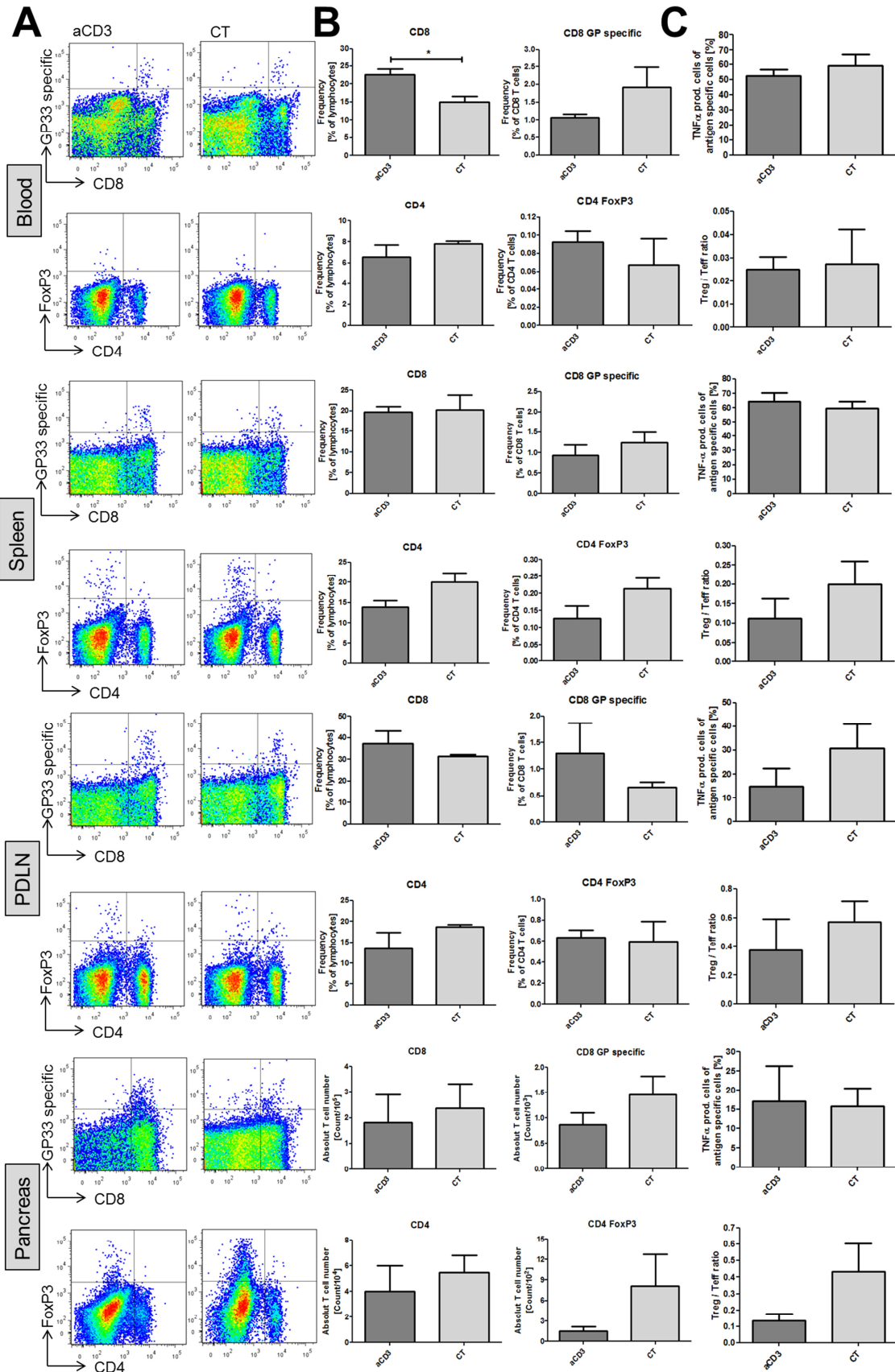


Figure 22: CT increased the Treg / Teff ratio in the pancreas of RIP-LCMV-GP mice.

Figure is displayed on the previous page. The mice were treated with isotype control, aCXCL10, aCD3 or CT and samples of blood, spleen, PDLN and pancreas were removed at day 182 post-infection. After lymphocyte isolation, the frequency of CD4 T cells, CD8 T cells, FoxP3⁺ CD4 T cells and islet antigen (GP33)-specific CD8 T cells were analysed by flow cytometry. In the pancreas the absolute T cell number of infiltrating cells was more important. Frequencies of islet antigen (GP33)-specific CD8 T cells in blood, spleen and PDLN and their absolute number in the pancreas were obtained by stimulation of isolated lymphocytes with LCMV-GP33 followed by intracellular IFN γ staining and flow cytometry. (A) Representative dot blots from flow cytometry are shown. (B) The frequencies and absolute number of CD4 T cells, CD8 T cells, FoxP3⁺ CD4 T cells and islet antigen (GP33)-specific CD8 T cells are displayed. (C) In addition, the ratio of islet antigen (GP33)-specific TNF α ⁺ CD8 T cells and Treg to Teff was calculated. Data are mean values \pm SD (n=4-5). Significant differences are indicated as follows: p < 0.05 (*); p < 0.01 (**); p < 0.001 (***).

9.2.8 The deficiency of CXCL10 reduced severity of T1D and thereby it created the basis to cure the majority of mice

By using CXCL10-deficient RIP-LCMV-GP mice we wanted to demonstrate the importance of CXCL10 on T1D and its influence on aCD3 therapy. Therefore, regular RIP-LCMV-GP mice were crossed with CXCL10-deficient mice (140). Homozygous CXCL10^{-/-} x RIP-LCMV-GP and CXCL10^{+/+} x RIP-LCMV-GP littermates were infected with LCMV and 3 μ g aCD3 were administered three times from day 10 to 12 post-infection or the mice were left untreated. CXCL10^{+/+} x RIP-LCMV-GP mice with or without aCD3 treatment behaved like regular RIP-LCMV-GP mice (Figure 15B) and resulted in 30 % and 10 % reversion of T1D, respectively (Figure 23). Two weeks after infection, a similar frequency of CXCL10^{-/-} x RIP-LCMV-GP mice developed T1D (70 %). Interestingly, almost half of them reverted T1D spontaneously, which resulted in a T1D incidence of 40 % at week 12 (Figure 23). It has to be noted that administration of aCD3 led to a 100 % reversion of this mild T1D in CXCL10^{-/-} x RIP-LCMV-GP mice within 8 weeks (Figure 23). This effect was even stronger than the impact of CT with aCXCL10. However, mice that received aCXCL10 showed an absence of CXCL10 only after T1D onset in contrast to mice with a CXCL10 deficiency, whose CXCL10 level was permanently reduced. Thus, this data indicated that CXCL10 had a strong impact on the course of T1D and it also showed the high potential of a combination of T cell inactivation with aCD3 together with a blockade of the T cell migration through a reduction of CXCL10.

Results

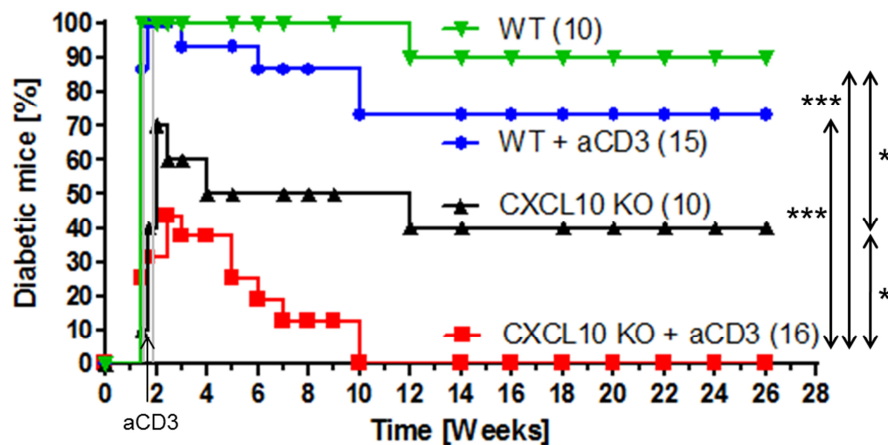


Figure 23: aCD3 cured all mice in the absence of CXCL10.

RIP-LCMV-GP mice (WT) and CXCL10-deficient RIP-LCMV-GP mice (CXCL10 KO) were infected with LCMV and treated with three daily injections of 3 μ g aCD3 at days 10-12 post-infection or mice were left untreated. BG levels were determined until week 26 after infection. Mice with BG levels >300 were considered to be diabetic and mice with a stable BG level <300 reverted T1D. The number of mice analysed in each group is indicated in brackets. Significant differences are indicated as follows: $p < 0.05$ (*); $p < 0.01$ (**); $p < 0.001$ (***)

9.2.9 CT reverted T1D in diabetic NOD mice

In order to confirm the results of the RIP-LCMV-GP model I used the well-established spontaneous diabetic NOD mouse model which is a mechanistically different T1D mouse model. These mice have a genetic polymorphism that is linked to the IL-2 production (141; 142) and a mutation in the CTLA-4 region (143). This resulted in the development of T1D in 55 % of the mice within 15-30 weeks (Figure 24A). First the aCD3 dose needed for the inactivation of almost half of all T cells was determined. Thus, diabetic female NOD mice were treated three times with 3 μ g, 10 μ g or 30 μ g aCD3. One day after the last aCD3 dose the T cells in the blood were analysed by flow cytometry.

This experiment revealed that in NOD mice 30 μ g aCD3 per mouse were needed for the inactivation of more than 50 % of the CD4 T cells. Interestingly, this dose of aCD3 showed only a minor impact on CD8 T cells (Figure 24B), similar to the 3 μ g aCD3 dose in the RIP-LCMV-GP model.

Consequently, I treated female NOD mice one week after turning diabetic (BG level >300 mg/dl) three times with 30 μ g aCD3 and then eight times with 100 μ g aCXCL10 or isotype control antibody (Figure 24C).

I found that all of the NOD mice stayed diabetic after administration of an isotype control antibody and that the aCD3 treatment only cured 30 % of female NOD mice. Importantly, there was a strong tendency that CT improved the effect of the monotherapy, indicated by a reversion of T1D in 55 % of NOD mice.

9.2.10 CT preserved the β -cell function, but the islets in the pancreas were still covered with infiltrates

Similar to the RIP-LCMV-GP mouse model, I also wanted to investigate the T cell response and insulin production directly in the pancreas. Therefore, 7 μ m pancreas sections of NOD mice treated with isotype control, aCD3 or CT were stained by immunohistochemistry (11.2.1.13) for insulin, CD4 and CD8 on day 21 after the first aCD3 dose (three days after the last aCXCL10 injection).

The islets of NOD mice were different to those of RIP-LCMV-GP mice (Figure 16). On the one hand NOD islets seemed to be larger, but on the other hand they were reduced in number. In addition, the number of infiltrated T cells around the islets was highly elevated in NOD mice (Figure 25). Even one day after a three days treatment with 30 μ g aCD3 (Figure 25A), a remarkable number of T cells was still present around the islets. Nevertheless, some islets of mice treated with aCD3 or CT only showed mild peri-insulinitis compared to the isotype control treated mice and 21 days after the first aCD3 dose the β -cells still produced insulin (Figure 25A+B). In contrast, in isotype control treated mice the β -cells were fully destroyed resulting in a disappearance of infiltrating T cells due to a lack of antigen (Figure 25B). Unfortunately, CT showed no clear benefit compared to aCD3 monotherapy 21 days and 182 days after the first aCD3 dose indicated by similar infiltration (Figure 25B+C+D). For that reason the T cell subtypes in the infiltrates were investigated by flow cytometry.

Results

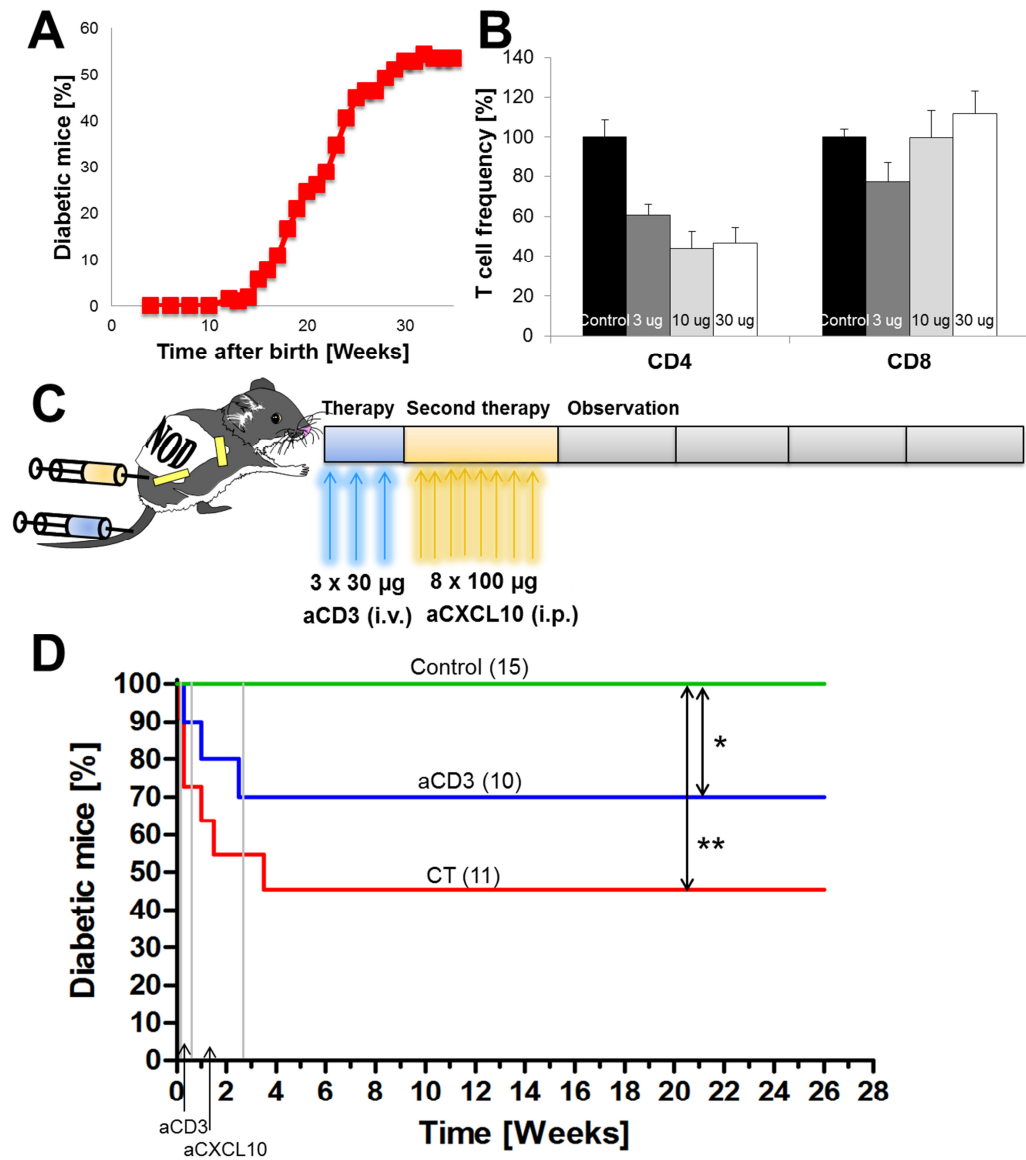


Figure 24: CT exceeded the effect of aCD3 treatment in NOD mice.

(A) The BG levels of NOD mice were determined once a week and mice with BG levels >300 were considered to be diabetic. (B) Diabetic NOD mice were treated with three daily injections of 3, 10, 30 µg aCD3 at days 0-2 after T1D onset and the relative blood CD4 and CD8 T cell frequencies were evaluated at day 3 after therapy began. (C) Diabetic NOD mice were treated with three daily injections of 30 µg aCD3 at days 0-2 after T1D onset and eight injections of 100 µg aCXCL10 or isotype control from day 3-18 after the initiation of the therapy. (D) BG levels were determined until week 26 after the therapy was initiated. Mice with BG levels >300 were considered to be diabetic and mice with a stable BG level <300 reverted autoimmune diabetes. The number of mice analysed in each group is indicated in brackets. Significant differences are indicated as follows: $p < 0.05$ (*); $p < 0.01$ (**); $p < 0.001$ (***)

Results

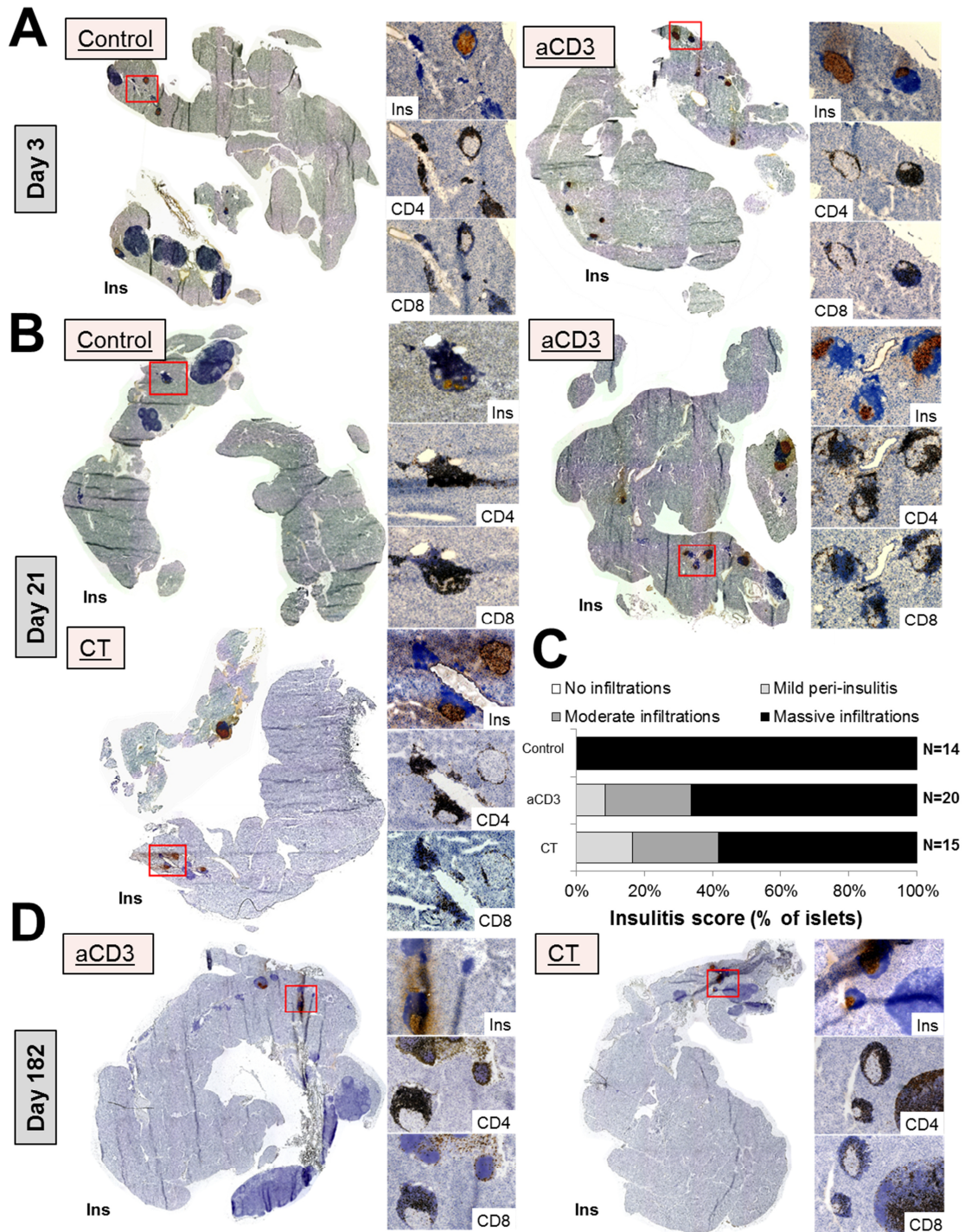


Figure 25: Immunohistochemistry revealed a preserved insulin production after CT and aCD3 administration in NOD mice.

Immunohistochemistry of pancreas tissue sections from NOD mice at day 3 (A), 21 (B) and 182 (D) after T1D onset was performed. The mice were treated with isotype control, aCD3 or CT as described above. Consecutive sections were stained for insulin (Ins), CD4 and CD8 T cells and positive staining is indicated by brown colour. Representative pancreas section overviews were reassembled from insulin pictures taken at a low magnification (4x) and blow ups were taken at a higher magnification (10x). (C) Semi-quantitative analysis of insulinitis of more than 100 individual islets from pancreas sections of three mice per group was performed. Islets were categorised into no infiltrations (white), mild peri-insulinitis (<20 %, light grey), moderate infiltrations (<50 %, dark grey) and massive infiltrations (>50 %, black).

9.2.11 CT treated mice showed a slight impact on Teff and Treg frequency

The lymphocytes from blood, spleen, PDLN and pancreas (11.2.1.6-11.2.1.9) of isotype control, aCD3 and CT treated NOD mice were isolated at day 21 after the initiation of the therapy. Afterwards the T cells were analysed by flow cytometry after stimulation with islet (NRP-V7)-specific peptide (11.2.1.11) and staining for CD4, CD8, FoxP3 (Treg), TNF α and IFN γ (islet antigen-specific T cells).

In contrast to the LCMV-GP model only 8-15 % of the IFN γ producing islet antigen-specific T cells also produced TNF α after stimulation with the immunodominant islet epitope NRP-V7 at day 21 after the initiation of the therapy (Figure 26A+B). The administration of CT or aCD3 showed no significant reduction of IFN γ / TNF α double positive T cells in blood and PDLN (Figure 26A+B). However, in the spleen and in the pancreas the frequency was dramatically reduced to 2 % in CT and aCD3 treated mice (Figure 26A+B). Similar to the RIP-LCMV-GP model, such a low frequency of TNF α -producing T cells indicated that most of the islet antigen-specific T cells had been only recently activated and therefore might originate from a T cell pool that regenerated after aCD3 treatment.

Results

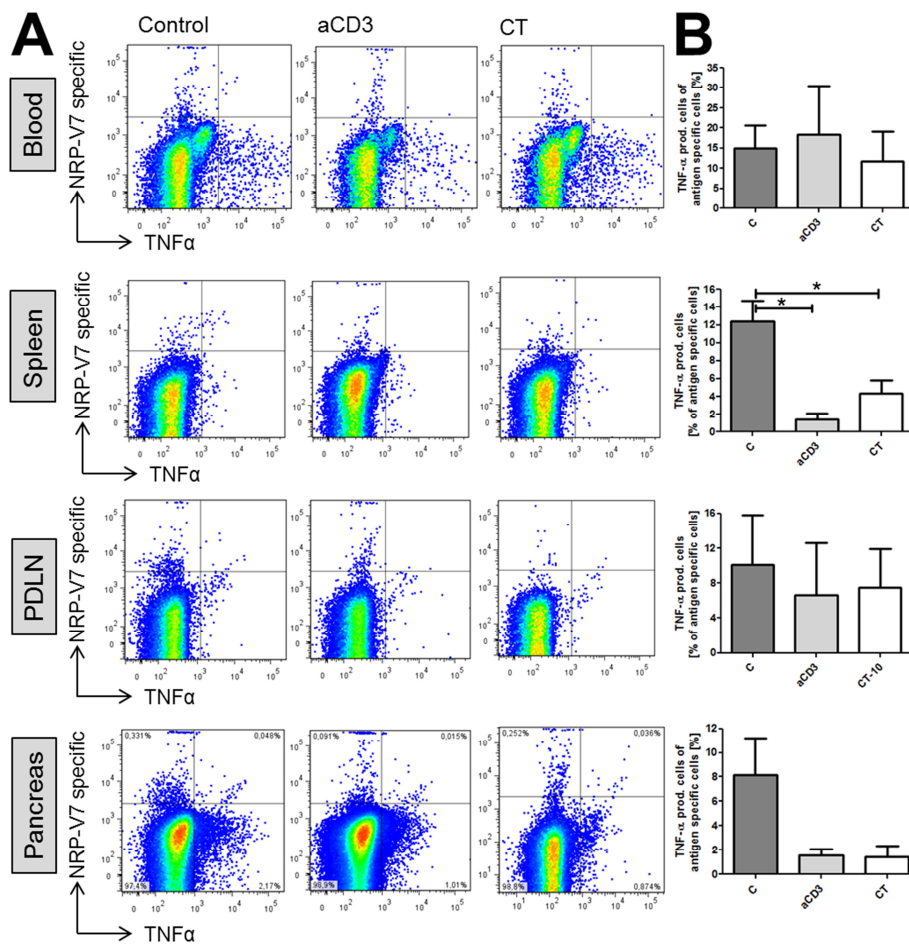


Figure 26: Less experienced CD8 T cells were present after aCD3 administration in NOD mice indicated by a lower TNF α production.

The NOD mice were treated with isotype control, aCD3 or CT and samples of blood, spleen, PDLN and pancreas were removed at day 21 after the initiation of the therapy. Frequencies of islet antigen (NRP-V7)-specific CD8 T cells in blood, spleen and PDLN as well as their absolute number in the pancreas were obtained by stimulation of isolated lymphocytes with the islet peptide NRP-V7 followed by intracellular IFN γ staining. (A) Representative dot blots from flow cytometry of lymphocytes harvested at day 21 after T1D onset are shown. (B) The ratio of NRP-V7-specific TNF α ⁺ double positive CD8 T cells was calculated. Data are mean values \pm SD (n=4-6). Significant differences are indicated as follows: p < 0.05 (*); p < 0.01 (**); p < 0.001 (***).

After completion of CT (day 21 after the first aCD3 dose) the CD8, but not the CD4, T cells were fully regenerated in blood, spleen and PDLN (Figure 27B). Unfortunately, I found no significant difference for islet antigen-specific or FoxP3⁺ regulatory T cells, due to the low number of investigated mice and high standard deviation. However, a strong tendency was observed after CT similar to RIP-LCMV-GP mice. The frequency of islet antigen-specific CD8 T cells was

Results

reduced in blood, spleen and PDLN of CT treated mice compared to the isotype control treated mice at day 21 after the first aCD3 dose by 92 %, 45 % or 75 %, respectively (Figure 27A+B). Similarly, the aCD3 monotherapy resulted in a reduction of the islet antigen-specific CD8 T cell frequency in the spleen and PDLN by 58 % and 84 %, respectively. In contrast, in the blood the inactivation of islet antigen-specific CD8 T cells in aCD3 treated mice was less pronounced than in CT treated mice (44 % reduction) (Figure 27A+B). Interestingly, the total number of islet antigen-specific CD8 T cells in the pancreas showed a marked reduction of 57 % in CT treated mice compared to aCD3 monotherapy (Figure 27A+B).

I found a low frequency and number of FoxP3⁺ CD4 T cells in general. Nevertheless, the frequency and the number of FoxP3⁺ CD8 T cells were more prominent. Accordingly, I focused on FoxP3⁺ CD8 T cells which were analysed in blood, spleen, PDLN and pancreas. CT demonstrated a strong tendency for an increase in FoxP3⁺ regulatory CD8 T cells. For instance I found a 2.9-fold, 2.6-fold or 3.9-fold increase in FoxP3⁺ regulatory CD8 T cells after CT compared to mice that received the isotype control antibody in blood, spleen and PDLN, respectively (Figure 27A+B). This effect was not observed in the RIP-LCMV-GP mouse model. In contrast, the aCD3 monotherapy could not induce FoxP3⁺ regulatory T cells in the spleen and PDLN. However, the FoxP3⁺ regulatory T cells frequency was increased 2.8-fold in the blood of aCD3 treated mice compared to the isotype control treated mice (Figure 27A+B). Importantly, both CT as well as aCD3 treatment increased the total number of FoxP3⁺ CD8 T cells in the pancreas 2.2-fold and 1.2-fold, respectively (Figure 27A+B). In addition, despite of the low FoxP3⁺ CD4 T cell number and frequency CT showed a similar tendency for an increase of FoxP3⁺ CD4 T cell in blood, spleen, PDLN and pancreas (Figure 27C).

Results

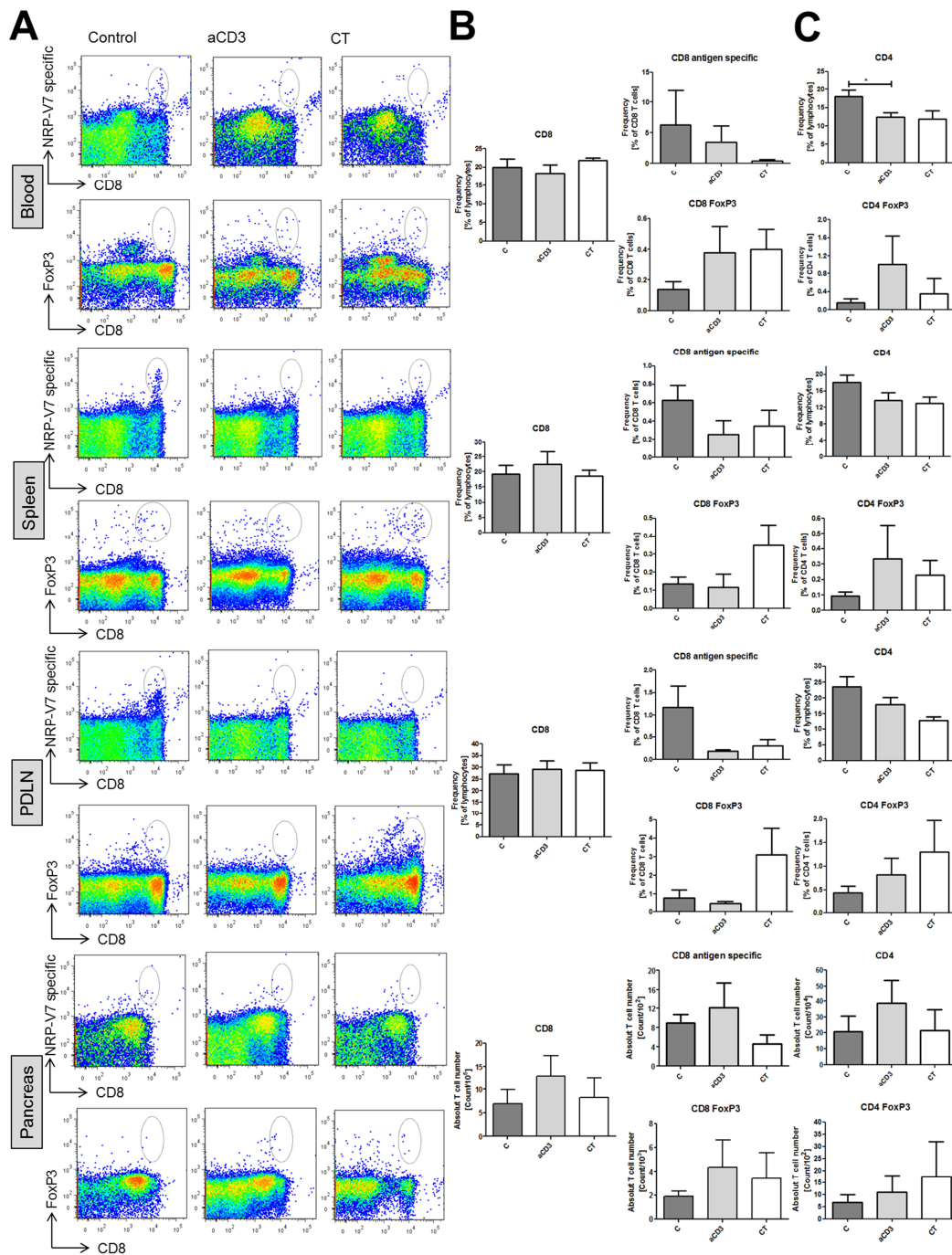


Figure 27: Flow cytometry analysis of NOD mice revealed a slight reduction of islet antigen-specific T cells as well as a slight increased Treg frequency after CT.

The NOD mice were treated with isotype control, aCD3 or CT and samples of blood, spleen, PDLN and pancreas were removed at day 21 after the initiation of the therapy. Frequencies of islet antigen (NRP-V7)-specific CD8 T cells in the blood, spleen and PDLN as well as their absolute number in the pancreas were obtained by stimulation of isolated lymphocytes with NRP-V7 followed by intracellular IFN γ staining and flow cytometry. (A) Representative dot plots from flow cytometry of lymphocytes harvested at day 21 after T1D onset are shown. (B+C) The frequencies and absolute number of CD4 T cells, CD8 T cells, FoxP3⁺ CD4 T cells, FoxP3⁺ CD8 T cells and NRP-V7-specific CD8 T cells are displayed. In the pancreas the absolute T cell number of infiltrating cells was more important. Data are mean values \pm SD (n=4-6). Significant differences are indicated as follows: p < 0.05 (*); p < 0.01 (**); p < 0.001 (**).

9.2.12 CT increased the Treg/Teff ratio in both mouse models

The FoxP3⁺ Tregs were further investigated by immunofluorescence co-staining for foxP3 (red) and CD4 (green) or CD8 (green) (Figure 28).

At day 21 after the first aCD3 dose, CT and aCD3 monotherapy showed a tendency towards a slightly increased CD4 and CD8 Treg (red) number in the pancreas compared to the isotype control treated mice similar as detected by flow cytometry analysis (Figure 28A+B). Notwithstanding the number of FoxP3⁺ CD4 T cells was higher than the number of FoxP3⁺ CD8 T cells in the pancreas (Figure 28A+B). However, CD8 FoxP3 T cells were present and strongly induced by CT (Figure 28A).

Thus, the impact of CT on islet antigen-specific T cells was stronger in the RIP-LCMV-GP than in the NOD model. In contrast, regulatory T cells (Tregs) were induced predominantly in NOD mice. Subsequently, the flow cytometry data was also assessed for the Treg/Teff ratio at day 21 after the first aCD3 dose (day 31 post-infection). I found a significant 4-fold increase in the pancreas of RIP-LCMV-GP mice and a 2.5-fold increase in the pancreas of NOD mice after CT administration compared to the isotype control treated mice (Figure 29). A similar 2-4-fold increased Treg/Teff ratio was observed after CT in blood, spleen and PDLN in both mouse models. CT achieved the most impressive effect in the PDLN of NOD mice with a 17-fold increase in Treg/Teff ratio (Figure 29). Interestingly, aCD3 administration did not result in a significant effect in any organ investigated (Figure 29).

In summary CT reduced the number of infiltrating T cells into the pancreas in RIP-LCMV-GP and NOD mice. Thereby the shift of the immune balance from effector to regulatory T cells was the basis for the impressive long-term effect of CT with aCD3 and aCXCL10.

Results

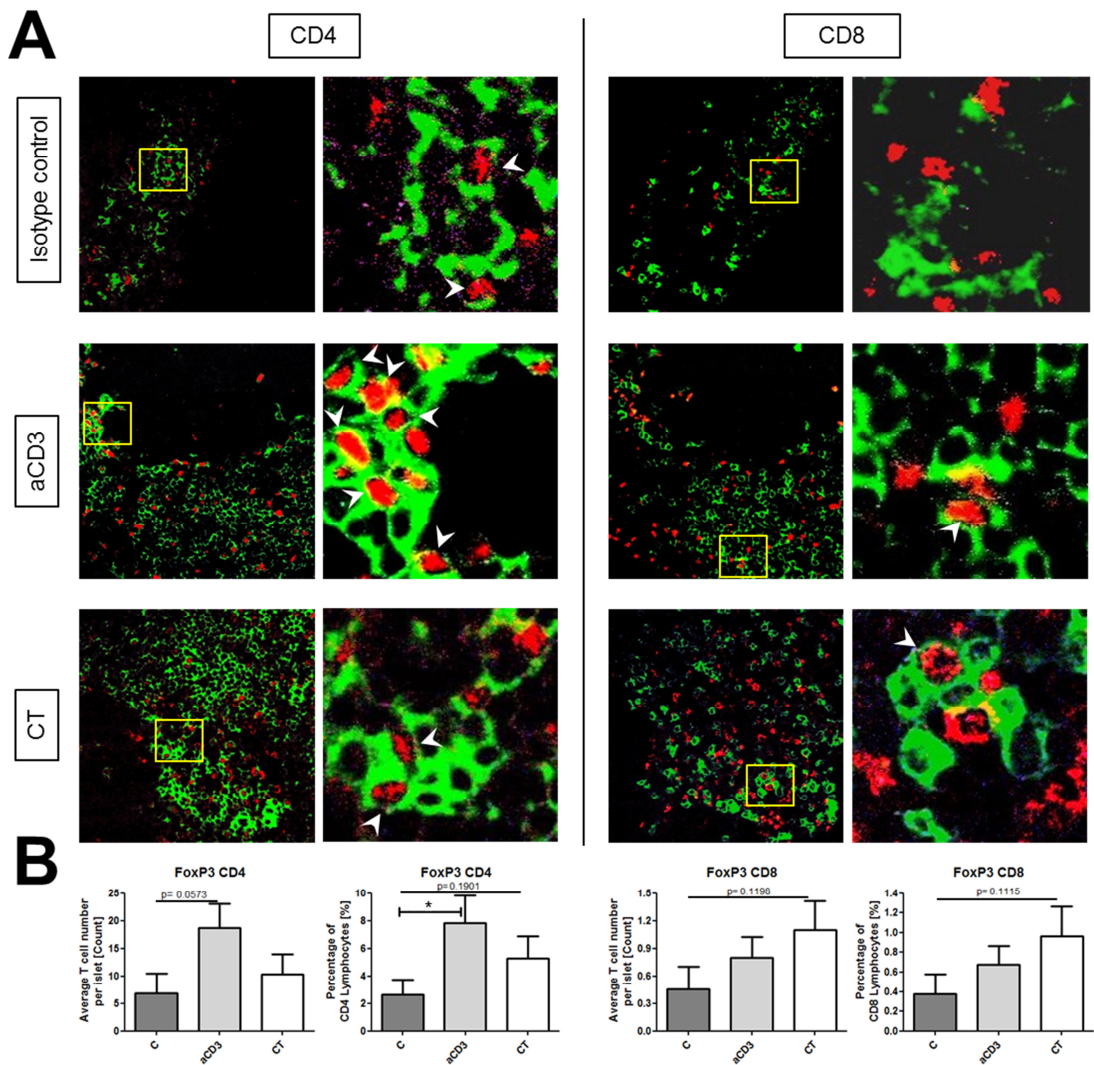


Figure 28: CT and aCD3 treatment increased the CD4 and CD8 Treg number evaluated by fluorescence staining.

Fluorescence immunohistochemistry of 7 μ m pancreas tissue sections from NOD mice at day 21 after T1D onset was performed. The mice were treated with isotype control, aCD3 or CT as described above. Sections were stained for CD4 or CD8 (green) and FoxP3 (red). Representative pancreas regions were taken at 40x magnification. (B) The frequency and number of CD4 and CD8 Tregs (FoxP3⁺) was counted. Data are mean values \pm SD (n=30 islets). Significant differences are indicated as follows: p < 0.05 (*); p < 0.01 (**); p < 0.001 (***).

Results

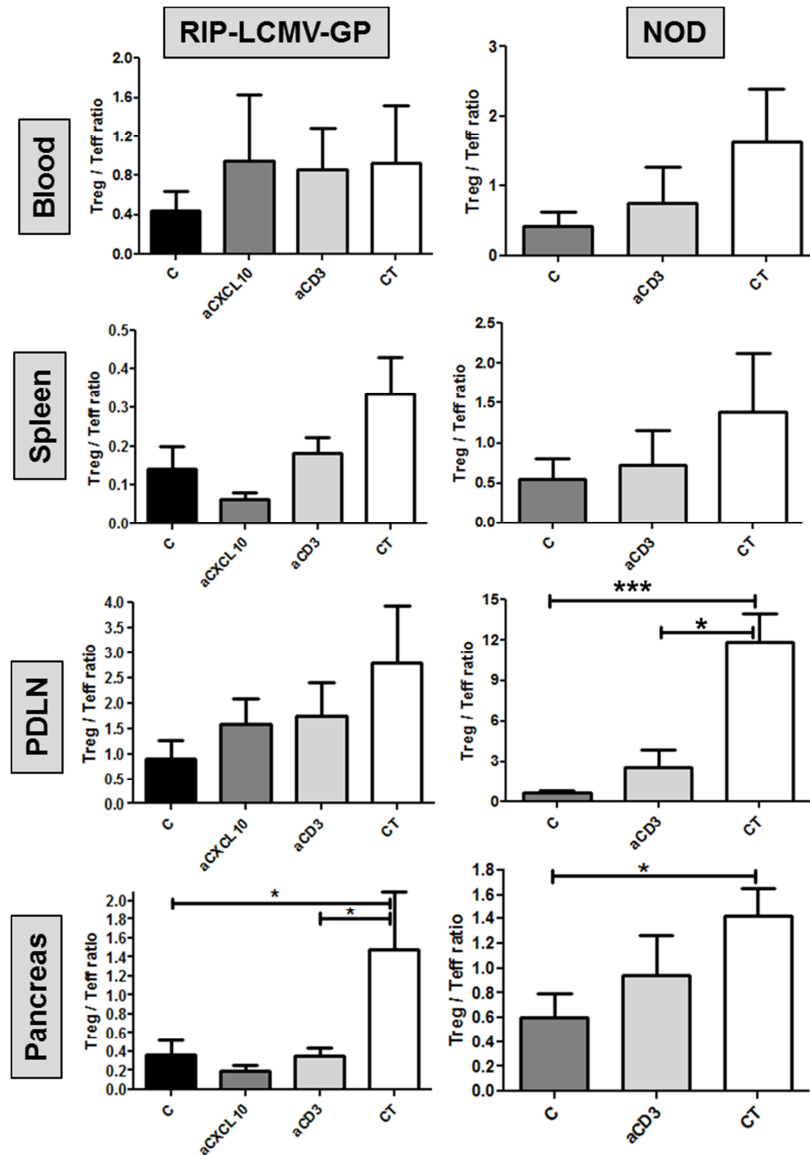


Figure 29: CT significantly elevated the Treg/Teff ratio in NOD and RIP-LCMV-GP mice.

The RIP-LCMV-GP or NOD mice were treated with isotype control, aCXCL10, aCD3 or CT and samples of blood, spleen, PDLN and pancreas were removed at day 21 after the therapy was initiated. The number of islet antigen-specific CD8 T cells (Teff) in blood, spleen, PDLN and pancreas was obtained by stimulation of isolated lymphocytes with LCMV-GP33 (RIP-LCMV-GP mice) or NRP-V7 (NOD mice) followed by intracellular IFN γ staining and flow cytometry. The ratio of Tregs (FoxP3⁺) to Teff was calculated. Data are mean values \pm SD (n=5-13). Significant differences are indicated as follows: p < 0.05 (*); p < 0.01 (**); p < 0.001 (***).

9.3 Combination therapy with aJAM-C

In a second approach I wanted to impair the transmigration of leukocytes through the endothelial layer into the pancreas after aCD3 treatment. Therefore, I used an antibody against the adhesion molecule Jam-C, which plays an important role in the transmigration process of leukocytes.

9.3.1 JAM-C was expressed by vascular endothelial cells

It has been shown in previous studies that JAM-C was upregulated during T1D development with a peak at day 10 and vascular as well as lymphatic endothelial cells were supposed to express JAM-C (129; 130). In order to evaluate this, mice were treated with aCD3 and an *in situ* staining of 7 μm RIP-LCMV-GP pancreas sections was performed. The sections were labelled by fluorescence immunohistochemistry for the co-expression of JAM-C and CD31 (vascular endothelial cells), podoplanin (lymphatic endothelial cells) or GFAP (pancreatic stellate cells) at day 13 post-infection.

Indeed, JAM-C (green) was co-expressed by CD31⁺ (red) vascular endothelial cells in the pancreas and PDLN indicated by yellow staining in the top row (Figure 30). However, neither podoplanin⁺ lymphatic endothelial cells nor GFAP⁺ (green) pancreatic stellate cells expressed JAM-C (green) in the pancreas and PDLN indicated by a lack of yellow staining in the second and third row (Figure 30). Interestingly, lymphatic endothelial cells were located close to vascular endothelial cells and encapsulated the islets and PDLN (Figure 30). In contrast to the lymphatic endothelial cells, the JAM-C expressing vascular endothelial cells also were present inside the islets. In addition, pancreatic stellate cells were located around the islets as well as in the PDLN and they encapsulated only the intact part of the islets (Figure 30). Upon aCD3 treatment the JAM-C expression profile remained unchanged. Due to the decreased destruction of islets after aCD3 administration compared to that in untreated mice, a higher number of vascular endothelial cells was present in the islets of aCD3 treated mice.

Results

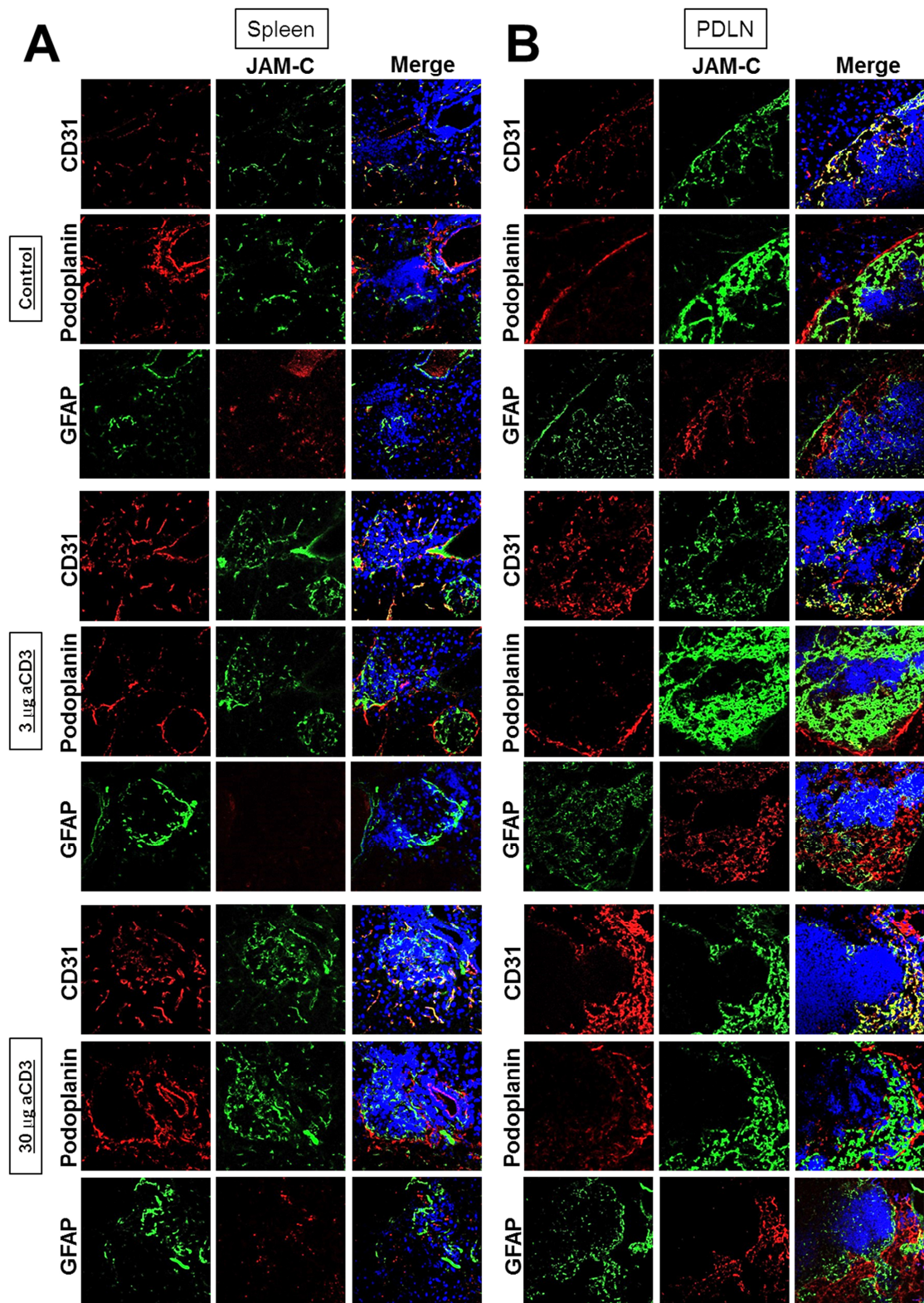


Figure 30: JAM-C was only expressed on CD31⁺ vascular endothelial cells.

Immunofluorescence of 7 μm pancreas tissue sections from RIP-LCMV-GP mice at day 13 after infection was performed. The mice were treated with 3 μg as well as 30 μg aCD3 or left untreated. Sections were co-stained for JAM-C (green, green, red) and CD31 (red), podoplanin (red) or GFAP (green). Representative pancreas (A) and PDLN (B) regions were taken at 25x magnification.

9.3.2 Production of aJAM-C

In order to block JAM-C with an anti-JAM-C antibody (aJAM-C), we first produced sufficient amounts of aJAM-C from a hybridoma cell line. Thus, the aJAM-C producing hybridoma cells obtained from Beat Imhof (University of Geneva, Switzerland) were cultured (11.2.1.1) and the supernatant was purified by using a Protein G column and FPLC (11.2.1.12) (Figure 31A). The purity was tested by SDS-PAGE (11.2.2.4).

The elution profile of aJAM-C showed one clear peak (blue line) shortly after the initiation of elution (green line; Figure 31A). The fractions (red) were evaluated in a Bradford assay and fractions containing a concentration above 1 mg/ml aJAM-C were pooled (Figure 31B). Following this, the concentration of the pooled fractions (red) of each batch was determined in a Bradford assay (Figure 31C). SDS-PAGE of the batches revealed a pure antibody with a light chain (25 kDa) as well as a heavy chain (50 kDa) similar to the control IgG antibody (Figure 31D). Thus, the aJAM-C demonstrated a high purity.

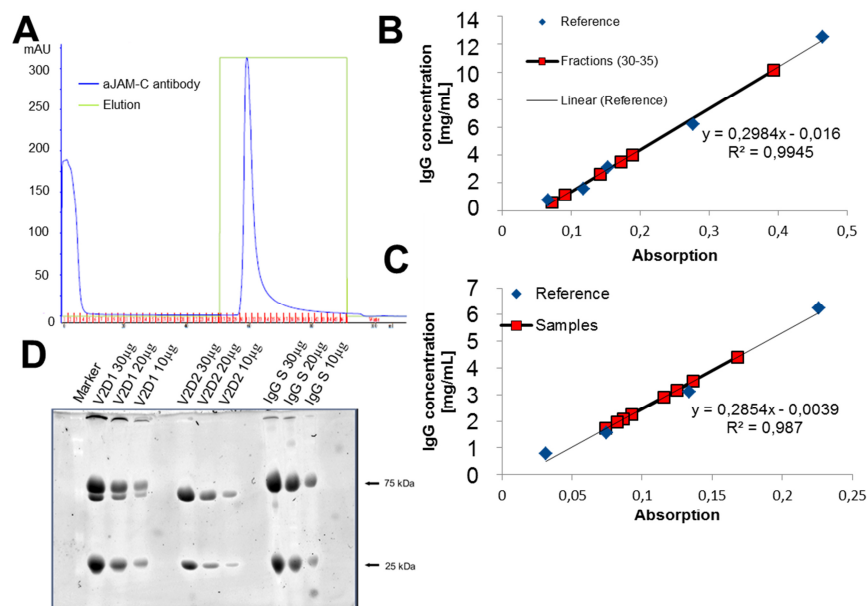


Figure 31: aJAM-C was of high purity.

(A) A representative elution diagram of aJAM-C purification by protein G FPLC chromatography is displayed. The concentrations of the fractions (red) (B) and whole pooled batches (red) (C) were determined by Bradford assay with a serial dilution of a standard control antibody (blue) and linear regression. (D) SDS-PAGE of representative batches aJAM-C and a control antibody at three different amounts (30, 20 and 10 µg) only showed two bands. One band was present at 50 kDa (heavy chain) and the other one at 25 kDa (light chain), indicating a purified antibody.

9.3.3 CT-J slightly improved the T1D remission of the aCD3 monotherapy

Since JAM-C was expressed by vascular endothelial cells located in the islets as well as PDLN and JAM-C might directly or indirectly influence the transmigration of T cells (125; 144), it was an interesting approach to inhibit JAM-C after aCD3 treatment to prevent the re-entry of T cells. The combination therapy with aJAM-C (CT-J) was designed similar to the combination therapy with aCXCL10 (CT). RIP-LCMV-GP mice were infected with LCMV and 3 µg aCD3 were injected intravenously for three days (10-12 post-infection). The next day the mice were treated eight times with 100 µg aJAM-C or isotype control antibody (three intraperitoneal injections/week). The last aJAM-C injection was given at day 28 after LCMV infection (Figure 32A).

At day 10 post-infection (initiation of the therapy) most of the mice were diabetic and CT-J resulted in a reversion of T1D in 51 % of the mice (Figure 32B). Indeed, the remission was significantly increased with CT-J compared to the monotherapy with aJAM-C (14 % remission) and the isotype control treated mice (16 % remission). Unfortunately, the effect of the aCD3 monotherapy (41 % remission) was not significantly increased by the addition of JAM-C treatment, however, there was a strong tendency (Figure 32B). Interestingly, at day 60 after infection the difference in T1D remission between CT-J and aCD3 treatment was 20 %. This difference decreased to 10 %, indicating that the remission occurs earlier in CT-J treated than aCD3 treated mice (Figure 32B). The comparison between the BG levels on day 10 (first aCD3 injection) revealed that over 80 % of the mice were diabetic or hyperglycaemic (BG >200 mg/dl) and the distribution of mice with diabetic, hyperglycaemic or normal BG level was similar in all groups. At day 35 (one week after the last aJAM-C dose) a very low portion of mice developed severe T1D (BG >500 mg/dl) after CT-J administration (26 %) compared to the isotype control (74 %), aJAM-C alone (57 %) or aCD3 alone (40 %) treated mice (Figure 32C). Moreover, the frequency of non-diabetic mice (BG <300 mg/dl) was increased after CT-J treatment (42 %) compared to the isotype control (8 %), aJAM-C (7 %) or aCD3 (28 %) treatment (Figure 32D).

Results

Thus, the addition of aJAM-C to aCD3 therapy influenced the T1D incidence. However, CT-J only resulted in a minor improvement over the aCD3 administration, indicated by a slight reduction in autoimmune diabetes incidence and a slight accelerated T1D remission.

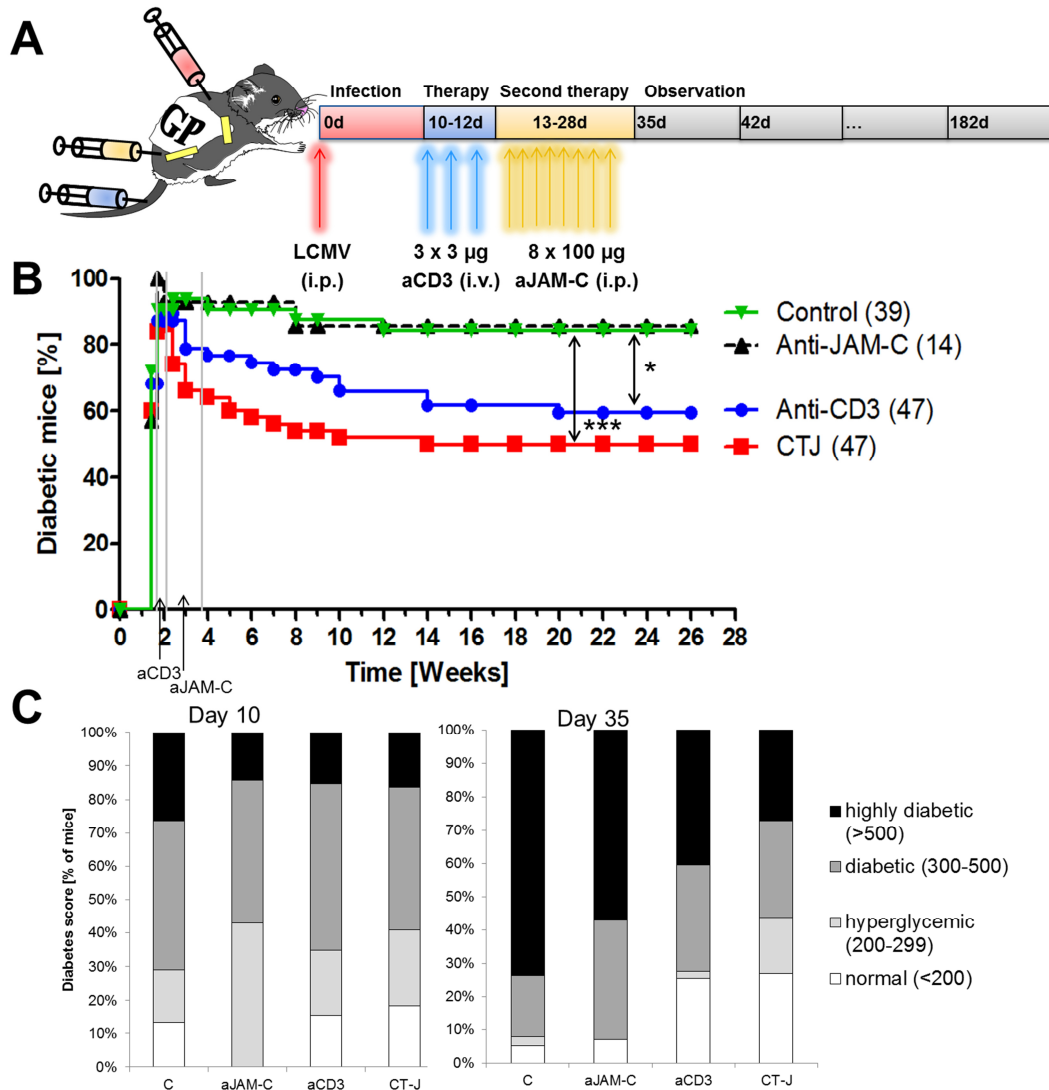


Figure 32: CT-J administration slightly improved the T1D reversion in RIP-LCMV-GP mice compared to aCD3 treated mice.

(A) RIP-LCMV-GP mice were infected with LCMV, treated with three daily injections of 3 µg aCD3 at days 10-12 post-infection and 8 injections of 100 µg aJAM-C from day 13-28 post-infection or isotype control. (B) BG levels were determined until week 26 after infection. Mice with BG levels >300 mg/dl were considered to be diabetic and mice with a stable BG level <300 mg/dl reverted T1D. The number of mice analysed in each group is indicated in brackets. Significant differences are indicated as follows: $p < 0.05$ (*); $p < 0.01$ (**); $p < 0.001$ (***). (C) BG levels of all mice from the incidence (B) were categorised into normal BG (BG: <200 mg/dl white), hyperglycaemic (BG: 200-299 mg/dl, light grey), diabetic (BG: 300-500 mg/dl, dark grey) and highly diabetic (BG: >500 mg/dl, black) at day 10 and 35.

9.3.4 CT-J and aCD3 treatment reduced the number of infiltrating T cells in the pancreas

The progression of T1D can be followed by analysing the integrity of the islets of Langerhans and their infiltration by immune cells. In the RIP-LCMV-GP model, JAM-C was upregulated at the same time as the T cells start to migrate into the pancreas (130). Thus, JAM-C might be directly or indirectly involved in the migration of T cells through the endothelial layer. For that reason 7 μ m pancreas sections of RIP-LCMV-GP mice treated with isotype control, aJAM-C, aCD3 or CT-J were stained by immunohistochemistry (11.2.1.13) for insulin (Ins), CD4 and CD8 at day 31 post-infection (three days after the last aCXCL10 injection).

The previous experiments showed that less T cells were present in aCD3 treated compared to untreated mice one day after the last dose aCD3 (day 13 post-infection) (Figure 11A). At day 31 after infection, the pancreas of mice that received the isotype control antibody or aJAM-C showed a reduced number of intact islets containing insulin producing β cells. In addition, the pancreas contained also many infiltrating T cells in the islets (Figure 33A). In contrast, aCD3 and CT treated mice demonstrated a marked insulin production combined with a reduced T cell infiltration. Nevertheless, some islets of both aCD3 and CT treated mice also showed a strong infiltration (Figure 33A+B). Unfortunately, the infiltration score only displayed small tendency for a reduction of infiltrates in CT-J treated mice compared to aCD3 administration (Figure 33B). It was shown that JAM-C interacts with MAC-1 on neutrophils resulting in a support of the migration through the endothelial layer (119; 145; 146). Due to this, I also stained for Ly-6G⁺ cells, which is expressed by neutrophils. Indeed, CT-J reduced the number of Ly-6G⁺ cells in the pancreas compared to the mice that received the isotype control antibody and monotherapies (Figure 33A).

Immunohistochemistry of the pancreas of cured mice at day 182 post-infection only showed a slight infiltration after CT treatment (Figure 33C). In contrast, the pancreas of cured aCD3 mice revealed some CD8 T cells in the islets at day 182 post-infection (Figure 33C). Thus, there was again a tendency that aJAM-C impaired the re-entry of T cells into the pancreas after aCD3 therapy.

Results

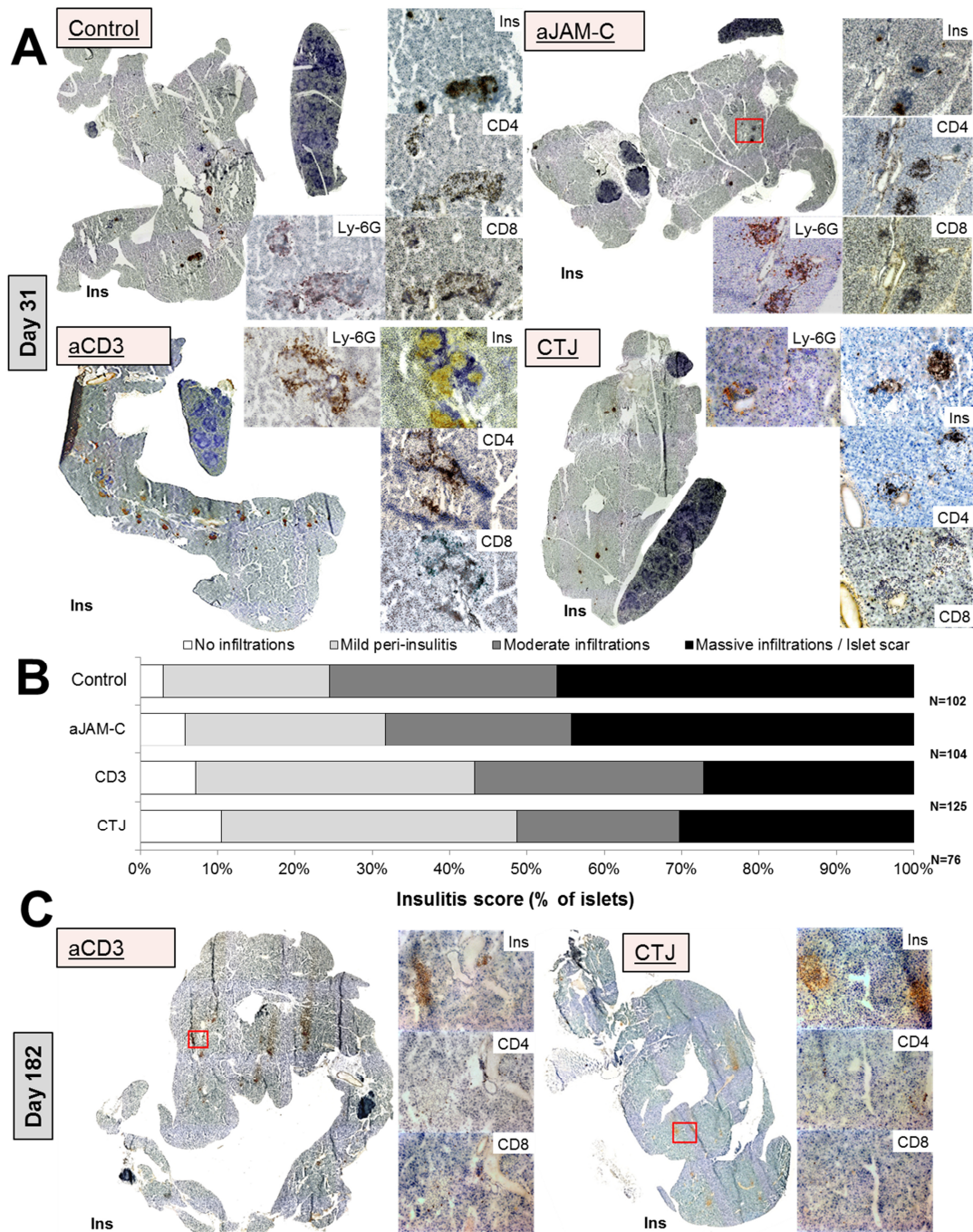


Figure 33: Immunohistochemistry of the pancreas of mice showed a reduced infiltration after CT-J.

(A) Immunohistochemistry of 7 μ m pancreas tissue sections from RIP-LCMV-GP mice at day 31 after infection was performed. The mice were treated with isotype control antibody, aJAM-C, aCD3 or CT-J as described above. Consecutive sections were stained for insulin (Ins), CD4 and CD8 T cells and positive staining is indicated by brown colour. Representative pancreas section overviews were reassembled from insulin pictures taken at a low magnification (4x) and blow ups were taken at a higher magnification (20x). (B) Semi-quantitative analysis of insulinitis of more than 100 individual islets from pancreas sections of four mice per group is shown. Islets were categorised into no infiltrations (white), mild peri-insulitis (<20 %, light grey), moderate infiltrations (<50 %, dark grey) and massive infiltrations (>50 %, black). Data are mean values \pm SD (n=4). (C) Immunohistochemistry of pancreas tissue sections from RIP-LCMV-GP mice at day 182 after infection was performed.

9.3.5 CT-J treatment diminished the number of islet specific T cells in the pancreas, but it did not significantly improve the aCD3 therapy

To further investigate the T cell frequencies and number, I isolated the lymphocytes from blood, spleen, PDLN and pancreas (11.2.1.6-11.2.1.9) of isotype control, aJAM-C, aCD3, and CT-J treated RIP-LCMV-GP mice at day 31 post-infection. The frequency and number of islet antigen-specific T cells were analysed by flow cytometry after stimulation with islet (LCMV-GP)-specific peptides (11.2.1.11).

Three days after the last dose of aJAM-C (day 31 after infection) the CD4 and CD8 T cells were almost fully regenerated in blood, spleen, and PDLN (Figure 34A+B) in all groups. Importantly, the frequency of islet antigen-specific CD8 T cells was significantly reduced by 60 % in the spleen of CT-J treated mice compared to isotype control treated mice. In contrast, the aCD3 or aJAM-C monotherapy only resulted in a reduction of islet antigen-specific CD8 T cell frequency by 48 % or had no effect, respectively (Figure 34A+B). In blood and PDLN, both CT-J and aCD3 demonstrated a significant impact on the islet antigen-specific CD8 T cell frequency indicated by a reduction of approx. 50 % compared to isotype control treated mice. However, according to the immunohistochemistry data, aCD3 therapy and CT-J showed no significant difference in the T cell frequencies (Figure 34A+B). In addition, none of the treatment groups altered the FoxP3⁺ regulatory T cell frequency (Figure 34A+B).

In the pancreas the absolute number rather than the relative frequency of T cells that are infiltrating the islets is crucial. For that reason the total number of infiltrating T cells was investigated. At day 31 post-infection the total number of CD4 as well as CD8 T cells was reduced by 30 % and 57 % in aCD3 treated mice compared to isotype control treated mice. This effect was even more pronounced after CT-J indicated by a 39 % and 73 % reduction of CD4 and CD8 T cells, respectively. Importantly, CT-J and aCD3 monotherapy showed a tendency to diminish the total number of islet antigen-specific CD8 T cells in the pancreas by 62 % and 55 %, respectively. However, it seemed that CT showed a small tendency to improve the effect of aCD3 in terms of T cell infiltration.

Results

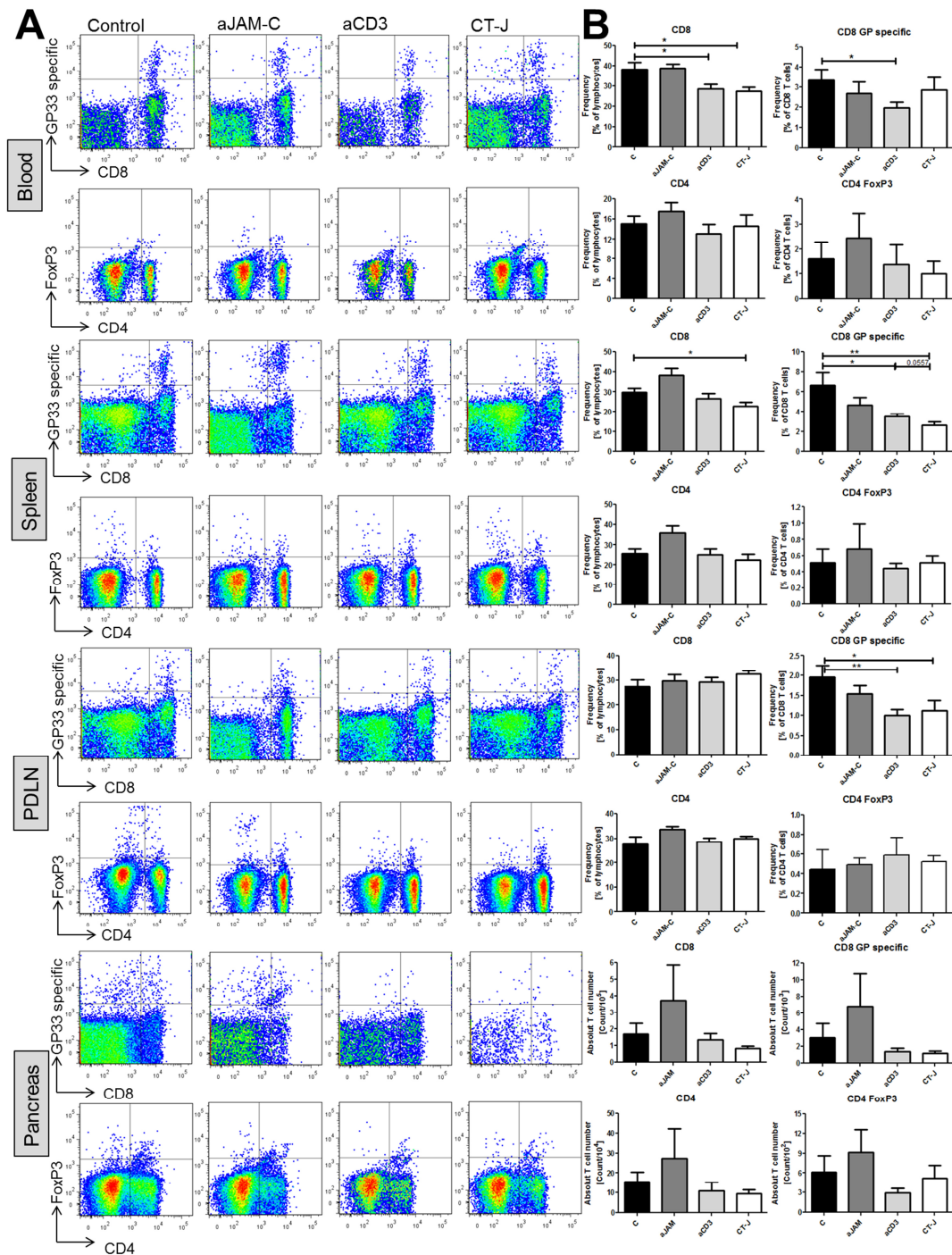


Figure 34: CTJ did not significantly improve the aCD3 effect in terms of T cell infiltration.

The mice were treated with isotype control, aJAM-C, aCD3 or CT-J and sample of blood, spleen, PDLN and pancreas were removed at day 31 after infection. Frequencies of islet antigen (LCMV-GP33)-specific CD8 T cells in blood, spleen and PDLN and their absolute number in the pancreas were obtained by stimulation of isolated lymphocytes with LCMV-GP33 followed by intracellular IFN γ staining and flow cytometry. (A) Representative dot plots from flow cytometry lymphocytes harvested at day 31 post-infection were shown. (B) The frequency and total number of CD4 T cells, CD8 T cells, FoxP3⁺ CD4 T cells and RIP-LCMV-GP33-specific CD8 T cells are shown. In the pancreas the absolute T cells number of infiltrating cells was more important. Data are mean values \pm SD (n=6-16). Significant differences are indicated as follows: $p < 0.05$ (*); $p < 0.01$ (**); $p < 0.001$ (***)

Results

Intriguingly, in the pancreas of aJAM-C treated mice the number of total and islet antigen-specific CD8 T cells was doubled (Figure 34A+B). It might be that the transmigration of already infiltrated T cells was blocked and the T cell accumulated in the pancreas.

At day 31 after infection an *in vivo* cytotoxicity assay was performed. We assume that this cytotoxicity assay will show a reduced killing of islet peptide loaded splenocytes in CT-J treated mice due to less cytotoxic T cells. The splenocytes were isolated from C57BL/6 mice and labelled with either a low or a high concentration of CFSE. Islet antigen GP33 loaded CFSE^{lo} splenocytes and an equal amount of unloaded CFSE^{hi} splenocytes were transferred into LCMV-infected mice that had been treated with CT-J, aCD3, aJAM-C or isotype control (11.2.3.4). The ratio of CFSE^{lo} and CFSE^{hi} splenocytes was calculated at several times after injection (Figure 35A+B).

The mice that received the isotype control antibody or aJAM-C revealed a marked reduction of islet antigen loaded target cells after 6 h (62 %; 44% respectively) and after 24 h almost all target cells were destroyed (20 %; 8 % respectively) (Figure 35A+B). Interestingly, the target cells were killed faster in aJAM-C treated mice, which was consistent with the observation of a higher frequency of islet antigen-specific CD8 T cells in the spleen of aJAM-C treated mice. In contrast, CT-J and aCD3 therapy prolonged the survival of target cells indicated by a 1.3 fold and 2.5 fold increased half-life (Figure 35C). However, there was no significant difference between administration of aCD3 or CT-J (Figure 35A-C). This confirmed the data obtained by immunohistochemistry and flow cytometry.

In summary after completion of CT-J the T cell frequency in the spleen was similar in all groups, which indicated a normal immune response. In contrast, aCD3 as well as CT-J treated mice showed a lower frequency of islet antigen-specific T cells and also a reduced general infiltration in the pancreas compared to isotype control treated mice. However, there only was a small tendency for slightly reduced T cell frequencies and number after CT-J compared to aCD3 treatment.

Results

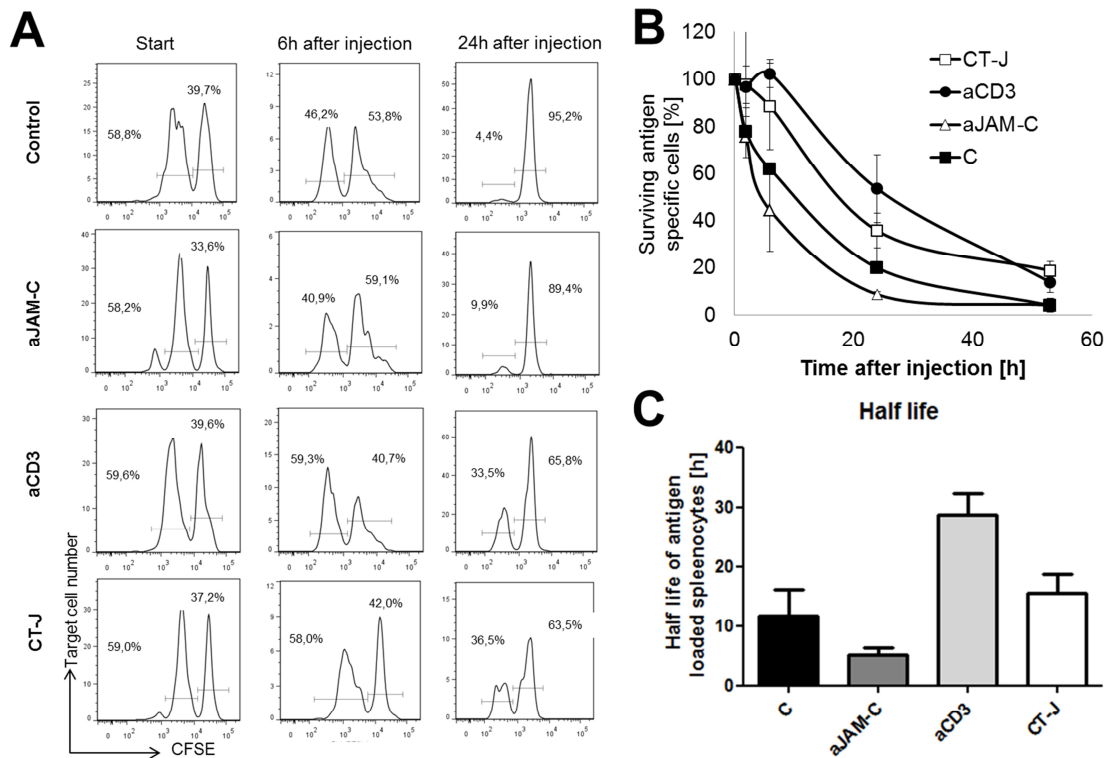


Figure 35: aCD3 as well as CT-J treatment reduced the cytotoxicity in RIP-LCMV-GP mice.

Splenocytes from uninfected C57BL/6 mice were isolated and loaded with the immunodominant CD8 peptide GP33 or left unloaded and labelled either with a low (CFSE^{lo}; peptide loaded) or high (CFSE^{hi}; unloaded) concentration CFSE. These two populations were mixed at a 1:1 ratio and injected into isotype control, aJAM-C, aCD3 or CT-J treated RIP-LCMV-GP mice at day 31 after infection. Blood samples were taken after 10 min, 2h, 6h, 24h and 53h after injection and the isolated lymphocytes were analysed by flow cytometry. (A) Representative histograms from flow cytometry are displayed. (B) The ratio of CFSE^{lo}/CFSE^{hi} was calculated and normalised to the ratio at the injection of target cells (10 min post-injection). (C) The half-life of target cells after injection is displayed. Data are mean values \pm SD (n=2-4). Significant differences are indicated as follows: p < 0.05 (*); p < 0.01 (**); p < 0.001 (***)

9.3.6 CT-J slightly influenced the neutrophil infiltration into the pancreas

The MAC-1 expressing neutrophils are one of the first cells infiltrating at the beginning of inflammation in T1D. Due to the interaction of JAM-C and MAC-1 (119; 126; 145), we suggest that aJAM-C may block the migration of neutrophils through the endothelial cell layer.

At day 31 post-infection the frequency of Ly-6G⁺ neutrophils was investigated after treatment of mice with isotype control, aCD3 or CT-J in blood, spleen, PDLN and pancreas by flow cytometry. The frequency of Ly-6G⁺ cells in blood, spleen and PDLN was not altered by administration of aCD3 as indicated by a similar frequency of Ly-6G⁺ cells to isotype control treated mice (Figure 36A+B). Importantly, in blood and PDLN of CT-J treated mice the frequency of Ly-6G⁺ cells was almost significantly decreased by 35 % ($p=0.0542$) and 52 % ($p=0.3132$), respectively (Figure 36B). Interestingly, CT-J increased the frequency of neutrophils 1.8 fold in the spleen (Figure 36B). It might be that aJAM-C blocked the migration out of the spleen and the neutrophils were captured. Indeed, the total number of neutrophils in the pancreas was significantly decreased by 47 % after CT-J compared to aCD3 monotherapy (Figure 36B). In addition, the number of Ly-6G⁺ cells in the pancreas of isotype control treated mice was also reduced, due to the progressed destruction process of islets, which resulted in a lower overall inflammation (Figure 36B). Thus, I found that the addition of aJAM-C to an aCD3 therapy influenced the Ly-6G⁺ cell frequency and it reduced the number of neutrophils in the pancreas. This reduction of neutrophils might be responsible for the slight tendency of decreased T cell frequencies and number, resulting in an accelerated as well as increased T1D remission. In contrast, the neutrophils frequency and number was not impaired after aCD3 administration.

9.3.7 aJAM-C reached the pancreas and was located on vascular endothelial cells in islets and PDLN

Since there only was a small effect of aJAM-C in addition to the aCD3 treatment I wanted to ensure that aJAM-C really reached the pancreas. Thus, the distribution of the injected rat derived aJAM-C was immunohistochemically investigated by *in situ* staining of 7 μm pancreas sections (11.2.1.13) with a secondary antibody against rat IgG.

Results

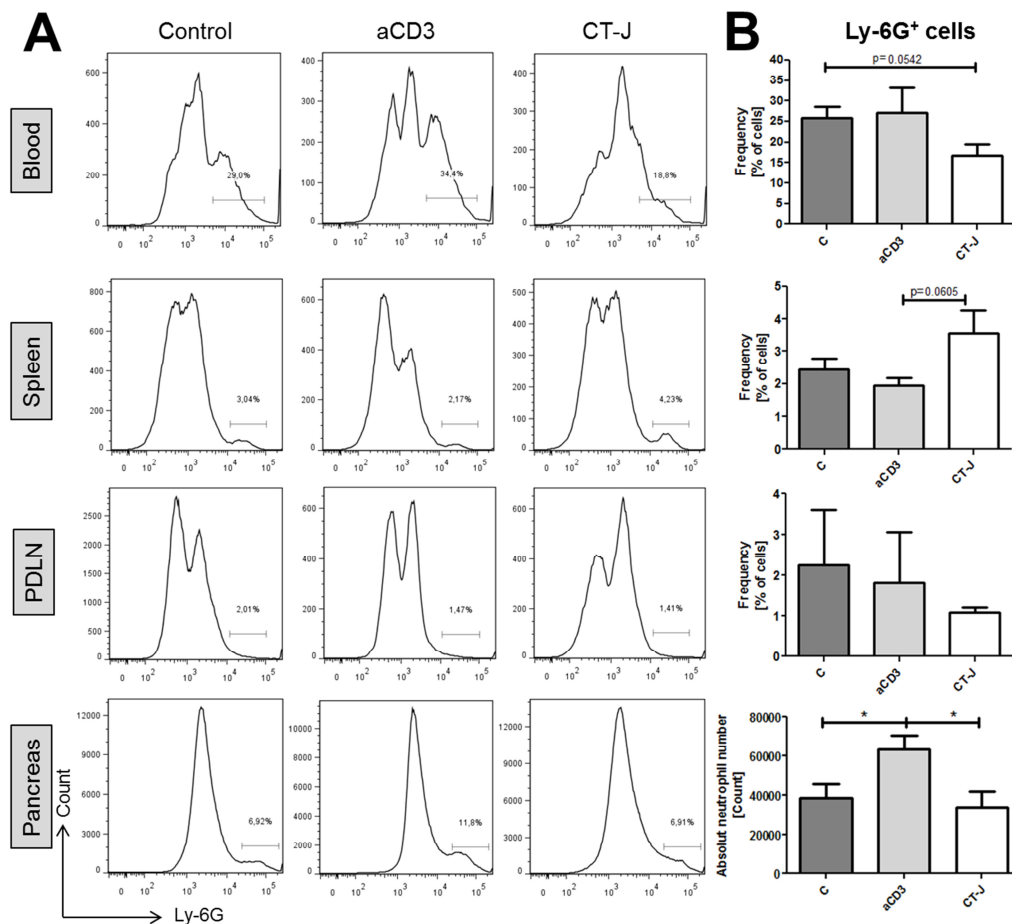


Figure 36: CT-J reduced the neutrophil infiltration into the pancreas compared to aCD3 therapy.

The mice were treated with isotype control, aJAM-C, aCD3 or CT-J and sample of blood, spleen, PDLN and pancreas were removed at day 31 after infection. (A) Representative histograms from flow cytometry of leukocytes harvested at day 31 post-infection are shown. (B) After leukocyte isolation, the frequency and number of Ly-6G⁺ neutrophils was analysed by flow cytometry. In the pancreas the absolute neutrophil number of infiltrating cells was more important. Data are mean values \pm SD (n=3-8). Significant differences are indicated as follows: p < 0.05 (*); p < 0.01 (**); p < 0.001 (***)

The staining revealed a distribution of aJAM-C in the pancreas of aJAM-C and CT-J treated mice at day three after the last antibody dose (Figure 37A). Interestingly, aJAM-C was located on vascular endothelial cells in the islets of Langerhans and formed a thin layer around them (Figure 37A). The distribution of aJAM-C was similar to the JAM-C expression pattern. Thus, aJAM-C seems to really decorate the JAM-C protein located around the islets of Langerhans and thereby might protect by blocking the JAM-C mediated infiltration into the islets. Although it seemed that aJAM-C was located on lymphatic endothelial

Results

cells (Figure 37A), but it was shown in the co-staining at day 13 post-infection that JAM-C was exclusively expressed by vascular endothelial cells which were close lymphatic endothelial cells. Moreover, in the spleen (Figure 38A) and PDLN (Figure 38B) the localisation of aJAM-C was similar the expression pattern of CD31 on vascular endothelial cells. After the end of the observation (day 182 post-infection) aJAM-C was not detectable anymore (Figure 37B).

In summary, the inhibition of the JAM-C interaction after aCD3 mediated inactivation of the T cells resulted in slightly improved as well as accelerated remission of T1D. This effect was accompanied by a reduction of neutrophils into the pancreas.

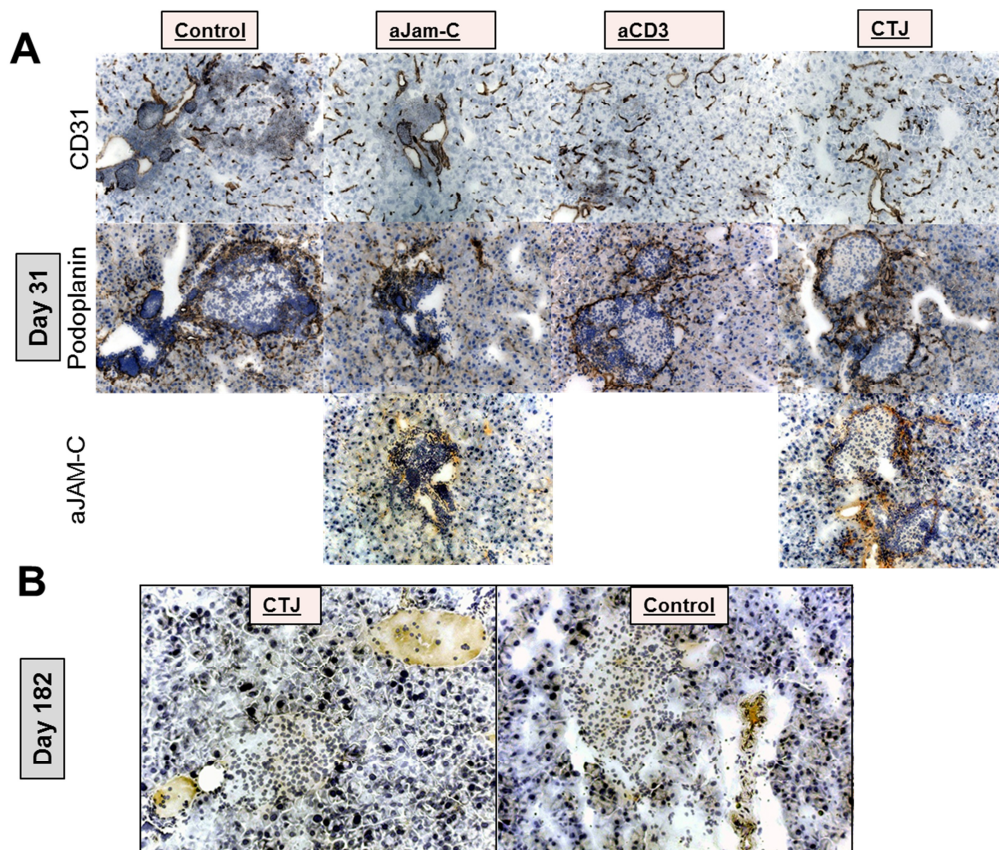


Figure 37: aJAM-C bound specifically to vascular endothelial cells in the pancreas and it formed a thin layer around islets.

Immunohistochemistry of 7 μ m pancreas tissue sections from RIP-LCMV-GP mice at day 31 after infection was performed. The mice were treated with three daily injections of 3 μ g aCD3 at days 10-12 post-infection and eight injections of 100 μ g aJAM-C from day 13-28 post-infection or isotype control. Sections were stained for the injected aJAM-C, vascular endothelial cells (CD31) and lymphatic endothelial cells (Podoplanin; Podo). Positive staining is indicated by brown colour. Representative pictures were taken at 20x magnification from the pancreas at day 31 post-infection (A) and at day 182 post-infection (B).

Results

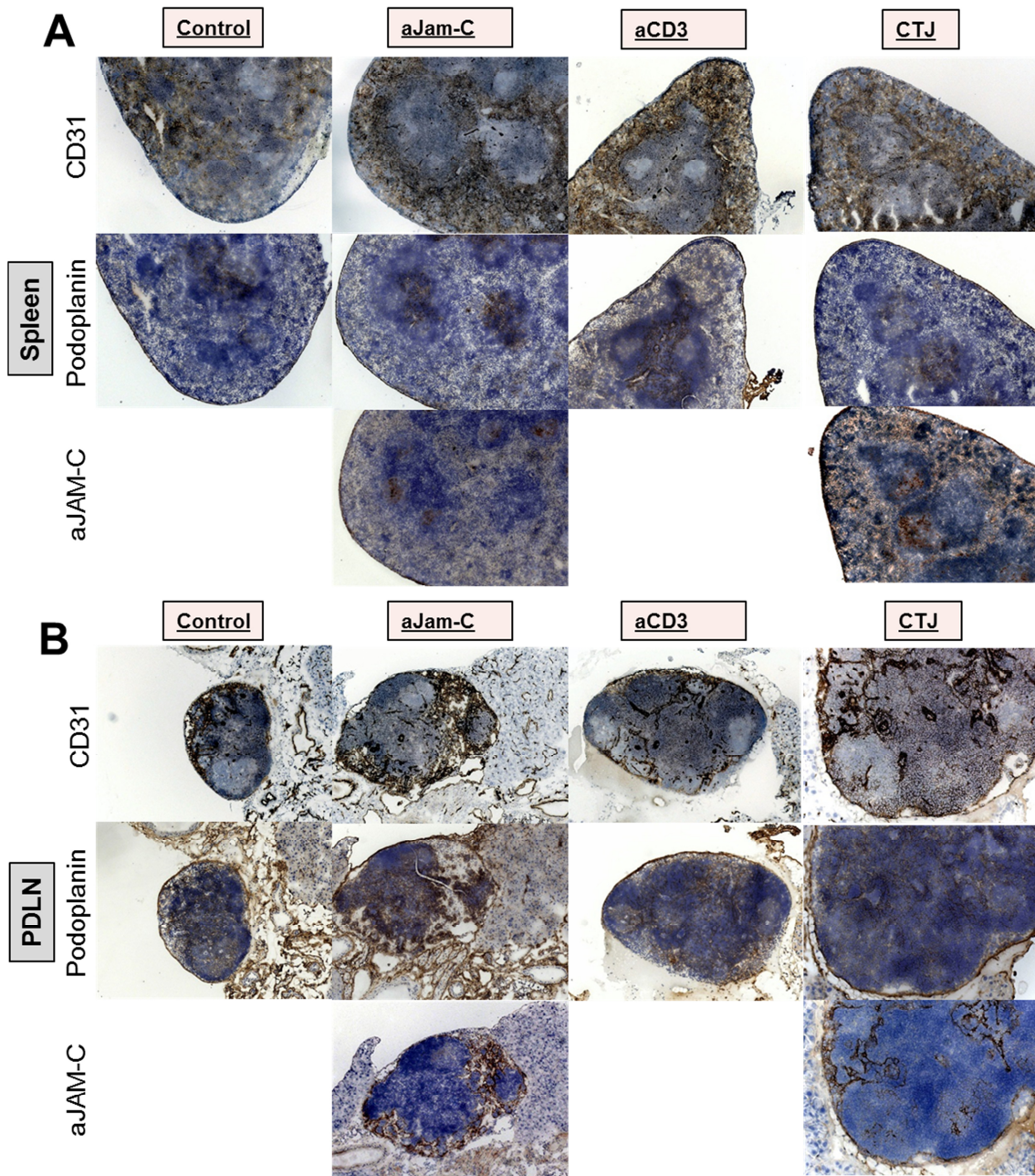


Figure 38: aJAM-C bound specifically to vascular endothelial cells in spleen and PDLN.

Immunohistochemistry of 7 μm pancreas tissue sections from RIP-LCMV-GP mice at day 31 after infection was performed. The mice were treated with three daily injections of 3 μg aCD3 at days 10-12 post-infection and eight injections of 100 μg aCXCL10 from day 13-28 post-infection or isotype control antibody. Sections were stained for the injected aJAM-C, vascular endothelial cells (CD31) and lymphatic endothelial cells (Podoplanin; Podo). Positive staining is indicated by brown colour. Representative pictures were taken at 20x magnification from the spleen (A) and PDLN (B).

Discussion

10 Discussion

Type 1 diabetes (T1D) is a chronic autoimmune disease which leads to the loss of β -cell mass. T cells are the main driver (147) and they destroy the β -cells, resulting in a lifelong need for insulin treatment. Despite of exogenous insulin administration, there are still some late complications like nephropathy, retinopathy and severe hypoglycaemia, which may reduce the life expectancy by 10-15 years (5). Several general immune suppressive drugs like cyclosporine (39) reduced the incidence of T1D, but they cause many adverse side effects. However, more specific interventions, such as monoclonal antibodies against T cells or B cells have been tested in clinical trials (41; 42). The anti-CD3 antibody (aCD3) for example, which is directed against T cells in general, was used in European (otelixumab, Defend-1 study (42; 51; 52) and American (teplizumab, protégé study (53; 54) phase 1-3 trials. aCD3 therapy showed a decreased insulin need in patients with T1D, but unfortunately after one year the insulin need increased again. Higher doses of aCD3 led to more side effects (55; 56). Importantly, repeated aCD3 treatment was ineffective in most individuals (57), because of a generation of anti-idiotypic antibodies. Up to 75 % of the patients develop these antibodies directed to aCD3 after the first treatment (51; 55; 56).

In order to achieve a long-lasting effect, several combinations of aCD3 and secondary treatments were attempted and they often improved the effect of the aCD3 monotherapy. For example T cell inactivation with aCD3 combined with B cell inactivation (aCD20 (59)), FTY720 (148), immunising agents (proinsulin (60); *Lactococcus Lactis* secreting proinsulin and IL-10 (61); GAD65 (62)), β -cell proliferation (Exendin-4 (63); dipeptidyl peptidase-4 inhibitor MK626 (64)) or β -cell protection (Vitamin D3 analogue TX527 (27)).

One possible explanation for the failure of the long-term effect is that the T cell regeneration is very fast. This is desired to re-establish a normal immune response against pathogens, but at the same time it enables a re-infiltration of the islets. With the exception of the experiments with FTY720 (148), which

retained T cells in the PDLN, none of the other combination therapies are directed against such a re-infiltration scenario.

Here, we targeted the re-entry of recovered T cells into the pancreas after T cell inactivation by aCD3. To achieve this we had two approaches: On the one hand the blocking of the chemokine CXCL10, which is important for T cell migration (109) and on the other hand the blocking of JAM-C, which might be involved in the transmigration of leukocytes through the endothelial layer (125; 128; 144; 149).

10.1 aCD3 therapy

Previous studies in NOD mice showed that treatment of recent onset diabetic NOD mice for five consecutive days with 5 µg/day of a regular aCD3 containing the IgG Fc-region was enough to cure over 60 % of the mice (47; 48). However, due to binding to the Fc receptor (FcR) the entire aCD3 IgG may activate the complement system which causes many side effects (55). The use of F(ab)₂-fragments of aCD3 reduced the side effects, but also the efficacy was slightly impaired (47; 150).

I found that a high dose of 30 µg/day F(ab)₂-fragment of aCD3 for three consecutive days cured also 60 % of recent onset diabetic RIP-LCMV-GP mice. This dose was enough to inactivate almost all CD4 T cells in these mice. Administration of 30 µg/day aCD3 for three days in mice corresponds to the cumulative aCD3 dose in humans that was used in the European phase 2 trial with oteelixumab (42). In this trial the aCD3 administration resulted in a reduction of the insulin need of the patients, but it also caused side effects such as cytokine release, fever and headache. In order to reduce the side effects a 16-fold lower aCD3 concentration was used in a subsequent phase 3 trial (DEFEND-1) (52). The patients showed almost no adverse events. However, the therapy left the insulin need unaltered compared to placebo treated patients. In this context, we used a 10-fold lower concentration of aCD3 (3 µg/day) to avoid strong side effects, but with the addition of a second therapy in order to preserve the efficacy. This dose of 3 µg aCD3 as a monotherapy led to an

Discussion

inactivation of 50 % of the CD4 T cells in RIP-LCMV-GP mice and still showed a reduction of the T1D incidence in 38 % of the mice.

In addition, I also investigated the effect of the aCD3 monotherapy in NOD mice. In contrast to our RIP-LCMV-GP model, even an administration of 30 μ g aCD3 for three consecutive days was not able to inactivate the majority of T cells in the pancreas. However, this dose inactivated 50 % of the CD4 T cells similar to the 3 μ g aCD3 dose in RIP-LCMV-GP mice. Accordingly, we used a dose of 30 μ g aCD3 for the treatment of NOD mice.

The infiltration of human islets in patients with T1D differs from that in islets of diabetic NOD mice (151). These mice displayed strong peri-insulitis whereas in humans only a few islets were infiltrated by T cells. Consequently, even a low aCD3 dose might be sufficient to inactivate an appropriate portion of T cells in the human pancreas. Nevertheless, the DEFEND-1 phase 3 trial with a 16-fold lower aCD3 concentration compared to the preceding phase 2 trial revealed a loss in efficacy (52). However, similar to the dose finding experiment in mice, an important parameter might be the aCD3 concentration needed for the inactivation of half of the T cells in the blood in humans.

A critical question concerns the precise time of aCD3 administration, especially in our RIP-LCMV-GP mouse model. An aCD3 therapy at a late phase of T1D might restore the immune balance at a time when most β -cells are already destroyed leading to the assumption that the aCD3 therapy was not beneficial. This hypothesis is consistent with the observation made by von Herrath et al. that a treatment of RIP-LCMV-GP mice from day 20 to 25 post-infection with aCD3 led to a loss in efficacy (49). Similarly, an aCD3 treatment prior to virus infection did not impair the development T1D. The trigger that deregulates the immune system appears later, accordingly, the intervention with aCD3 cannot affect the consequences of the triggering event. Moreover, Chatenoud et al. demonstrated in NOD mice that there was no benefit from the administration of aCD3 at 4 and 8 weeks of age (48), indicated by a similar development of autoimmune diabetes in aCD3 treated and untreated mice. Usually NOD mice develop T1D up on week 15 of age. Interestingly, Chatenoud et al. showed that the treatment with aCD3 at week 12 of age delayed the incidence of T1D by almost 2 months (48). In the virus induced RIP-LCMV-GP mouse model an

Discussion

early immune intervention (day 8-12) with the F(ab)₂-fragment aCD3 results in a complete prevention of T1D without interfering with the virus clearance (49). Similarly, I found that all at day ten after infection not yet diabetic RIP-LCMV-GP mice were protected from T1D development after aCD3 treatment starting at day ten. In contrast, most of untreated mice developed T1D later.

It is possible to identify people with a high risk to develop T1D on the basis of genetics, relatives and autoantibodies (152). However, there is no correlation of the appearance of autoantibodies and the degree of insulinitis. For that reason there is a lack of reliable biomarkers to identify patients with a beginning autoimmune destruction and most of the patients are not diagnosed until clinical symptoms become apparent (36; 153; 154). Therefore, we pursued a therapeutic approach and treated mice with aCD3 directly after being diagnosed through a diabetic blood glucose (BG) level (NOD model) or when most of the mice were diabetic (day 10 in the RIP-LCMV-GP model).

Chatenoud et al. claimed that aCD3 was not only depleting the T cells, but even more it inactivated most of them by inducing a state of unresponsiveness (anergy) (155). I confirmed this by comparing active IFN γ producing T cells and general islet antigen-specific (tetramer-positive / Tet⁺) T cells. The tetramer also labelled islet antigen-specific T cells that did not produce IFN γ after stimulation with the islet antigen GP33, due to an aCD3 mediated anergy. The experiment revealed that three times 3 μ g aCD3 resulted in an inactivation of approx. 40 % of the islet antigen-specific T cells and 30 % of them were really depleted. Moreover, a higher dose of aCD3 left the ratio of inactivated to depleted T cells unaltered.

Interestingly, I found that more CD4 T cells were inactivated than CD8 T cells. A low dose of aCD3 reduced the frequency of CD8 T cells to approx. 60 %. Administration of a high aCD3 dose did not improve the inactivation achieved by a low aCD3 dose indicated by a similar inactivation of CD8 T cells. Other groups reported the same phenomenon (27; 61). The T cells recovered very fast displayed by a similar frequency of T cells in all groups two weeks after the last aCD3 dose. Therefore, the overall immune function was restored. Importantly, shortly after aCD3 treatment, the frequency of FoxP3⁺ CD4 Tregs of all CD4 T cells was enhanced although the frequency of CD4 in general

declined. Nevertheless, the absolute amount of FoxP3⁺ CD4 T cells in the pancreas was not affected and all groups showed a similar number of FoxP3⁺ CD4 T cells. Thus, the reason for the increased frequency probably was a stronger inactivation of normal CD4 T cells, rather than the induction of new FoxP3⁺ CD4 T cells. This is controversially discussed in the literature. On the one hand there are several reports according to which aCD3 induced Tregs (28; 48; 156; 157). On the other hand it was suggested that aCD3 stimulate the CD4 or CD8 Tregs induction neither in mice (49) nor in humans (158). New findings indicate that Tregs were resistant to aCD3 (157; 159; 160), and due to this the relative Treg frequency increased shortly after aCD3 treatment. A possible explanation might be that Tregs underwent an antigen modulation of the CD3 receptor and are therefore somewhat protected from aCD3 induced anergy and/or depletion.

Chatenoud et al. mentioned a higher specificity of aCD3 for specific allo-reactive T cells in islet transplantation (161) and it was demonstrated that human activated T cells were more susceptible to aCD3 treatment than the resting ones *in vitro* (159). I found that aCD3 strongly inactivated islet (LCMV-GP)-specific T cells in RIP-LCMV-GP mice. Possibly, the CD3 receptor is upregulated on activated T cells. However, Liu et al. showed that the CD3 complex was downregulated after ligation by MHC peptides (162). Another hypothesis is that the CD3 receptor is upregulated on recently developed T cells to ensure direct activating to fight against pathogens.

In conclusion, up to the present most of the diabetic patients are diagnosed only after clinical symptoms appeared. High doses of aCD3 decreased the insulin need in humans. Unfortunately, it caused severe side effects. However, lower doses were less effective and therefore there is a need for a second therapy. In the RIP-LCMV mouse model aCD3 predominantly affects CD4 T cells rather than CD8 T cells. In contrast, the islet (LCMV-GP)-specific T cells were susceptible to the aCD3 induced inactivation, whereas the FoxP3⁺ CD4 T cells were resistant to the aCD3 treatment.

10.2 Combination therapy with aCXCL10

In this study I showed that a combination of aCD3 and anti-CXCL10 antibody (aCXCL10) (CT) persistently reversed T1D in two different mouse models. CT followed an exact time schedule. First a low dose aCD3 was administered to diabetic mice, which inactivated approx. 50 % of the T cells, especially the disease driving islet antigen-specific CD8 T cells. The second therapy with aCXCL10 (injection of 8 doses) was initiated one day after the last dose of aCD3 was administered and it aimed at the blockade of the re-infiltration of recovered T cells into the pancreas. The second therapy had to be given directly after aCD3 treatment, because the T cells recovered within one week after the last aCD3 dose. Importantly, three days after the last dose of aCXCL10 the antibody still was detectable in the islets.

I found that CT resulted in a remission of T1D in 67 % of the mice in the inducible RIP-LCMV-GP and 55 % in the spontaneous NOD mouse model. The effect of CT was stronger than that of the monotherapies with either aCD3 or aCXCL10 in both mouse models (30-40 % remission of T1D). In addition, none of the therapies reverted T1D in mice with a BG level higher than 500 mg/dl at the initiation of the therapy (day 10 post-infection). Immunohistochemistry and flow cytometry revealed a marked reduction of general T cell infiltration in the pancreas of CT treated mice.

The islet antigen-specific T cells are of high importance in T1D, since Velthuis et al. were able to measure islet antigen-specific T cells in T1D patients using a combinatorial quantum dot major histocompatibility complex multimer technique. They found that the frequency of insulin B₁₀₋₁₈ specific CD8 T cells was higher in most of the recent-onset T1D patients than in all healthy controls (163). Further these islet antigen-specific T cells were still detectable 8 years after clinical diagnose of T1D (164) evaluated by in situ MHC-peptide tetramer staining of pancreas tissue. Interestingly, the frequency of islet antigen-specific CD4 T cells was similar in T1D and T2D (165). However, the frequency of islet antigen-specific CD8 T cells was significantly higher in T1D patients, which suggests that general β -cell stress drives a CD4 T cell immune response. In contrast, islet antigen-specific CD8 T cells led to a specific attack of the β -cells,

resulting in a rapid β -cell loss. This underpinned the importance of the CT treatment, which showed a significantly lower frequency and number of islet antigen-specific CD8 T cells in blood, spleen, PDLN and pancreas.

For instance I found a similar number of islet antigen-specific T cells in the pancreas of CT and aCD3 treated RIP-LCMV-GP mice 7 days after the last aCD3 dose. However, 18 days later there was a tendency that the number of infiltrating islet antigen-specific T cells increased in aCD3 treated RIP-LCMV-GP mice. Accordingly, the BG levels increased again in aCD3 treated RIP-LCMV-GP mice after day 21. In contrast, in CT treated RIP-LCMV-GP mice the number of infiltrating islet antigen-specific T cells was still reduced by 78 % and their BG level further declined (Figure 39).

Similarly, there was a tendency towards a lower frequency of islet antigen-specific CD8 T cells after CT administration in the NOD model. However, the islets of both, CT and aCD3 treated mice were still strongly infiltrated. Interestingly, a tendency towards an increased frequency and an absolute number of FoxP3⁺ CD4 and FoxP3⁺ CD8 T cells was also found in CT treated NOD mice. An increase of FoxP3⁺ CD4 T cells had been shown in previous experiments with an aCD3 therapy and their functionality was demonstrated by autoimmune diabetes prevention after adoptive transfer into NOD mice (27-30). In contrast, the FoxP3⁺ CD8 T cell population was not investigated in this way. This population had been detected after aCD3 therapy in the collagen-induced arthritis model (166) and they were induced by aCD3 *in vitro* with human PBMC's (167) as well as *in vivo* in humans (168). Liu et al. showed for the first time the *in vivo* suppression effect of CD8 FoxP3⁺ T cells in an animal model of inflammatory bowel disease (169).

In humans the CXCR3 receptor was predominantly expressed on Th1 cells rather than on Tregs (98; 99; 170) and approx. 90 % of the LCMV specific CD8 T cells expressed the CXCR3 receptor (95; 99; 171). Consequently, one could speculate that the aCXCL10 therapy blocked especially the migration of effector T cells (Teff) rather than the migration of Tregs. This hypothesis is consistent with the observation that the ratio between FoxP3⁺ Tregs and islet antigen-specific CD8 Teff was significantly higher in the pancreas of both RIP-LCMV-GP and NOD mice after CT treatment.

Discussion

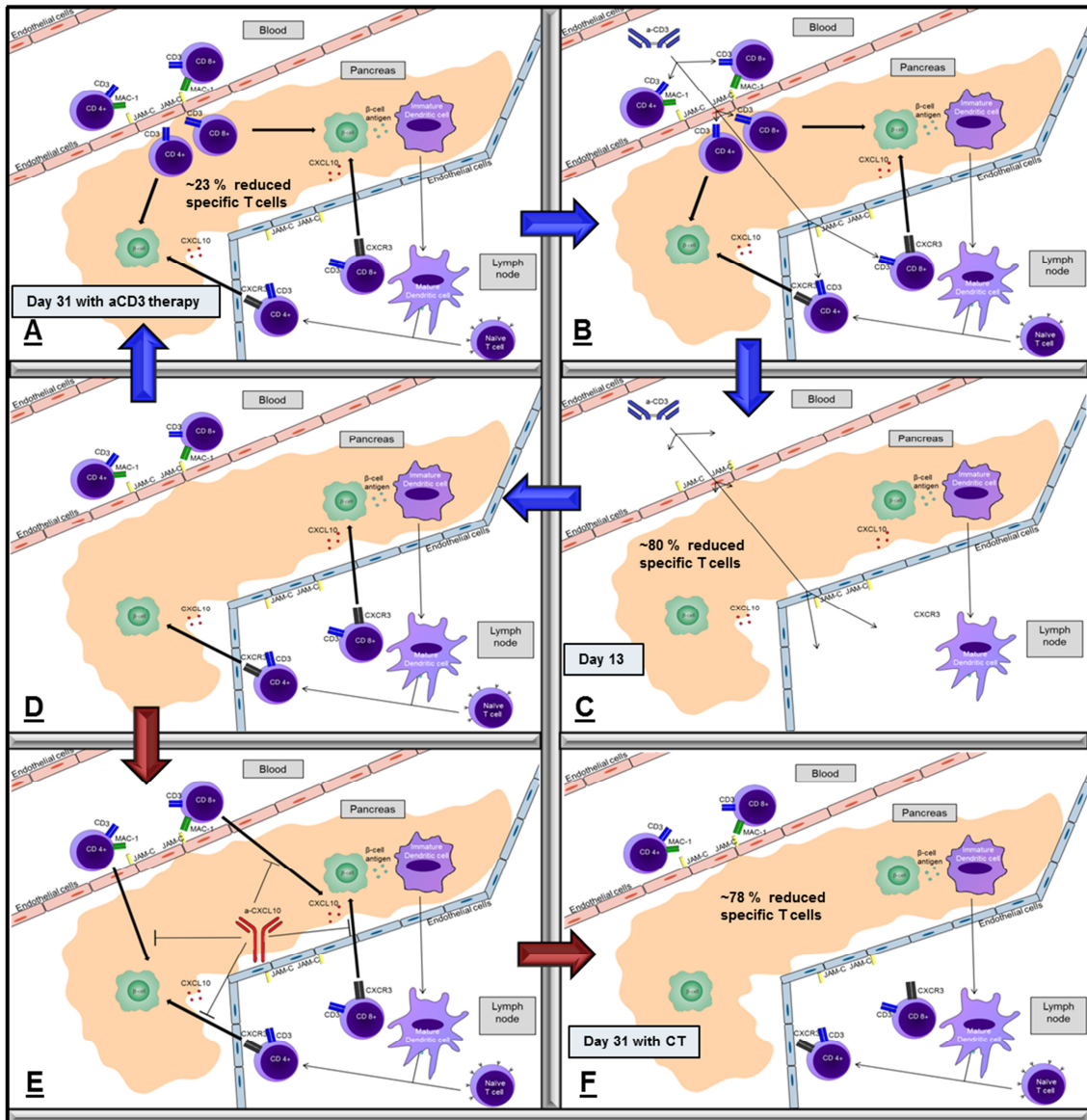


Figure 39: Overview of the CT effect.

(A) Environmental and genetic factors may lead to an increased antigen uptake of dendritic cells in the pancreas. In the PDLN the antigen is presented by matured dendritic cells to T cells. Accordingly, there might be a potential activation of cross-reactive T cells by specific antigens. These aggressive T cells migrate through a CXCL10/CXCR3 mediated mechanism into the pancreas. Subsequently, these T cells attack the antigen presenting β -cells in the pancreas. (B+C) The administration of aCD3 induces a significant inactivation of T cells in lymphoid organs and in the infiltrated tissues. In the pancreas, approx. 80 % of the islet antigen-specific T cells were inactivated in aCD3 treated RIP-LCMV-GP mice at day 13 after infection (D) Soon after, the immune system regenerates and new T cells are produced. (D→A) Unfortunately, without a second therapy these recovered T cells migrate into the pancreas and they attack yet again the β -cells in the pancreas (pathway marked with blue arrows). Consistently, the islet antigen-specific T cells were only reduced by approx. 23 % in aCD3 treated RIP-LCMV-GP mice at day 31 post-infection (E) Administration of aJAM-C blocks the transmigration of leukocytes (pathway marked with yellow arrows) and results in a slight improvement of the aCD3 therapy (F). For instance at day 31 after infection the islet antigen-specific T cell number of CT treated RIP-LCMV-GP mice was still diminished by 78 %, respectively.

In addition, the aCXCL10 was not detectable anymore in the pancreas half a year after infection in spite of its very long half-life of several months (data not shown). Nevertheless, the protective effect of CT was stable for at least 20 weeks after T1D remission and all cured CT treated RIP-LCMV-GP mice stayed largely without insulinitis, whereas cured aCD3 monotherapy treated RIP-LCMV-GP mice partially showed infiltrations in the islets. This effect was linked with an elevated Treg/Teff after CT treatment compared to aCD3 administration, suggesting a long-term shift of the immune balance towards regulation.

Interestingly, in NOD mice, after CT as well as aCD3 treatment, many T cells were detectable around the islets half a year after T1D reversion. One could speculate if CT created a long-term regulatory milieu and thereby curbs the autoreactive T cells. In addition, the remaining islet antigen-specific T cells also produced less IFN γ per cell indicated by a reduced intensity of the IFN γ signal in flow cytometry. Due to that, the peri-insulinitis of NOD mice might be similar to the non-destructive infiltrations observed in 8-11 weeks old NOD mice (172) or that shown in cured NOD mice after combinational anti-cell adhesion therapy at day 52 and 215, where the T cells around the islets mainly produce IL-10 and almost no IFN γ (173). Nevertheless, human islets show only a mild infiltration of some islets similar to the RIP-LCMV-GP mouse model (151). Due to this, the non-destructive infiltrations might not be important in humans, if CT fully prevent the re-entry of recovered T cells.

In RIP-LCMV mice CXCL10 was induced directly after virus infection with a peak induction at day 1 in the PDLN and day 4-10 in the pancreas (108). Although CXCR3 is the only receptor for CXCL10 it seemed that the impact of a blockade of CXCR3 was not as strong as the blockade of CXCL10. CXCR3 deficient mice showed a delay in T1D in the RIP-LCMV-GP mouse model (93; 174). However, these data are controversial since the observation time was very short and new studies with CXCR3 deficient mice as well as treatment with the CXCR3 antagonist NIBR2130 revealed no influence on T1D incidence in RIP-LCMV-GP mice (174; 175). Importantly, clinical studies demonstrated only a small impact of CXCR3 antagonists in other diseases like arthritis, lupus nephritis and encephalomyelitis (176-178).

Discussion

Interestingly, I found that the CXCL10-deficient RIP-LCMV-GP mice showed a milder form of T1D development and some mice showed a spontaneous remission of T1D. In addition, the incidence of T1D was significantly lower in CXCL10-deficient RIP-LCMV-GP mice compared to littermates. These data stand in contrast to a recent observation by Coppieters et al. who found almost no difference on T1D development in CXCL10-deficient mice compared to normal RIP-LCMV-GP mice (175). However, the mice were only observed till day 14 after infection with a final T1D incidence of 90 %. In our case, at this point of time a similar frequency of 70 % of CXCL10-deficient RIP-LCMV-GP mice were diabetic, even so almost half of them turned to normal glycaemia later.

Similar inconsistent data was published in terms of the prevention of autoimmune diabetes with aCXCL10. On the one hand Christen et al. showed a prevention of 69 % of RIP-LCMV-GP mice after aCXCL10 administration in 2003 (95) and it was demonstrated that aCXCL10 prevents T1D in the NOD model (179). On the other hand Coppieters et al. found no significant effect in the RIP-LCMV model in 2013 (175). In addition, overexpression of CXCL10 did not accelerate T1D in the RIP-LCMV-GP mouse model, certainly due to its already fast T1D onset. In contrast, the overexpression showed an acceleration in the slow onset RIP-LCMV-NP model (109).

In the present study diabetic RIP-LCMV-GP mice were treated with an aCXCL10 monotherapy for 19 days, resulting in a reversion of T1D in 36 % of the mice. For that reason and due to late remission of T1D in CXCL10-deficient RIP-LCMV-GP mice, it is possible that aCXCL10 is important in the chronic phase of autoimmune diabetes. In line with this assumption, the CXCL10 level was elevated in the blood of NOD mice (106) and in new onset T1D patients (81; 180; 181).

As mentioned before in CXCL10 deficient RIP-LCMV-GP mice the absence of CXCL10 alone delayed the T1D onset. Importantly, the administration of aCD3 to CXCL10 deficient RIP-LCMV-GP mice at day 10 after infection, led to an impressive reversion of T1D in all mice. These data indicated a high potential of a combination of aCD3 with aCXCL10.

Discussion

All in all the data on CXCL10 and CXCR3 neutralisation are intriguing and it seems that the success depends strongly on timing of treatment as well as intensity of disease and degree of infiltration.

Interestingly, CXCL10 is the major chemokine for the CXCR3 (97) and no receptor independent function was described. Notwithstanding, the blockade of CXCR3 had only a marginal influence on T1D whereas the blockade of CXCL10 partially showed an impressive effect. One possibility might be that CXCL9 and CXCL10 have opposite effects. However, a simultaneous neutralisation of CXCL9 and CXCL10 did not diminish the therapeutic effect of CXCL10 in the RIP-LCMV model (95). In any case, it is obvious that a monotherapy with aCXCL10 is not the solution to cure T1D, but there is evidence that CXCL10 has an influence, indeed.

In addition, after injection aCXCL10 was localised directly among the T cells of in the infiltrates in the islets of Langerhans. Consequently, it might be that diabetogenic T cells are also able to produce CXCL10 to attract further T cells to the side of inflammation. Indeed, it has been shown that T cells itself may produce CXCL10 in certain circumstances (182-184) It was also shown that β -cells themselves produced CXCL10 under inflammatory stress (93; 107). Thereby CXCL10 formed a gradient around the islets, which attracted islet antigen-specific T cells. However, it is not clear whether the β -cells, T cells or other cell types were responsible for the chemokine gradient in our experiments.

In conclusion, I found a combination therapy which improves the aCD3 monotherapy and led to a persistent reversion of T1D in diabetic RIP-LCMV-GP and NOD mice. This combination of aCD3 and aCXCL10 allowed a ten-fold reduction of the required aCD3 dose in RIP-LCMV-GP mice. Moreover, this low dose of aCD3 inactivates half of the T cells, especially the islet antigen-specific T cells. In a second step aCXCL10 prevents the re-entry of recovered T cells into the pancreas. Thereby it creates a protective environment by altering the immune balance towards regulation. Moreover, an aCXCL10 monotherapy was already used in a phase 1 trial for the treatment of ulcerative colitis and showed

Discussion

a reduction of infiltration in immunohistochemistry (185). Since aCD3 also is available as well as tested in humans and the patients are only treated for a short period of time after T1D onset, this combination therapy may be a novel treatment for T1D patients.

10.3 Combination therapy with aJAM-C

In the second approach I showed that a combination of aCD3 and an anti-JAM-C antibody (aJAM-C) slightly improved the remission of T1D compared to the aCD3 monotherapy. Eight doses of the second antibody were injected into the mice one day after the last of three doses aCD3.

In order to block the migration of leukocytes into the inflamed tissue, JAM-C seems to be a good target, since it was shown that the blockade of JAM-C resulted in a reduction of leukocytes at the side of inflammation (129; 186; 187). JAM-C was predominantly found on fibroblasts (188) and in vascular cell-cell interactions (128-130; 149). Correspondingly, I found that in the pancreas CD31⁺ vascular endothelial cells express JAM-C. However, neither podoplanin expressing lymphatic endothelial cells nor the GFAP expressing pancreatic stellate cells co-express JAM-C. In contrast, Zimmerli et al. found that JAM-C was expressed by lymphatic sinusoids of lymph nodes (189). However, they used LYVE-1 instead of podoplanin as lymphatic endothelial cell marker, since it has been shown that both podoplanin and LYVE-1 were expressed on lymphatic endothelial cells (190; 191). Nevertheless, it is possible that the vascular endothelial cells under the capsule of lymph nodes also express LYVE-1.

Several members of the endothelial adhesion molecule family are known, for example VCAM-1 and ICAM-1. They both play an important role in the adhesion and rolling of leukocytes on endothelial cells. ICAM-1 binds to LFA-1 and was also upregulated in pancreatitis (192). However, the blocking of ICAM-1 with an antibody showed almost no effect in the treatment of autoimmune diabetes (115). In contrast, an antibody mediated inhibition of VCAM-1, which binds to VLA-4 and supported the chemotaxis of monocytes (193; 194), delayed the onset of T1D in NOD mice (115). Different to these two adhesion molecules JAM-C was involved in the transmigration of leukocytes (125; 144; 146; 195). Therefore an antibody against JAM-C may have a high potential to block the leukocyte infiltration into inflamed tissue.

The aJAM-C monotherapy showed no benefit when administered at T1D onset, indicated by a similar T cell infiltration in the pancreas and incidence of T1D to

isotype control antibody treated mice. However, JAM-C was upregulated in RIP-LCMV-NP mice at day 10-14 after infection and preventive aJAM-C administration delayed T1D development (130). For that reason JAM-C might be more important in the pre-diabetic rather than in the chronic phase. Interestingly, Christen et al. showed that the T cell infiltration did not differ in aJAM-C treated and untreated RIP-LCMV-NP mice at day 7 or 28 after infection (130). In contrast, in a cerulean induced pancreatitis mouse model, where JAM-C was also upregulated, aJAM-C reduced the infiltration (129). Moreover, it was demonstrated that aJAM-C or soluble JAM-C interfered with the transmigration of lymphocytes (125; 128). Intriguingly, I found a tendency for an increased rather than decreased number of T cells in the pancreas of mice after CT-J administration compared to isotype control antibody treated mice. Many T cells were already in the islets at the moment when aJAM-C treatment was initiated in diabetic RIP-LCMV-GP mice. Possibly, the T cells could not migrate out of the pancreas and accumulated in the pancreas.

JAM-C overexpression did not influence the course of T1D, not even in the slow onset RIP-LCMV-NP model (130). Since LCMV alone induced JAM-C expression, it is hardly surprising that overexpression of JAM-C did not further enhance the infiltration in the RIP-LCMV model. In contrast, JAM-C overexpression increased the influx of inflammatory cells in a lung related disease (196).

In CT-J the treatment with aCD3 reduced the insulinitis to a status similar to the pre-diabetic phase with a reduced number of infiltrated T cells in the pancreas. The addition of aJAM-C should prevent directly or indirectly the re-infiltration of recovered T cells into the pancreas. Unfortunately, similar to the prevention study with aJAM-C in RIP-LCMV-NP mice (130), the addition of aJAM-C to the aCD3 therapy did not improve the aCD3 monotherapy in terms of islet antigen-specific T cell as well as general T cell number or frequency. It is possible that other factors compensate the lack of JAM-C.

Since there was only a slight tendency for a difference in the T cell number, frequency and ratio we investigated the direct effect of JAM-C on the transmigration of leukocytes. JAM-C was suggested to be involved in neutrophil transmigration (127; 186; 197; 198) by its interaction with MAC-1, which is

expressed by neutrophils (119; 126; 145). However, Sircar et al. claimed that JAM-C did not influence the neutrophil migration (199). Nevertheless, the studies were performed *in vitro* under flow condition with a HUVEC cell line and *in vivo* the JAM-C interactions might be more complex. In the present study the addition of aJAM-C to the aCD3 treatment reduced the neutrophil frequency and number in blood, PDLN and pancreas. In line with this finding Zen et al. demonstrated that an aJAM-C antibody reduced the neutrophil (PMN) migration (200). The reduction of neutrophils might be the reason for the slight influence on T cell number and frequency (Figure 40). Intriguingly, I found a higher frequency of neutrophils in the spleen. One may speculate that the neutrophils accumulate upon day 13 (moment of first aJAM-C injection) in the spleen. Possibly, the neutrophils cannot migrate into the tissues and accumulate in the lymphatic system, including the spleen, during aJAM-C therapy. Consistently, Aurrand-Lions et al. also showed that the T cell homing was unaffected by a JAM-C blockade, the retention in LN, however, was indirectly prolonged (201). This may also be a possible scenario in the spleen.

Due to this marginal effect in the pancreas and the high expression of JAM-C on vascular endothelial cells, JAM-C might play a more important role in heavily vascularised tissue such as the lung (196). aJAM-C reduced angiogenesis by rearranging the cell-cell interactions (133), implicating an influence of tumour development (202). MAC-1 is expressed by macrophages and therefore it was not surprising that aJAM-C reduced the number of macrophages in cancer (132; 133). For the reason that macrophages express angiogenic factors (203), a reduction of the number of macrophages also reduced angiogenesis.

In conclusion, I found a combination therapy which slightly improved the aCD3 monotherapy and led to an acceleration of autoimmune diabetes remission. Treatment of diabetic RIP-LCMV-GP mice directly after disease onset with an antibody against JAM-C, did not show a therapeutic effect. Nevertheless, the addition of aJAM-C to the aCD3 monotherapy demonstrated an increased T1D remission, although it did not significantly influence the T cell number, frequency or ratio compared to the aCD3 monotherapy. However, administration CT-J reduced the neutrophil number in the pancreas of mice compared to aCD3 therapy.

Discussion

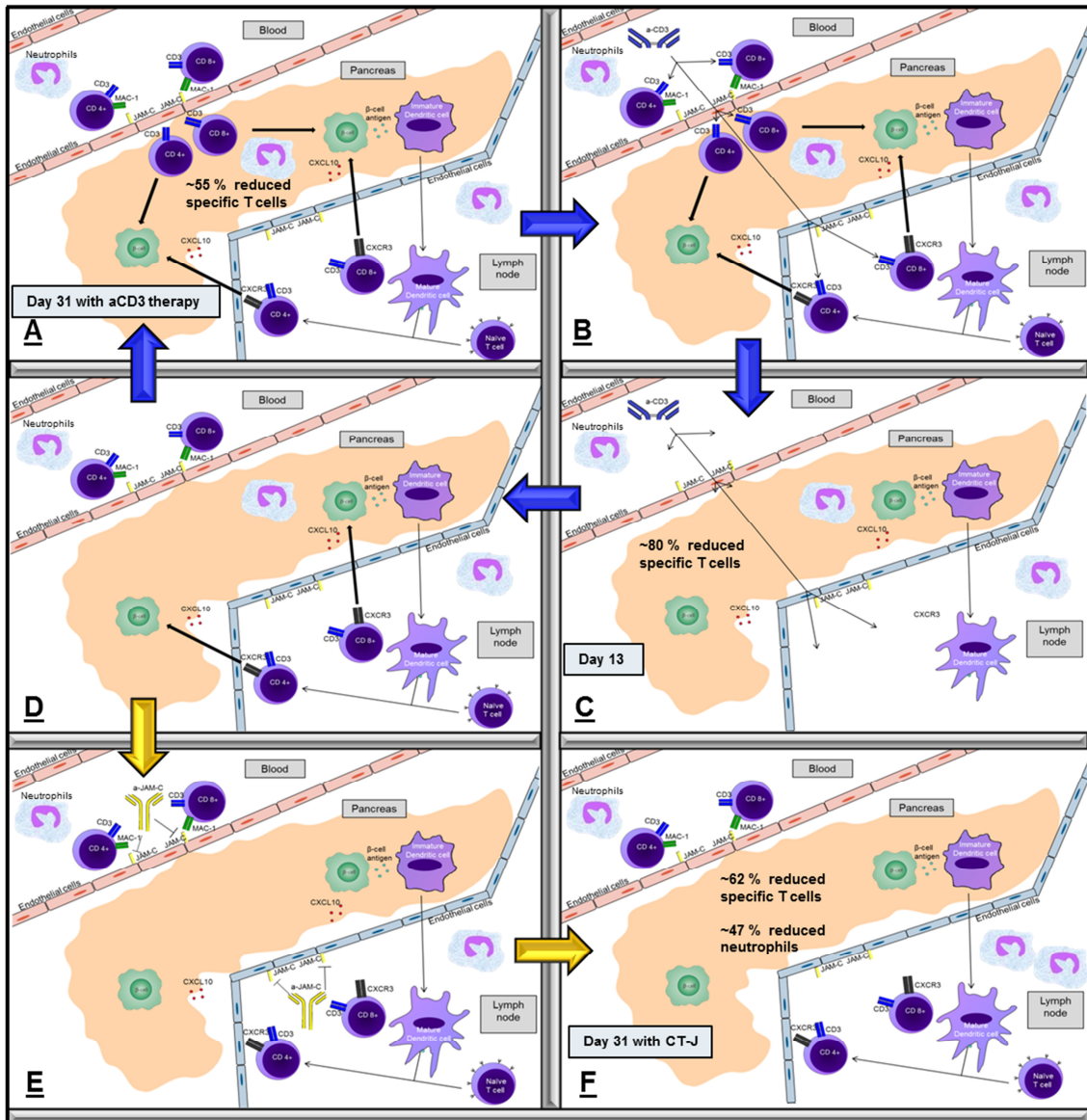


Figure 40: Overview of the CT-J effect.

(A) Environmental and genetic factors may lead to an increased antigen uptake of dendritic cells in the pancreas. In the PDLN the antigen is presented by matured dendritic cells to T cells. Accordingly, there might be a potential activation of cross-reactive T cells by specific antigens. These aggressive T cells and also neutrophils migrate into the pancreas through a CXCL10/CXCR3 or JAM-C/MAC-1 mediated mechanism, respectively. Neutrophils support the attraction of T cells by secreting CXCL10. Subsequently, these T cells attack the antigen presenting β -cells in the pancreas. (B+C) The administration of aCD3 induces a significant inactivation of T cells in lymphoid organs and in the infiltrated tissues. In the pancreas, approx. 80 % of the islet antigen-specific T cells were inactivated in aCD3 treated RIP-LCMV-GP mice at day 13 after infection (D) Soon after, the immune system regenerates and new T cells are produced. (D→A) Unfortunately, without a second therapy these recovered T cells migrate into the pancreas and they attack yet again the β -cells in the pancreas (pathway marked with blue arrows). Consistently, the islet antigen-specific T cells were only reduced by approx. 55 % in aCD3 treated RIP-LCMV-GP mice at day 31 post-infection (E) Administration of aJAM-C blocks the transmigration of leukocytes (pathway marked with yellow arrows) and results in a slight improvement of the aCD3 therapy (F). For instance the neutrophil and islet antigen-specific T cell number was diminished by 47 % and 62 %, respectively.

10.4 Closing remarks

Many combinations with aCD3 exist which address different mechanisms. Many of the approaches to combine aCD3 with general immunosuppressive drugs failed (48; 58; 204). Other combinations of aCD3 with aCD20 (inactivated B cells) (59) or FTY720 (retained T cells in the PDLN) (148) showed an effect at a very early stage of T1D (BG <270 mg/dl). Nevertheless, they did not provide long term remission of T1D. However, some approaches were very promising. They addressed the β -cell proliferation with exendin-4 (63) or aimed at the regulatory T cell induction by (pro)-insulin (60; 61; 205) or GAD65 (62). In our combination therapies as well as in many other approaches the mice with a BG level higher than 500 mg/dl were not treatable with an immune intervention/regulation. In humans, at the diagnosis of T1D the number of insulin producing β -cells was reduced (<30 %), predominantly due to cell death. However, the remaining β -cell mass is still higher, but because of inflammatory stress the insulin production is impaired (36). Consequently, after successful aCD3 therapy it is more likely that recovering β cells re-initiate insulin production rather than β cell regeneration restores the initial mass.

In my opinion, the only way to treat T1D is a combination therapy targeting several aspect of its pathogenesis similar to the therapy suggested by Ludvigsson (206). First of all it is important to attenuate the auto destructive process by immune intervention, for example with aCD3. Second, the recurrence of islet infiltration has to be prevented by a second therapy such as aCXCL10. Third, immunomodulatory measures that create a protective environment by inducing Tregs, such as the addition of Vitamin D₃ (207-210) or treatment with (pro)-insulin (44; 45; 60) as well as GAD65 (43) have to be included. And last, the β -cell mass has to be restored by enhancing β -cell regeneration (211-215) or by islet as well as whole pancreas transplantation (216).

Material and Methods

11 Materials and Methods

11.1 Materials

11.1.1 Molecular weight marker for protein electrophoresis

Prestained Protein Molecular Weight Marker (Carl Roth GmbH):

This is a Mix of following proteins:

Table 1: Proteins of the molecular weight marker.

Protein	Source	Molecular weight [Da]
Myosin	Bovine	245.000
β -galactosidase	E. coli	123.000
Serum albumin	Bovine	95.000
Ovalbumin	Chicken	50.000
Carbonic anhydrase		33.000
Trypsin inhibitor	Soya	23.000
Lysozyme	Chicken	17.000



Figure 41: Banding pattern of the prestained protein marker.

Each protein of the prestained protein marker indicates a specific molecular weight. Myosin (245 kDa), β -galactosidase (123 kDa), serum albumin (95 kDa), ovalbumin (50 kDa), carbonic anhydrase (33 kDa), trypsin inhibitor (23 kDa) and lysozyme (17 kDa) are displayed.

11.1.2 Antibodies

Flow cytometry:

Table 2: Antibodies for flow cytometry.

Antibody	Manufacturer
PerCP-anti-mouse CD3e (Clone 145-2C11)	BD Pharmingen; 553067
APC-anti-mouse CD4/L3T4 (Clone GK 1.5)	Southern Biotech; 1540-11
FITC-anti-mouse CD4/L3T4 (Clone GK 1.5)	Southern Biotech; 1540-02
V450-anti-mouse CD4 (Clone RM4-5)	BD Horizon; 560468
APC-anti-mouse CD8a/Lyt-2 (Clone 53-6.7)	Southern Biotech; 1550-11
APC-Cy7-anti-mouse CD8a/Lyt-2 (Clone 53-6.7)	BD Pharmingen; 557654
FITC-anti-mouse CD8a/Lyt-2 (Clone 53-6.7)	Southern Biotech; 1550-02
PE-Cy5.5-anti-mouse CD8a/Lyt-2 (Clone 53-6.7)	Southern Biotech; 1550-16
PE-Cy7-anti-mouse CD86	BD Pharmingen; 560582
APC-anti-mouse CD11c (p150/90)	eBioscience; 17-0114-81
PE-anti-mouse FoxP3	eBioscience; 12-5773-82
APC-anti-mouse IFN	BD Pharmingen; 554412
PE-anti-mouse IFN	BD Pharmingen; 554413
FITC-anti-mouse IL10	eBioscience; 11-7101-82
V450-anti-mouse MHC class II	eBioscience; 48-5321-82
PE-anti-mouse PDL1 (Clone MIH5)	BD Pharmingen; 558091
Streptavidin-APC	eBioscience; 17-4317-82

Materials and Methods

Immunohistochemistry:

Table 3: Antibodies for immunohistochemistry.

Antibody	Manufacturer
Rat anti-mouse CD4/L3T4 (Clone GK 1.5)	BD Pharmingen; 553043
Rat anti-mouse CD8a/Lyt-2 (Clone 53-6.7)	BD Pharmingen; 553027
Rat anti-mouse Foxp3	eBioscience; 14-5773
Polyclonal guinea pig anti-swine insulin	DakoCytomation; A0564
Biotinylated anti-guinea Pig IgG (H+L)	Vector; BA-7000
Biotinylated anti-rat IgG (H+L)	Vector; BA-4001
Goat anti-mPodoplanin	R&D Systems; AF3244
Goat anti-JAM-C	R&D Systems; AF3244
Rabbit anti-JAM-C	Own production
Rat anti-CD31	BD Pharmingen 557355
Rabbit anti-GFAP	Dako; Z0334
Goat anti-rat Alexa Fluor 488	Invitrogen; A11006
Goat anti-rat Alexa Fluor 594	Invitrogen; A11007
Donkey anti-rabbit Alexa Fluor 488	Invitrogen; A21206
Donkey anti-goat Alexa Fluor 594	Invitrogen; A11058

Treatment:

Table 4: Antibodies for treatment.

Antibody	Manufacturer
Monoclonal CD3 antibody (145-2C11 F(ab') ₂ fragment), Armenian hamster	BioXcell; Be0001-1FAB 4294/0212
Monoclonal CXCL10 antibody (1F11, IgG 2), hamster	Own production
Monoclonal JAM-C antibody (H33, IgG 2), rat	Own production

11.1.3 Enzymes and proteins

Table 5: Enzymes and proteins.

Protein	Manufacturer
Collagenase P	Roche; 11 213 857 001
Collagenase IV	Sigma
CXCL10	eBioscience; 14-8967-80
Dexamethasone	Sigma; D4902
DNase	Sigma; DN25
GM-CSF (recombinant mouse)	R&D Systems; 415-ML
IL-2	Sigma-Aldrich
IL-4 (recombinant mouse)	Peptotech; 214-14
Proteinase K	Carl Roth; 7528.1
Taq-polimerase	Peqlab Biotechnology GmbH; 01-1030

11.1.4 Nucleotides and peptides

Table 6: Nucleotides and peptides.

Peptides (Sequence)	Manufacturer
GP ₃₃ peptide (KAVYNFATM)	
GP ₆₁ peptide (GLKGPDIYKGVYQFKSVEFD)	
NP ₃₁₁ peptide (EGWPYIACRTSIVGR)	
NP ₃₉₆ peptide (FQPQNGQFI)	
GP F Primer (5.' GGG AAA GGA GAA TCC TGG AC 3.')	
GP R Primer (5.' GCA ATC TGA CCT CTG CCT TC 3.')	
NP F Primer (5.' AAT CCA TGT AGG AGC GTT GG 3.')	
NP R Primer (5.' AAC AGC GAG GAC CTC TTG AA 3.')	
CXCL10 KO F Primer (5' TTT TGG CTA AAC GCT TTC ATT 3')	
CXCL10 KO R Primer (5' AAG TGC TGC CGT CAT TTT CT 3')	
dNTP	Peqlab; 20-2011

11.1.5 Kits

Table 7: Kits.

Kit	Manufacturer
ABC-Kit	Vector; PK-7100
Avidin/Biotin blocking Kit	Vector; SP-2001
Peroxidase Substrate Kit DAB	Vector; SK-4100

11.1.6 Cell lines

Rat hybridoma cells for anti-JAM-C antibody production:

Rat hybridoma cells are Sp2/0 cells that were fused with splenocytes from JAM-C antibody immunised male Fisher rats and were originally received from Prof. Beat A. Imhof from the University of Geneva. The cells were grown in DMEM, Na-pyruvate (1mM), Pen//Strep (1%) and FBS (20%)

Hamster hybridoma cells for anti-CXCL10 antibody production:

Hamster hybridoma cells are P3x63 cells that were fused with splenocytes from hamster immunised with Ecoli producing murine CXCL10 and were originally received from Prof. A. D. Luster from the Harvard medical school. The cells were grown in DMEM, Na-pyruvate (1mM), Pen//Strep (1%), NEAA (1mM), HEPES (10mM), FBS (10%) and BME (0.1%).

T_H1 cells for migration assay:

Murine T_H1 cells were received from Prof H. H. Radeke from the University Hospital Frankfurt. The cells were grown in RPMI 1640, L-glutamine (2mM), pen/strep (1%), NEAA (0.1mM) and FBS (10%).

11.1.7 Virus

The Armstrong strain of LCMV, clone 53b, was used for all experiments. LCMV was plaque purified three times on Vero cells (ATCC CCL-81), and stocks were prepared by a single passage on hamster kidney fibroblast cell line BHK-21 (ATCC CCL-10, American Type Culture Collection, Manassas, VA).

11.1.8 Mouse Strains

Transgenic mice (H-2b x H-2d [bx_d]) with rat insulin promoter (RIP) fused to cDNA encoding the NP or GP of LCMV-Arm were made for direct expression of LCMV viral proteins by pancreatic β cells. (217)

RIP-LCMV-GP x CXCL10 KO double transgenic mouse lines were generated by crossing CXCL10 KO single transgenic mice (140) to RIP-LCMV-GP single transgenic lines.

NOD mice were received were initially purchased from The Jackson Laboratories, Bar Harbor, ME, USA and have been bred in the local breeding facility of the Georg-Speyer Haus (GSH), Frankfurt, Germany.

Wild-type C57BL/6 mice were purchased from the breeding colony of Harlan Netherlands.

Experiments were carried out with age- and sex-matched animals kept under specific pathogen free (SPF) conditions and in accordance with German regulations. All animal experiments were approved by the local Ethics Animal Review Board (Darmstadt, Germany).

11.1.9 Chemicals

Table 8: List of used chemicals.

Chemical	Manufacturer
A	
Acetic acid	Sigma Aldrich Chemie GmbH; 33209
Acetone	Sigma Aldrich Chemie GmbH; 32201
Acrylamid (30 %)	Merck Chemicals KGaA
Agarose	Sigma Aldrich Chemie GmbH; A9539
Ammonium acetate	Merck Chemicals KGaA; 1.01116
Ammonium chloride	Merck; 1.01145

Materials and Methods

Ammonium peroxide sulphate (APS)	Sigma Aldrich Chemie GmbH; A3678
Ammonium sulphate	Merck Chemicals KGaA; 101211
Aquamount	Merck Chemicals KGaA; 1.08562
B	
β -mercaptoethanol	Gibco; 31350-010
Bisacrylamide (2 %)	Rothphorese
Brefeldin A	Sigma Aldrich Chemie GmbH; B6542
Bromophenol blue	Roth; 512.1
C	
Calcium chloride di-hydrate	Merck Chemicals KGaA; 1.02382
Chloroform	Sigma Aldrich Chemie GmbH; 32211
Collagen	Corning
Comassie R 250	Bio-Rad; 161-0400
Crystal violet	Sigma Aldrich Chemie GmbH; HT90132
CSFE	Invitrogen
D	
Dimethyl sulfoxide (DMSO)	Sigma Aldrich Chemie GmbH; D5879
Dithiothreitol (DTT)	Fluka; 43817
DMEM + GlutaMax I	Gibco; 61965
E	
Ethylenediamintetraacetic acid (EDTA)	AppliChem; A1103.1000
Ethanol absolute	Sigma Aldrich Chemie GmbH; 24102

Materials and Methods

F	
FACS Clean	BD Biocience; 340345
FACS Flow	BD Biocience; 342003
FACS Shutdown	BD Biocience; 334224
FBS (Foetal bovine serum)	Biochrom AG; S0115
Formaldehyde	Roth; 6749-2
G	
GelRed nucleic acid gel stain	Biotium; 41003
Glucose	Merck; 104074
Glycerol	Roth; 3783.1
Glycine	Roth; 3908.2
H	
Hydrogen peroxide	Roth; 8070.1 Sigma Aldrich Chemie GmbH; 216763 (Histology)
Hydrogen chloride	Riedel-de Haën; 30721
Haematoxylin	AppliChem A4840.1000
HEPES	Sigma Aldrich Chemie GmbH; H0887
I	
Instruplus	Viruguard; 0481
Isoflurane	Abbott; B506
Isopropyl alcohol	Prolabo; R11-36-67

Materials and Methods

K	
Kwik-Stop Styptic Powder	ARC laboratories 106012
L	
Lipopolysaccharide (LPS)	Sigma Aldrich Chemie GmbH; L 2654
M	
Methanol	Roth; T909.1
Mounting Medium Vectashield Hard Set	Vector Laboratories; H-1400
N	
Non-Essential Amino Acids	Gibco; 11140
O	
OCT solution (Tissue-Tek)	Sakura; 4583
P	
Paraformaldehyde	Merck; 1.04005.1000
PBS	Gibco; 14190
Potassium acetate	Sigma Aldrich Chemie GmbH; P1190
Potassium chloride	Roth; 6781.1
Potassium di-phosphate	Merck; 1.05099
di-Potassium phosphate	Roth; 3904.1
Pen/Strep	Gibco; 15140
Percoll	GE Healthcare; 17-0891-01
Peroxidase substrate	Vector; SK-4100
Polyethylene glycol 200 (PEG200)	Sigma Aldrich Chemie GmbH; P3015

Materials and Methods

Protein assay standard I	Bio-Rad; 500-0005
Protein G Matrix (HiTrap)	GE Healthcare; 17-0405-01
R	
Roti Quant (Bredford solution)	Roth; K015.1
RPMI 1640 + GlutaMax I	Gibco; 61870
S	
Saponin	Sigma Aldrich Chemie GmbH;; S7900
Sodium azide	Roth; K305.1 (old) Appchem; A1430 (new)
Sodium chloride	Sigma Aldrich Chemie GmbH; 31434
Sodium hydroxide	Riedel-de Haën; 30620
di-Sodium phosphate di-hydrate	VWR; 28029.292
Sodium dodecyl sulphate (SDS)	Roth; 2326.2
Sodium pyruvate	Gibco; 11360
T	
TEMED	Roth; 2367.3
Triethanolamine	Sigma Aldrich Chemie GmbH; 90278
Tris	Roth; 4855.2
Tris-HCl	Roth; 9090.2
Triton X-100	Sigma Aldrich Chemie GmbH; T8787
Trypan blue	Sigma Aldrich Chemie GmbH; T8154
TWEEN 20 (Polyethylen-Sorbitan-Monolaureat)	Sigma Aldrich Chemie GmbH; P7949

11.1.10 Consumable material and equipment

Table 9: List of consumable material and equipment.

Equipment or material	Manufacturer
A	
Anesthesia unit 1200	Univentor
Autoclave v-150	Systec
B	
Blood glucose test strips dyna Valeo	Dynami CARE; 0537
Blood glucose testing unit dyna Valeo	Dynami CARE
Blood collecting tube, microvette	Sarstedt; 20.1345
C	
Capillary (Heparin coated)	Fisher scientific; 02-668-10
Chromatography unit, äkta-FPLC - Fraction collector FRAC-920 - Mixing Chamber M-925 - 2 Pumps P-920 - Photometer: UVicord VW 2251 - Motor Valve INV-907 - Flow Restrictor FR-904 - Control unit CU-950 - Control Monitor UPC-900	GE
Cell culture flasks (25, 75, 175 cm ²)	Cellstar
Cell scraper	Sarstedt; 83.1830
Cell strainer (70 µm)	BD Falcon; 352350
Cell strainer (100 µm)	BD Falcon; 352360

Materials and Methods

Centrifuge, 5804	Eppendorf
Centrifuge, Multifuge 3 S-R	Thermo Scientific
Column HighTrap XL (5 ml)	GE Healthcare
Cooling unit 4 °C, KSR3PX31	Bosch
Cooling unit 4 °C, comfort	Liebherr
Cooling unit -20 °C, comfort GP4013	Liebherr
Cooling unit -20 °C, economic	Bosch
Cooling unit -80 °C, Herafreeze	Thermo
Cover slip (4 mm)	Menzel-Gläser
Cryotome CM1850 UV	Leica
Cryotubes, Cryo.S (2 ml)	Greiner Bio One
Cryotubes, Cryo pure (2 ml)	Sarstedt; 72.379.002
D	
Disposal base molds	Thermo; 93019402
Disposal bag IK210-C	Sarstedt
Dry block heater, Thermomixer 5436	Eppendorf
Dry block heater, DB20	Techne
E	
Electrophorese Unit Power Pac 1000	Bio Rad
Eppendorf tubes (1,5 ml / 2 ml)	Eppendorf
F	
(Sterile) Filter, Bottle-Top-Filter (250, 500 ml)	Millipore; SCGPU05RE
FACS Unit Canto II	BD

Materials and Methods

FACS tubes	BD Falcon; 352052
G	
Gel Doc, universal hood II	BioRad
Glassware	Schott
Gloves, Vasco Nitril (L)	Braun
Gloves, Latex (M)	VWR; 112-1566
I	
Incubation unit Electron HBSNSR5220	Thermo
Incubation unit BBD 6220	Thermo
Incubation unit (Mice) 3698	Ehret
M	
Magnetic stirrer, RCT-B	IKA-Werke; 885067
Micro scale, CP153	Sartorius
Microliter pipettes, 1000 μ l, 200 μ l, 20 μ l, 10 μ l	Eppendorf, Middleton, USA
Mircotainer SST tubes	BD; 365951
Microtiter plate (96 well, V-bottom)	Anicrin; 3911924
Microtiter plate (96 well, U-bottom)	Anicrin; 3911923
Micro wave	Bosch
Microscope Axiovert 25C	Zeiss
Confocal Microscope LSM 510 META	Zeiss
Microscope Axioskop 2 (with axiocam)	Zeiss
Microscope Biozero, BZ-8000K	Keyence
Multichannel pipette, 200 μ l	Eppendorf, Hamburg

Materials and Methods

N	
Needles (23G, 25G, 27G, 30G)	BD Microlance
P	
Paper towels, clean and clever	Igefa
Parafilm "M" Laboratory Film	American National Can., Chicago, USA
pH-Meter, MultiLab 540	WTW
Pipetting aid unit, accuJet pro	Brand
Pipetting aid unit, Pipetboy	Integra
Plastic pipettes (5, 10, 25, 50 ml)	Corning INC
R	
Rocking platform Shaker SSL4	Stuart
Rocking platform Shaker Duomax 1030	Heidolph
S	
Scale, PT3100	Sartorius, Göttingen
Scanner, 1133	Dell
Slide A lyzer cassette (1-3ml / 10000 MWCO)	Pierce, 66425
Slide A lyzer cassette (3-12ml / 3500 MWCO)	Thermo, 66110
Slides (Sialin coated)	Menzel-Gläser
Slides (Superfrost plus)	Thermo; J1800AMN
Software FACS Diva	BD
Software Flowjo 7.6.5	Treestar

Materials and Methods

Software Prism 5	Graphpad
Software Magellan 5.0	Tecan
Software Epson Scan	Epson
Syringes (1 ml)	Terumo; BS-01T
Syringes (1 ml with needle), omnican	Braun; 91511335
Syringes (3, 5, 10, 20 ml)	Braun
T	
Tabletop centrifuge, Biofuge pico	Thermo Scientific
Tabletop centrifuge, Biofuge fresco	Thermo Scientific
Tissue culture dishes	Cellstar
Tissue culture plates (6, 12, 24, 48, 96 well)	Cellstar
Transfer Membrane	PolyScreen; NEF1002
Transmigration MTP (3 μ m)	Corning 3385
(Falcon) Tubes (15, 50 ml)	Cellstar
V	
Vortex unit, MS2	IKA
W	
Washing machine, UXTHS-GH	Hobart
Water bath, Isotemp 215	Fisher Scientific

11.1.11 Solutions, buffers and culture media

The following solutions are prepared with double dest. water, if not mentioned otherwise.

Table 10: List of used buffers and solutions.

Solution	Composition
A	
ABC reagent solution (Peroxidase substrate kit DAB)	5 ml ddH ₂ O 2 drops of buffer 4 drops of DAB stock solution 2 drop of hydrogen peroxide solution
Ammonium acetate stock	NH ₄ Ac 8 M
APS stock (10%)	APS 10 % (w/v) Store at -20 °C
C	
Calcium chloride solution	Calcium chloride 25 mM
Collagenase P stock	150 U/ml (approx.. 100 mg/ml) 1 x PBS
Comassie staining solution for SDS-PAGE	Comassie R-250 0,2 % (w/v) Acetic acid 10 % (v/v) Methanol 0.1 % (v/v)
Coomassie destain solution for SDS-PAGE	Acetic acid 10 % (v/v) Methanol 10 % (v/v)
Coomassie destain solution for SDS-PAGE (fast)	Acetic acid 10 % (v/v) Methanol 40 % (v/v)
CSFE stock	CSFE 5 mM

Materials and Methods

Culture Medium (1F11)	DMEM Na-pyruvate 1 mM Pen//Strep 1 % (100 u/ml) NEAA 1 mM HEPES 10 mM FBS 10 % (v/v) BME 0.1 % (v/v)
Culture Medium (H33)	DMEM Na-pyruvate 1 mM Pen//Strep 1 % (100 u/ml) FBS 20 % (v/v)
Culture Medium (Migration assay)	RPMI 1640 BSA 1% HEPES 1 mM
Culture Medium (RPMI complete)	RPMI 1640 L-Glutamine 2 mM Pen//Strep 1 % (100 u/ml)
Culture Medium (T _H 1 Cell line)	RPMI 1640 L-Glutamine 2 mM Pen//Strep 1 % (100 u/ml) NEAA 0.1 mM FBS 10 % (v/v) IL-2 2 µg/ml
D	
Dialysis buffer	1x PBS
DNase stock	DNase 20 µg/ml
E	
EDTA solution	EDTA 0.5 M

Materials and Methods

Elution buffer	Glycine 0.1 M pH 2.7
F	
FACS buffer	1 x PBS FBS 1 % NaN ₃ 0.1% pH 7.5
FACS fixation buffer (+PFA)	1 x PBS FBS 1 % NaN ₃ 0.1% PFA 1 % pH 7.5
FACS saponin buffer	1 x PBS FBS 1 % NaN ₃ 0.1% Saponin 0.1 % pH 7.5
FACS saponin fixation buffer (+PFA)	1 x PBS PFA 4 % Saponin 0.1 % pH 7.5
Glycine	0.1M pH 2.7
H	
Histo H ₂ O ₂ solution	H ₂ O ₂ 0.3 % NaN ₃ 0.1 % 1x PBS

Materials and Methods

Histo PFA solution (4%)	PFA 4 % (w/v) K ₂ HPO ₄ 80 mM KH ₂ PO ₄ 20 mM pH 7,3-7,4
L	
2x Laemmli sample buffer	Tris 50 mM Glycerol 10 % SDS 2 % DTT 40 mM pH 6.8
LCMV stock	2 x 10 ⁵ PFU
M	
Mouse tail buffer	SDS 0.5 % NaCl 100 mM Tris (pH8) 50 mM EDTA 3 mM
P	
PCR gel buffer (6x)	Glycerine 12 % (v/v) Bromophenol blue
PCR gel marker mix	Marker 10 % (v/v) PCR gel buffer 1x
Phosphate buffered saline (PBS)	NaCl 140 mM KCl 10 mM Na ₂ HPO ₄ 6,4 mM KH ₂ PO ₄ 2 mM

Materials and Methods

PBS Tween-Puffer	NaCl 140 mM KCl 10 mM Na ₂ HPO ₄ 6,4 mM KH ₂ PO ₄ 2 mM Tween 20 0,05% (v/v) BSA 1 %
Percoll gradient	1 x PBS Percoll 40 % (v/v) 10 x PBS 4.4 % (v/v)
Proteinase K	Proteinase K 10 mg/ml Tris-HCl 10 mM pH 7.5
Protein sample buffer (4x) reducing	SDS PAGE – Upper gel buffer 40 % (v/v) Glycerol 40 % (v/v) Bromophenol blue 10 % (v/v) SDS 2 mM DTT 40 mM
R	
Red blood cell lysis buffer (0.74%)	NH ₄ Cl 0.74 %
Red blood cell lysis buffer (0.83%)	NH ₄ Cl 0.83 %
Running buffer (10x)	Tris 250 mM Glycine 1.92 M SDS 1 % pH 8.3
S	
SDS-Stock (10%)	SDS 10 % (w/v)
SDS PAGE - Lower gel buffer	Tris 1,5 M pH 8.8

Materials and Methods

SDS PAGE - Upper gel buffer	Tris 0.5 M Bromophenol blue 10 % (w/v) pH 6.8
Sodium chloride solution	Sodium chloride 5 M
Sodium azide solution	Sodium azide 10 %
T	
TAE buffer	Tris-Acetate 40 mM EDTA 1 mM
Tris buffer (pH10)	Tris 1 M pH 10.0
Tris buffer (pH8)	Tris 1 M pH 8.0
Tris buffer (pH7.5)	Tris 1 M pH 7.5

11.2 Methods

11.2.1 Cell biological methods

11.2.1.1 Cultivation of cells

Cells were cultured in plastic cell culture flasks (25, 75 or 175 cm²) at 37 °C (5 % CO₂, relative humidity 95 %) with appropriate medium. Not adherent cells were split every 3 or 4 days. Cells were centrifuged (For T_H1 cells: 260 x g for 6 minutes at 4 °C in Falcon tubes). Medium was removed. Finally the cells were resuspended in appropriate medium and split.

11.2.1.2 Freezing of cells

Cryotubes were pre-cooled for 30 minutes at 4 °C. The freezing medium was prepared containing 90 % FBS and 10 % DMSO and also pre-cooled at 4 °C. Cells were counted, centrifuged at 260 x g for five minutes and the supernatant discarded. The pellet was resuspended to a concentration of 6×10^6 cells/ml with pre-cooled freezing medium and 1 ml aliquots were transferred into cryotubes. The aliquots were placed into a polystyrene box and stored in the -80 °C deep freezer. The polystyrene box ensures that the cell samples are cooled down to -80 °C at a rate of approx. 1 °C/min. After 24 hours, the cryotubes were transferred to the liquid nitrogen tank (-196 °C).

11.2.1.3 Thawing of cells

A 15 ml tube with 9 ml 37 °C warm medium was prepared. Cell aliquots were taken out of the liquid nitrogen tank and warmed immediately in a water bath (37 °C) until cells started to thaw. 1 ml of warm medium was added and transferred back to the 15 ml tube. This step was repeated until all cells were thawed. This is important to dilute the DMSO as fast as possible to avoid cell damage. After centrifuging cells at 260 x g for five minutes, the supernatant was discarded and cells were cultured in appropriate medium.

11.2.1.4 Determining the density of a cell suspension

The cellular density of a suspension was determined by mixing the cell suspension with trypan blue solution. The cells in the resulting suspension were counted directly in a Neubauer chamber using a microscope. Dead cells had a cytoplasmic staining with trypan blue. A grid at the bottom of the chamber was used to count the cells and the cell density (cells per ml) was calculated with the following formula:

Cellular density (cells/ml) = number of cells on the grid x dilution factor x 10^4 ml^{-1}

11.2.1.5 Migration assay

Needed wells of the 96-well MTP with a 3 μm insert were incubated with 235 μl migration medium at 37 $^{\circ}\text{C}$ until further use. $\text{T}_{\text{H}}1$ cells of a T75 flask were split and transferred into two falcons (approx. 1.5×10^7 cells/falcon). The cells were centrifuged at 550 x g for five minutes at 4 $^{\circ}\text{C}$, then the medium was sucked off and one pellet was resuspended in 10 ml cold migration medium and the other one in 10 ml cold PBS. This washing step was repeated two times and one pellet was resuspended in 1 ml cold migration medium and the other one in 1 ml cold PBS. After counting both cell suspensions a concentration of 2.7×10^6 cells/ml was adjusted with migration medium for the medium cell suspension and a concentration of 5×10^6 cells/ml was adjusted with PBS for the PBS cell suspension. Both suspensions were stored at 4 $^{\circ}\text{C}$ until further use. The medium of the MTP was removed and 235 μl of migration medium containing 20 μM CXCL10 and 50 $\mu\text{g/ml}$ of the specific antibody were pipetted into each well. The membrane insert was put on the plate and 75 μl medium cell suspension were pipetted into the wells of the insert. The plate was incubated at 37 $^{\circ}\text{C}$ and 5 % CO_2 for two hours.

A final concentration of 0.5 μM CSFE was adjusted in the PBS cell suspension and it was incubated for ten minutes at RT in the dark. After filling up the suspension to 10 ml with FACS staining buffer, the cells were centrifuged at 550 x g for five minutes at 4 $^{\circ}\text{C}$, then the medium was sucked off and the pellet was resuspended in FACS staining buffer. This washing step was repeated 3 times and the pellet was resuspended in 1 ml FACS fixing buffer. The cells were counted and a concentration of 2×10^6 cells/ml was adjusted with FACS fixing buffer.

The MTP was centrifuged at 100 x g for two minutes at 4 $^{\circ}\text{C}$ to stop the assay. The insert was removed and the suspension from the insert was sucked off. 150 μl suspension from the 96-well plate were transferred into a V-bottom 96-well plate and it was centrifuged 550 x g for five minutes at 4 $^{\circ}\text{C}$. The medium was discarded and the remaining cells from the MTP were transferred into the same wells of the V-bottom 96-well plate like before. The cells were centrifuged again at 550 x g for five minutes at 4 $^{\circ}\text{C}$, then the medium was discarded and the pellet was resuspended with 175 μl FACS fixing buffer

containing 0.05×10^6 cells/ml CFSE labelled cells. The cells were transferred to FACS tubes and analysed by flow cytometry with a BD FACS Canto II.

11.2.1.6 Isolation of lymphocytes from pancreatic islet cells

The pancreas was extracted from mice and stored in 5 ml cold RPMI. The medium was sucked off and lymphocytes from pancreatic islet cells were isolated by injecting 3 ml of collagenase P solution (1.2 U/ml in RPMI) into the pancreas. After 30 minutes incubation at 37 °C the warm RPMI was removed and 10 ml of cold RPMI containing 20 µg/ml DNase I were added. The pancreas was shaken for one minute and pressed through a 70 µm cell strainer. The suspension was transferred into a 50 ml falcon tube and filled up with RPMI containing 20 µg/ml DNase I to 50 ml. The cells were centrifuged at 550 x g for five minutes at 4 °C, then the medium was sucked off and the pellet was resuspended in 1 ml RPMI containing 20 µg/ml DNase I. 5 ml 40 % Percoll in a 50 ml Falcon tube were prepared and with 1 ml cell suspension overlaid. The gradient was centrifuged at 600 x g for 20 minutes at 4 °C. After that the pellet was transferred with a transfer pipette in a new 15 ml tube with 10 ml cold RPMI. The cells were centrifuged at 550 x g for five minutes at 4 °C, then the medium was sucked off and the pellet was resuspended in RPMI complete.

11.2.1.7 Isolation of splenocytes

The spleen was extracted from mice and stored in 5 ml cold RPMI. Splenocytes were isolated by pressing the spleen through a 70 µm cell strainer. The suspension was centrifuged at 550 x g for five minutes at 4 °C and the supernatant was discarded. To eliminate the red blood cells the pellet was resuspended in 2 ml 0.83 % NH₄Cl in PBS and incubated two minutes at RT under occasional shaking. 10 ml RPMI were added to stop the reaction and the clot was extracted by using a transfer pipette. The cells were centrifuged at 550 x g for five minutes at 4 °C, the supernatant discarded and the pellet was resuspended in RPMI complete.

11.2.1.8 Isolation of lymphocytes from pancreatic draining lymph nodes

The PDLN was extracted from mice and stored in 5 ml cold RPMI. Lymphocytes were isolated by pressing the lymph node through a 70 µm cell strainer. The suspension was centrifuged at 550 x g for five minutes at 4 °C, the supernatant discarded and the pellet was resuspended in RPMI complete.

11.2.1.9 Isolation of lymphocytes from blood

The blood was extracted from mice and stored in 5 ml cold RPMI. Lymphocytes were isolated by centrifuging at 550 x g for five minutes at 4 °C and the supernatant was discarded. To eliminate the red blood cells the pellet was resuspended in 6 ml 0.83 % NH₄Cl in PBS and incubated 5 minutes at RT under occasional shaking. 8 ml RPMI was added to stop the reaction and the clot was extracted by using a transfer pipette. The cells were centrifuged at 550 x g for five minutes at 4 °C, the supernatant discarded and the pellet was resuspended in RPMI complete.

11.2.1.10 Flow cytometry

Cells from blood, spleen, pancreatic draining lymph nodes and pancreas were isolated like described above. Around 10⁶ cells were transferred to a V-bottom 96-well plate. The cells were centrifuged at 550 x g for five minutes at 4 °C, the supernatant discarded and the cells were resuspended with 150 µl FACS PBS/staining buffer. The washing step was repeated and the cells were stained with the respective fluorochrome labelled antibody in 50 µl FACS PBS/staining buffer for 30 minutes at 4 °C in the dark. Then the cells were centrifuged again at 550 x g for five minutes at 4 °C, the supernatant discarded and the cells were resuspended with 150 µl FACS PBS/staining buffer. The washing step was repeated twice. After the last washing step the cells were fixed in 200 µl FACS-fixation buffer, transferred to FACS tubes and analysed by flow cytometry with a BD FACS Canto II.

11.2.1.11 Intracellular cytokine stain (ICCS)

Restimulation of lymphocytes:

Approx. 10^6 cells were added per well of a U-bottom 96-well plate. The cells were centrifuged at 550 x g for five minutes at 4 °C, the supernatant discarded and the cells were resuspended in RPMI complete containing specific stimulant (2 µg/ml GP₃₃, NP₁₉₆ or 4 µg/ml GP₆₁) and 2 µg/ml Brefeldin A to block secretion of IFN γ . The plate was incubated overnight (Max.16 hours) at 37 °C and 5 % CO₂.

Staining:

The cells were transferred to a V-bottom 96-well plate. The cells were centrifuged at 550 x g for five minutes at 4 °C, the supernatant discarded and the cells were resuspended with 150 µl FACS PBS/staining buffer. The washing step was repeated and the cells were stained with fluorochrome labelled antibody of choice in 50 µl FACS PBS/staining buffer for 30 minutes at 4 °C in the dark. Then the cells were centrifuged again at 550 x g for five minutes at 4 °C, the supernatant discarded and the cells were resuspended with 150 µl FACS PBS/staining buffer. The washing step was repeated twice and after the last washing step the cells were fixed and permeabilised with 100 µl of PFA/saponin solution for 10 minutes at RT. The cells were centrifuged at 550 x g for five minutes at 4 °C, the supernatant discarded and the cells were resuspended with 150 µl FACS PBS/saponin buffer. The washing step was repeated and the cells were stained with APC-conjugated anti-mouse-IFN- γ and/or PE-conjugated anti-mouse-FoxP3 antibody in 50 µl PBS/saponin buffer for 30 minutes at 4°C in the dark. The cells were centrifuged at 550 x g for five minutes at 4 °C, the supernatant discarded and the cells were resuspended with 150 µl FACS PBS/saponin buffer. The washing step was repeated twice with FACS PBS/saponin buffer and once with FACS PBS/staining buffer. The cells were fixed in 200 µl FACS-fixation buffer, transferred to FACS tubes and analysed by flow cytometry with a BD FACS Canto II.

11.2.1.12 Antibody production and purification

Preparation:

Rat hybridoma cells were grown in appropriate medium. Nine parts collected supernatants were diluted with one part 10x PBS and filtered with 0.22 µm polystyrene filter.

Purification:

For the purification of the antibody 5 ml Protein G sepharose 4 fast flow column and FPLC was used. Sepharose G column was washed with 10x column capacity 1x PBS with a separate pump.

5 l supernatant were loaded to the column over night at 4°C and with a speed of 250 ml/h with a separate pump.

The column was connected to the FPLC and after washing the pumps the column was washed with 10x column capacity 1x PBS. The antibodies were eluted with 8x column capacity 0.1 M glycine (pH 2.7) and 2 ml fractions were collected in 15 ml Falcons containing 74 µl 1 M Tris pH 10 to immediately neutralise the solution. The column was washed with 0.1 M glycine (pH 2.7) till no antibody was bounded anymore to the column and then it was washed with 10x column capacity PBS. The loading and elution step were repeated once and at the end the column was washed with 20 % ethanol.

Analyses:

The concentrations of the fractions were measured by Bradford assay and fractions, which exceed a concentration of 1 mg/ml were pooled. The solution was dialysed against 5 l 1x PBS overnight and after changing the PBS it was dialysed again for 6-8 hours. The antibody was centrifuged at 1940 x g for five minutes at 4 °C and the supernatant was split into 1 ml aliquots. At the end the antibody concentration and the purity was measured by Bradford assay and SDS-PAGE. The aliquots were stored at -80 °C until use.

11.2.1.13 Immunohistochemistry stainings

Organs were harvested at the times indicated and embedded in Tissue-Tek OCT. The OCT was quick-frozen on dry ice and stored at -80 °C. After incubating the samples for one hour at -20 °C 6-7 µm tissue sections were cut using a cryomicrotome at -20 °C and mounted on sialin-coated slides. One sample was stained with haematoxylin to identify regions with many islets under the microscope and consecutive sections were taken. The sections were stored at -20 °C until use.

Fixing:

Fixing A: Sections were fixed in 95 % ethanol or 1:1 diluted ethanol/acetone at -20 °C for 15 minutes and after drying the slides on a paper towel for ten minutes circles were drawn around the specimen with a wax pencil.

Fixing B: Circles were drawn around the specimen with a wax pencil and thawed for a short time. 2-3 drops 4 % (w/v) Histo PFA solution were added to each specimen and it was incubated at RT for 15 minutes.

Blocking:

The sections were washed two times in PBS for two minutes and each specimen was incubated with 100-200 µl Histo H₂O₂ solution (0.3 % H₂O₂ / 0.1 % NaN₃ in PBS) for 10 minutes at RT. After washing twice in PBS for two minutes two drops of avidin were added to each specimen and each was incubated for 10 minutes at RT. The sections were washed again two times in PBS for two minutes and two drops of biotin were added to each specimen and each was incubated for 10 minutes at RT. The sections were washed again twice in PBS for two minutes. 100-200 µl 10 % FBS in PBS was added and the sections were incubated for 30 minutes at RT.

Staining:

The 10 % FBS in PBS was tapped off and 100 µl of the first antibody diluted 1:50-1:1000 in 10 % FBS in PBS were added to each specimen and the sections were incubated for two hours at RT in a humidified chamber in the dark. After tapping off the first antibody solution, the sections were washed

twice in PBS for four minutes and 120 µl of biotinylated secondary antibody diluted 1:400-1:500 in 10 % FBS in PBS were added to each specimen and it was incubated for one hour at RT in a humidified chamber in the dark. The secondary antibody solution was tapped off and sections were washed two times for four minutes in PBS. Each specimen was incubated for 30 minutes at RT with one drop ABC reagent solution. The sections were washed two times in PBS for four minutes and 120 µl peroxidase substrate was added to each specimen and the sections were incubated for two to five minutes at RT. The reaction was stopped by washing in PBS for five minutes and the sections were counterstained in haematoxylin solution for three to five minutes at RT. After washing twice in PBS for four minutes two drops of aquamount were added to each section and a coverslip was placed onto each slide. Then the sections were incubated at RT overnight and pictures were taken with a microscope (Biozero BZ-8000, Keyence / Zeiss).

11.2.1.14 Immunofluorescence stainings

Organs were harvested at the times indicated and embedded in Tissue-Tek OCT. The OCT was quick-frozen on dry ice and stored at -80 °C. After incubating the samples for one hour at -20 °C 6-7 µm tissue sections were cut using a cryomicrotome at -20 °C and mounted on sialin-coated slides. One sample was stained with haematoxylin to identify regions with many islets under the microscope and consecutive sections were taken. The sections were stored at -20 °C until use.

Fixing:

Fixing A: Sections were fixed in 95 % ethanol at -20 °C for 15 minutes and after drying the slides on a paper towel for ten minutes circles were drawn around the specimen with a wax pencil.

Fixing B: Circles were drawn around the specimen with a wax pencil and thawed for a short time. 2-3 drops 4 % (w/v) Histo PFA solution were added to each specimen and it was incubated at RT for 15 minutes.

Blocking:

The sections were washed two times in PBS for two minutes and each specimen was incubated with 100-200 μ l 10 % FBS in PBS for 30 minutes at RT.

Staining:

The 10 % FBS in PBS was tapped off and 100 μ l of the first antibody diluted 1:50-1:1000 in 10 % FBS in PBS were added to each specimen and the sections were incubated for two hours at RT in a humidified chamber in the dark. After tapping off the first antibody solution, the sections were washed twice in PBS for four minutes and 120 μ l of fluorophore labelled secondary antibody diluted 1:400-1:500 in 10 % FBS in PBS were added to each specimen. It was incubated for one hour at RT in a humidified chamber in the dark. The secondary antibody solution was tapped off and sections were washed two times for four minutes in PBS. After washing one drop of Vectashield Hard Set was added to each section and a coverslip was placed onto each slide. Then the sections were incubated at RT overnight and pictures were taken with a confocal microscope (Zeiss LSM 510 META).

11.2.2 Molecular biological methods

11.2.2.1 Mouse tail DNA isolation

Tail biopsies (0.3 cm) were digested overnight at 55°C with 500 μ l Mouse tail buffer containing 0.1 mM proteinase K, 75 μ l 8 M KOAc and 500 μ l chloroform were added and the tubes were inverted several times. The samples were incubated for 15 minutes at -80 °C and after thawing they were centrifuged at 16060 x g for ten minutes at 4 °C in a micro-centrifuge. Then the water phase was transferred to new tubes containing 1 ml 95 % ethanol and stored at 4 °C overnight.

After centrifugation at 16060 x g for ten minutes at 4 °C the supernatant was removed and 1 ml 70 % ethanol was added. The samples were centrifuged again at 16060 x g for ten minutes at 4 °C and the supernatant was removed.

Materials and Methods

The DNA pellet was air-dried for 20 to 30 minutes and then dissolved in 100 μ l TE buffer and stored at 4 °C.

11.2.2.2 Polymerase chain reaction (PCR)

PCR was used to amplify the transgenic insert of the RIP-LCMV-GP, RIPLCMV-NP, and CXCL10 mice for screening.

Table 11: The components of the PCR reaction.

	NP, CXCL10	GP
ddH ₂ O	19.9 μ l	14.3 μ l
10x PCR buffer	2.5 μ l	2 μ l
10 mM dNTP-Mix	0.5 μ l	1.6 μ l
10 μ m reverse Primer	0.5 μ l	0.5 μ l
10 μ m forward Primer	0.5 μ l	0.5 μ l
TAQ-Polymerase	0.1 μ l	0.1 μ l
DNA	1 μ l	1 μ l
Volume	25 μ l	20 μ l

All buffers and reaction components had to be stored at 4 °C and they were pipetted into micro Eppendorf tubes in the same order as in the table above. For all reactions a water sample and an antigen negative sample were included as negative controls and an antigen positive sample to confirm the efficiency of the PCR result.

Table 12: Cycling.

	NP, CXCL10	GP
initial denaturation at	94 °C > 5 min	94 °C > 3 min
Cycles	35	35
denaturation at	94 °C > 30 sec	94 °C > 45 sec
primer annealing at	56 °C > 30 sec	56 °C > 45 sec
elongation at	72 °C > 1 min	72 °C > 1 min
additional elongation at	72 °C > 3 min	72 °C > 3 min
Cool to	4 °C	4 °C

PCR products were analysed by agarose gel electrophoresis.

11.2.2.3 DNA agarose gel electrophoresis

Separation of DNA fragments of different sizes was achieved by agarose gel electrophoresis. 1 % agarose gel was prepared. Therefore agarose was dissolved in TAE buffer by heating it in the microwave. After cooling to hand temperature 0.5 x GelRed was added and the solution was poured into a gel tray with combs. After setting, the gel was placed into an electrophoresis container containing 1 x TAE as running buffer and the combs were removed. 16.6 % of 6x DNA loading dye were added to the samples and the slots were loaded with a DNA molecular weight marker and DNA samples. The separation was performed with 100V for 15-20 minutes and pictures were taken with the Gel Doc unit.

11.2.2.4 SDS-PAGE

Proteins were separated by SDS-PAGE. An appropriate separating gel was prepared using a 0.75 mm spacer:

Materials and Methods

Table 13: Lower SDS-gel.

% Acrylamide	7.5 %	10 %	12 %	15 %	20 %
Acrylamide (30 %; 0.8 % bisacrylamide)	2.50 ml	3.33 ml	4.00 ml	5.00 ml	6.67 ml
Lower gel buffer	2.50 ml	2.50 ml	2.50 ml	2.50 ml	2.50 ml
Dist. water	4.90 ml	4.07 ml	3.40 ml	2.40 ml	0.73 ml
SDS (20 %)	50 μ l	50 μ l	50 μ l	50 μ l	50 μ l
TEMED	5 μ l	5 μ l	5 μ l	5 μ l	5 μ l
APS (10 % w/v)	50 μ l	50 μ l	50 μ l	50 μ l	50 μ l

Just after adding the TEMED and APS, the acrylamide solution was poured into the chamber to about 5 cm from the top and an isopropanol or water overlay was added. After one hour of polymerisation the overlay was removed and an appropriate stacking gel was prepared:

Table 14: Upper SDS gel.

% Acrylamide	3 %	4 %
Acrylamide (30 %; 0.8 % bisacrylamide)	0.50 ml	0.67 ml
Upper gel buffer	1.25 ml	1.25 ml
Dist. water	3.25 ml	3.08 ml
SDS (20 %)	25 μ l	25 μ l
TEMED	5 μ l	5 μ l
APS (10 % w/v)	25 μ l	25 μ l

The acrylamide solution was poured and immediately after pouring, the comb was added. The gel was cooled down for 30 minutes and after setting it was mounted in the electrophoresis unit. The inner and outer chamber was filled

with 1x Running buffer. The comb was removed and the wells were washed with 1x Running buffer to remove any unpolymerised acrylamide. Samples were heated for 5 minutes at 95 °C in 4x Laemmli sample buffer and the Roti prestained marker was heated for 5 minutes at 70 °C. 10 µl of the samples and the Roti prestained marker were loaded. Electrophoresis was performed at 140 V until the blue front reached the bottom of the gel (1-1.5 hours) and pictures were taken with the Gel Doc unit.

11.2.2.5 Bradford assay

Protein concentrations were measured with the Bio-Rad Protein assay. 99 µl Elution buffer (Dilution buffer of the samples) and 1 µl protein sample were mixed and serial diluted 1:2 with Elution buffer over 11 steps in duplicates in a 96-well flat bottom plate. The standard solution (2 mg/ml) was serial diluted 2-fold with Elution buffer over 11 steps in duplicates and two wells were filled with 100 µl Elution buffer as blank controls. Colour developer Roti-Quant was diluted 1:5 in dist. water, 200 µl were added to all wells and the plate was measured at 595 nm with an ELISA micro plate reader (Sunrise, Tecan).

11.2.3 Experiments with mice

11.2.3.1 Blood collection

Mice were anaesthetised with isoflurane and blood samples were taken retrobulbar with a heparin coated capillary. The blood samples were stored in 5 ml RPMI at 4 °C for a short time until further use.

11.2.3.2 Blood glucose levels

Blood samples were obtained from the tail vein. Blood glucose (BG) was monitored with a dyna Valeo glucometer from dynamiCARE at weekly intervals. Animals with BG levels >300 mg/dl were considered diabetic (79) and levels >600 mg/dl cannot be measured and were considered to be 600 mg/dl.

11.2.3.3 Injections

LCMV-Arm:

The LCMV-Arm stock was diluted to 1×10^5 PFU/ml with cold PBS and stored at 4 °C. 100 µl of the LCMV-Arm dilution (1×10^4 PFU) were injected i.p. into the mice with a syringe.

Anti-CD3 antibody:

If not mentioned otherwise the anti-CD3 antibody was diluted to 300 or 30 µg/ml with cold PBS and stored at 4 °C. 100 µl of the anti-CD3 antibody dilution (30 µg or 3 µg) were injected i.v. retrobulbar into mice with a syringe at day 10, 11 and 12 after LCMV-infection in RIP-LCMV-GP mice or 0, 1, 2 days after therapy start in NOD mice. Every dose was given at the same time in the afternoon.

Anti-CXCL10 antibody:

The anti-CXCL10 antibody (aCXCL10) was diluted to 1 mg/ml with cold PBS and stored at 4 °C. 100 µl of the aCXCL10 dilution (100 µg) were injected i.p. into mice with a syringe at day 13, 14, 17, 19, 21, 24, 26 and 28 after LCMV-infection in RIP-LCMV-GP mice or at day 3, 4, 7, 9, 11, 14, 16 and 18 after therapy start in NOD mice. Every dose was given either on Monday mornings, on Wednesday/Thursday middays or on Friday afternoons.

Anti-JAM-C antibody:

The anti-JAM-C antibody (aJAM-C) was diluted to 1 mg/ml with cold PBS and stored at 4 °C. 100 µl of the aJAM-C dilution (100 µg) were injected i.p. into mice with a syringe at day 13, 14, 17, 19, 21, 24, 26 and 28 after LCMV-infection in RIP-LCMV-GP mice or at day 3, 4, 7, 9, 11, 14, 16 and 18 after therapy start in NOD mice. Every dose was given either on Monday mornings, on Wednesday/Thursday middays or on Friday afternoons.

11.2.3.4 In vivo cytotoxic assay

Cultivation:

Lymphocytes were isolated from spleen of wild-type C57BL/6 mice and up to three spleens were stored in a 15 ml Falcon tube filled with 10 ml RPMI. Splenocytes were isolated by pressing the spleen through a 70 μm cell strainer. The suspension was centrifuged at 550 x g for five minutes at 4 °C and the supernatant was discarded. To eliminate the red blood cells the pellet was resuspended in 6 ml 0.83 % NH_4Cl in PBS and incubated two minutes at RT under occasional shaking. 8 ml RPMI was added to stop the reaction and the clot was extracted by using a transfer pipette. The cells were centrifugated at 550 x g for five minutes at 4 °C, the supernatant discarded and the pellet was resuspended in 10 ml RPMI complete. After counting the cells a concentration of 5×10^6 cells/ml was adjusted with RPMI complete. The suspension was split into two portions and one portion also received the peptide GP_{33} at a final concentration of 2 $\mu\text{g}/\text{ml}$. 10 ml portions were transferred in each uncoated tissue culture dish and the suspensions were incubated overnight at 37 °C and 5 % CO_2 .

Staining:

On the next day the cells were harvested, if necessary with a cell scraper and transferred in falcon tubes. The cells were centrifuged at 550 x g for five minutes at 4 °C, the supernatant discarded and the pellet was resuspended in 10 ml RPMI (without FBS). After counting the cells a concentration of 5×10^6 cells/ml was adjusted with RPMI (without FBS). CFSE was given to peptide unloaded cells at a final concentration of 5 μM and it was given to peptide loaded cells at a final concentration of 0.5 μM . The suspensions were incubated for 10 minutes at RT in the dark and then the tubes were filled up with RPMI complete. The cells were centrifuged at 550 x g for five minutes at 4 °C, the supernatant discarded and the pellet was resuspended in RPMI complete. This washing step was repeated twice and after counting the cells for each cell suspension a concentration of 1.5×10^8 cells/ml was adjusted with RPMI. Always 10 μl were taken out for FACS analyses and the peptide loaded and

unloaded cells were mixed. 200 μ l of this mix (1.5×10^7 peptide loaded and 1.5×10^7 unloaded cells) were injected i.v. into mice.

Sample preparation:

100 μ l Blood of mice was collected 10 min, 2 h, 6 h 24 h and 48 h after injection of lymphocytes in 5 ml RPMI. The samples were centrifuged at 550 x g for five minutes at 4 °C and the supernatant was discarded. To eliminate the red blood cells the pellet was resuspended in 6 ml 0.83 % NH_4Cl in PBS and incubated four minutes at RT under occasional shaking. 8 ml RPMI was added to stop the reaction. The cells were centrifuged at 550 x g for five minutes at 4 °C, the supernatant discarded and the pellet was resuspended in 200 μ l FACS fixation buffer. The samples were transferred into FACS tubes and analysed by flow cytometry with a BD FACS Canto II. The ratio between the percentages of CFSE^{low} and $\text{CFSE}^{\text{high}}$ cells ten minutes after transfer were used as 100% and all consecutive points of time were calculated as percentages of that ratio.

11.2.4 Statistical evaluations

11.2.4.1 Mechanistic experiments

Cell frequencies, number and ratios were analysed using the unpaired, two-tailed test (GraphPad Prism 5.02 software).

11.2.4.2 Incidence studies

T1D incidence curves (“survival curves”) were analysed using the Log-Rank (Mantel-Cox) test.

Literature

12 Literature

1. Berg JM, Tymoczko JL, Stryer L: *Biochemistry*. New York, W. H. Freeman, 2007
2. Brinkmann V, Reichard U, Goosmann C, Fauler B, Uhlemann Y, Weiss DS, ... Zychlinsky A: Neutrophil extracellular traps kill bacteria. *Science* **2004**;303:1532-1535
3. Rose NR, Mackay IR: *The autoimmune diseases*. Amsterdam ; London, Elsevier Academic Press, 2006
4. Ueda H, Howson JM, Esposito L, Heward J, Snook H, Chamberlain G, ... Gough SC: Association of the T-cell regulatory gene CTLA4 with susceptibility to autoimmune disease. *Nature* **2003**;423:506-511
5. Liu E, Eisenbarth GS: Type 1A diabetes mellitus-associated autoimmunity. *Endocrinol Metab Clin North Am* **2002**;31:391-410, vii-viii
6. Gardner DG, Shoback DM, Greenspan FS: *Greenspan's basic and clinical endocrinology*. New York, McGraw-Hill Medical ; London : McGraw-Hill [distributor], 2011
7. Pozzilli P, Di Mario U: Autoimmune diabetes not requiring insulin at diagnosis (latent autoimmune diabetes of the adult): definition, characterization, and potential prevention. *Diabetes Care* **2001**;24:1460-1467
8. Chiang JL, Kirkman MS, Laffel LM, Peters AL, Type 1 Diabetes Sourcebook A: Type 1 diabetes through the life span: a position statement of the American Diabetes Association. *Diabetes Care* **2014**;37:2034-2054
9. Bach JF: Insulin-dependent diabetes mellitus as an autoimmune disease. *Endocr Rev* **1994**;15:516-542
10. Greenbaum CJ, Schatz DA, Cuthbertson D, Zeidler A, Eisenbarth GS, Krischer JP: Islet cell antibody-positive relatives with human leukocyte antigen DQA1*0102, DQB1*0602: identification by the Diabetes Prevention Trial-type 1. *J Clin Endocrinol Metab* **2000**;85:1255-1260
11. Todd JA, Bell JI, McDevitt HO: HLA-DQ beta gene contributes to susceptibility and resistance to insulin-dependent diabetes mellitus. *Nature* **1987**;329:599-604
12. Todd JA: Etiology of type 1 diabetes. *Immunity* **2010**;32:457-467

Literature

13. Staines A, Hanif S, Ahmed S, McKinney PA, Shera S, Bodansky HJ: Incidence of insulin dependent diabetes mellitus in Karachi, Pakistan. *Arch Dis Child* **1997**;76:121-123
14. Unger WW, Laban S, Kleijwegt FS, van der Slik AR, Roep BO: Induction of Treg by monocyte-derived DC modulated by vitamin D3 or dexamethasone: differential role for PD-L1. *Eur J Immunol* **2009**;39:3147-3159
15. Fronczak CM, Baron AE, Chase HP, Ross C, Brady HL, Hoffman M, ... Norris JM: In utero dietary exposures and risk of islet autoimmunity in children. *Diabetes Care* **2003**;26:3237-3242
16. Bizzarri C, Pitocco D, Napoli N, Di Stasio E, Maggi D, Manfrini S, ... Group I: No protective effect of calcitriol on beta-cell function in recent-onset type 1 diabetes: the IMDIAB XIII trial. *Diabetes Care* **2010**;33:1962-1963
17. Laitinen OH, Honkanen H, Pakkanen O, Oikarinen S, Hankaniemi MM, Huhtala H, ... Hyoty H: Coxsackievirus B1 is associated with induction of beta-cell autoimmunity that portends type 1 diabetes. *Diabetes* **2014**;63:446-455
18. Oikarinen S, Tauriainen S, Hober D, Lucas B, Vazeou A, Sioofy-Khojine A, ... VirDiab Study G: Virus antibody survey in different European populations indicates risk association between coxsackievirus B1 and type 1 diabetes. *Diabetes* **2014**;63:655-662
19. Bason C, Lorini R, Lunardi C, Dolcino M, Giannattasio A, d'Annunzio G, ... Puccetti A: In type 1 diabetes a subset of anti-coxsackievirus B4 antibodies recognize autoantigens and induce apoptosis of pancreatic beta cells. *PLoS One* **2013**;8:e57729
20. von Herrath MG, Fujinami RS, Whitton JL: Microorganisms and autoimmunity: making the barren field fertile? *Nat Rev Microbiol* **2003**;1:151-157
21. Serreze DV, Fleming SA, Chapman HD, Richard SD, Leiter EH, Tisch RM: B lymphocytes are critical antigen-presenting cells for the initiation of T cell-mediated autoimmune diabetes in nonobese diabetic mice. *J Immunol* **1998**;161:3912-3918
22. Willcox A, Richardson SJ, Bone AJ, Foulis AK, Morgan NG: Analysis of islet inflammation in human type 1 diabetes. *Clin Exp Immunol* **2009**;155:173-181
23. Bradley BJ, Haskins K, La Rosa FG, Lafferty KJ: CD8 T cells are not required for islet destruction induced by a CD4+ islet-specific T-cell clone. *Diabetes* **1992**;41:1603-1608
24. Wong FS, Visintin I, Wen L, Flavell RA, Janeway CA, Jr.: CD8 T cell clones from young nonobese diabetic (NOD) islets can transfer rapid onset

- of diabetes in NOD mice in the absence of CD4 cells. *J Exp Med* **1996**;183:67-76
25. Rabinovitch A, Suarez-Pinzon WL, Sorensen O, Bleackley RC, Power RF: IFN-gamma gene expression in pancreatic islet-infiltrating mononuclear cells correlates with autoimmune diabetes in nonobese diabetic mice. *J Immunol* **1995**;154:4874-4882
 26. Seewaldt S, Thomas HE, Ejrnaes M, Christen U, Wolfe T, Rodrigo E, ... von Herrath MG: Virus-induced autoimmune diabetes: most beta-cells die through inflammatory cytokines and not perforin from autoreactive (anti-viral) cytotoxic T-lymphocytes. *Diabetes* **2000**;49:1801-1809
 27. Baeke F, Van Belle TL, Takiishi T, Ding L, Korf H, Laureys J, ... Mathieu C: Low doses of anti-CD3, ciclosporin A and the vitamin D analogue, TX527, synergise to delay recurrence of autoimmune diabetes in an islet-transplanted NOD mouse model of diabetes. *Diabetologia* **2012**;55:2723-2732
 28. Li L, Nishio J, van Maurik A, Mathis D, Benoist C: Differential response of regulatory and conventional CD4(+) lymphocytes to CD3 engagement: clues to a possible mechanism of anti-CD3 action? *J Immunol* **2013**;191:3694-3704
 29. Salomon B, Lenschow DJ, Rhee L, Ashourian N, Singh B, Sharpe A, Bluestone JA: B7/CD28 costimulation is essential for the homeostasis of the CD4+CD25+ immunoregulatory T cells that control autoimmune diabetes. *Immunity* **2000**;12:431-440
 30. Chen Z, Herman AE, Matos M, Mathis D, Benoist C: Where CD4+CD25+ T reg cells impinge on autoimmune diabetes. *J Exp Med* **2005**;202:1387-1397
 31. Makino S, Kunimoto K, Muraoka Y, Mizushima Y, Katagiri K, Tochino Y: Breeding of a non-obese, diabetic strain of mice. *Jikken Dobutsu* **1980**;29:1-13
 32. Grinberg-Bleyer Y, Baeyens A, You S, Elhage R, Fourcade G, Gregoire S, ... Piaggio E: IL-2 reverses established type 1 diabetes in NOD mice by a local effect on pancreatic regulatory T cells. *J Exp Med* **2010**;207:1871-1878
 33. Tang Q, Adams JY, Penaranda C, Melli K, Piaggio E, Sgouroudis E, ... Bluestone JA: Central role of defective interleukin-2 production in the triggering of islet autoimmune destruction. *Immunity* **2008**;28:687-697
 34. Ohashi PS, Oehen S, Buerki K, Pircher H, Ohashi CT, Odermatt B, ... Hengartner H: Ablation of "tolerance" and induction of diabetes by virus infection in viral antigen transgenic mice. *Cell* **1991**;65:305-317

Literature

35. von Herrath MG, Dockter J, Oldstone MB: How virus induces a rapid or slow onset insulin-dependent diabetes mellitus in a transgenic model. *Immunity* **1994**;1:231-242
36. Steele C, Hagopian WA, Gitelman S, Masharani U, Cavaghan M, Rother KI, ... Herold KC: Insulin secretion in type 1 diabetes. *Diabetes* **2004**;53:426-433
37. Lo B, Swafford AD, Shafer-Weaver KA, Jerome LF, Rakhlin L, Mathern DR, ... Lenardo MJ: Antibodies against insulin measured by electrochemiluminescence predicts insulinitis severity and disease onset in non-obese diabetic mice and can distinguish human type 1 diabetes status. *J Transl Med* **2011**;9:203
38. Chee J, Ko HJ, Skowera A, Jhala G, Catterall T, Graham KL, ... Krishnamurthy B: Effector-memory T cells develop in islets and report islet pathology in type 1 diabetes. *J Immunol* **2014**;192:572-580
39. Feutren G, Papoz L, Assan R, Vialettes B, Karsenty G, Vexiau P, ... et al.: Cyclosporin increases the rate and length of remissions in insulin-dependent diabetes of recent onset. Results of a multicentre double-blind trial. *Lancet* **1986**;2:119-124
40. Parving HH, Tarnow L, Nielsen FS, Rossing P, Mandrup-Poulsen T, Osterby R, Nerup J: Cyclosporine nephrotoxicity in type 1 diabetic patients. A 7-year follow-up study. *Diabetes Care* **1999**;22:478-483
41. Pescovitz MD, Greenbaum CJ, Krause-Steinrauf H, Becker DJ, Gitelman SE, Goland R, ... Type 1 Diabetes TrialNet Anti CDSG: Rituximab, B-lymphocyte depletion, and preservation of beta-cell function. *N Engl J Med* **2009**;361:2143-2152
42. Keymeulen B, Walter M, Mathieu C, Kaufman L, Gorus F, Hilbrands R, ... Pipeleers D: Four-year metabolic outcome of a randomised controlled CD3-antibody trial in recent-onset type 1 diabetic patients depends on their age and baseline residual beta cell mass. *Diabetologia* **2010**;53:614-623
43. Ludvigsson J, Krisky D, Casas R, Battelino T, Castano L, Greening J, ... Baron S: GAD65 antigen therapy in recently diagnosed type 1 diabetes mellitus. *N Engl J Med* **2012**;366:433-442
44. Skyler JS, Krischer JP, Wolfsdorf J, Cowie C, Palmer JP, Greenbaum C, ... Leschek E: Effects of oral insulin in relatives of patients with type 1 diabetes: The Diabetes Prevention Trial--Type 1. *Diabetes Care* **2005**;28:1068-1076
45. Nanto-Salonen K, Kupila A, Simell S, Siljander H, Salonsaari T, Hekkala A, ... Simell O: Nasal insulin to prevent type 1 diabetes in children with HLA genotypes and autoantibodies conferring increased risk of disease: a double-blind, randomised controlled trial. *Lancet* **2008**;372:1746-1755

Literature

46. You S, Candon S, Kuhn C, Bach J-F, Chatenoud L: Chapter 2 CD3 Antibodies as Unique Tools to Restore Self-Tolerance in Established Autoimmunity. **2008**;100:13-37
47. Chatenoud L, Thervet E, Primo J, Bach JF: Anti-CD3 antibody induces long-term remission of overt autoimmunity in nonobese diabetic mice. *Proc Natl Acad Sci U S A* **1994**;91:123-127
48. Chatenoud L, Primo J, Bach JF: CD3 antibody-induced dominant self tolerance in overtly diabetic NOD mice. *J Immunol* **1997**;158:2947-2954
49. von Herrath MG, Coon B, Wolfe T, Chatenoud L: Nonmitogenic CD3 antibody reverses virally induced (rat insulin promoter-lymphocytic choriomeningitis virus) autoimmune diabetes without impeding viral clearance. *J Immunol* **2002**;168:933-941
50. Norman DJ, Chatenoud L, Cohen D, Goldman M, Shield CF, 3rd: Consensus statement regarding OKT3-induced cytokine-release syndrome and human antimouse antibodies. *Transplant Proc* **1993**;25:89-92
51. Keymeulen B, Vandemeulebroucke E, Ziegler AG, Mathieu C, Kaufman L, Hale G, ... Chatenoud L: Insulin needs after CD3-antibody therapy in new-onset type 1 diabetes. *N Engl J Med* **2005**;352:2598-2608
52. Aronson R, Gottlieb PA, Christiansen JS, Donner TW, Bosi E, Bode BW, ... Group DI: Low-dose oteelixumab anti-CD3 monoclonal antibody DEFEND-1 study: results of the randomized phase III study in recent-onset human type 1 diabetes. *Diabetes Care* **2014**;37:2746-2754
53. Sherry N, Hagopian W, Ludvigsson J, Jain SM, Wahlen J, Ferry RJ, Jr., ... Protege Trial I: Teplizumab for treatment of type 1 diabetes (Protege study): 1-year results from a randomised, placebo-controlled trial. *Lancet* **2011**;378:487-497
54. Herold KC, Gitelman SE, Willi SM, Gottlieb PA, Waldron-Lynch F, Devine L, ... Bluestone JA: Teplizumab treatment may improve C-peptide responses in participants with type 1 diabetes after the new-onset period: a randomised controlled trial. *Diabetologia* **2013**;56:391-400
55. Herold KC, Hagopian W, Auger JA, Poumian-Ruiz E, Taylor L, Donaldson D, ... Bluestone JA: Anti-CD3 monoclonal antibody in new-onset type 1 diabetes mellitus. *N Engl J Med* **2002**;346:1692-1698
56. Herold KC, Gitelman SE, Masharani U, Hagopian W, Bisikirska B, Donaldson D, ... Bluestone JA: A single course of anti-CD3 monoclonal antibody hOKT3gamma1(Ala-Ala) results in improvement in C-peptide responses and clinical parameters for at least 2 years after onset of type 1 diabetes. *Diabetes* **2005**;54:1763-1769

Literature

57. Herold KC, Gitelman SE, Ehlers MR, Gottlieb PA, Greenbaum CJ, Hagopian W, ... Ab ATEST: Teplizumab (anti-CD3 mAb) treatment preserves C-peptide responses in patients with new-onset type 1 diabetes in a randomized controlled trial: metabolic and immunologic features at baseline identify a subgroup of responders. *Diabetes* **2013**;62:3766-3774
58. Valle A, Jofra T, Stabilini A, Atkinson M, Roncarolo MG, Battaglia M: Rapamycin prevents and breaks the anti-CD3-induced tolerance in NOD mice. *Diabetes* **2009**;58:875-881
59. Hu C, Ding H, Zhang X, Wong FS, Wen L: Combination treatment with anti-CD20 and oral anti-CD3 prevents and reverses autoimmune diabetes. *Diabetes* **2013**;62:2849-2858
60. Bresson D, Togher L, Rodrigo E, Chen Y, Bluestone JA, Herold KC, von Herrath M: Anti-CD3 and nasal proinsulin combination therapy enhances remission from recent-onset autoimmune diabetes by inducing Tregs. *J Clin Invest* **2006**;116:1371-1381
61. Takiishi T, Korf H, Van Belle TL, Robert S, Grieco FA, Caluwaerts S, ... Mathieu C: Reversal of autoimmune diabetes by restoration of antigen-specific tolerance using genetically modified *Lactococcus lactis* in mice. *J Clin Invest* **2012**;122:1717-1725
62. Bresson D, Fradkin M, Manenkova Y, Rottembourg D, von Herrath M: Genetic-induced variations in the GAD65 T-cell repertoire governs efficacy of anti-CD3/GAD65 combination therapy in new-onset type 1 diabetes. *Mol Ther* **2010**;18:307-316
63. Sherry NA, Chen W, Kushner JA, Glandt M, Tang Q, Tsai S, ... Herold KC: Exendin-4 improves reversal of diabetes in NOD mice treated with anti-CD3 monoclonal antibody by enhancing recovery of beta-cells. *Endocrinology* **2007**;148:5136-5144
64. Ding L, Gysemans CA, Stange G, Heremans Y, Yuchi Y, Takiishi T, ... Mathieu C: Combining MK626, a novel DPP-4 inhibitor, and low-dose monoclonal CD3 antibody for stable remission of new-onset diabetes in mice. *PLoS One* **2014**;9:e107935
65. Li X, Qi Y, Ma X, Huang F, Guo H, Jiang X, ... Wang S: Chemokine (C-C motif) ligand 20, a potential biomarker for Graves' disease, is regulated by osteopontin. *PLoS One* **2013**;8:e64277
66. Sellam J, Rouanet S, Hendel-Chavez H, Miceli-Richard C, Combe B, Sibilia J, ... Mariette X: CCL19, a B cell chemokine, is related to the decrease of blood memory B cells and predicts the clinical response to rituximab in patients with rheumatoid arthritis. *Arthritis Rheum* **2013**;65:2253-2261

67. Narumi S, Takeuchi T, Kobayashi Y, Konishi K: Serum levels of ifn-inducible PROTEIN-10 relating to the activity of systemic lupus erythematosus. *Cytokine* **2000**;12:1561-1565
68. Cheng W, Chen G: Chemokines and chemokine receptors in multiple sclerosis. *Mediators Inflamm* **2014**;2014:659206
69. Rot A, von Andrian UH: Chemokines in innate and adaptive host defense: basic chemokines grammar for immune cells. *Annu Rev Immunol* **2004**;22:891-928
70. Charo IF, Ransohoff RM: The many roles of chemokines and chemokine receptors in inflammation. *N Engl J Med* **2006**;354:610-621
71. Nomiya H, Osada N, Yoshie O: The evolution of mammalian chemokine genes. *Cytokine Growth Factor Rev* **2010**;21:253-262
72. Kelner GS, Kennedy J, Bacon KB, Kleyensteuber S, Largaespada DA, Jenkins NA, ... et al.: Lymphotactin: a cytokine that represents a new class of chemokine. *Science* **1994**;266:1395-1399
73. Nomiya H, Hieshima K, Osada N, Kato-Unoki Y, Otsuka-Ono K, Takegawa S, ... Yoshie O: Extensive expansion and diversification of the chemokine gene family in zebrafish: identification of a novel chemokine subfamily CX. *BMC Genomics* **2008**;9:222
74. Nomiya H, Osada N, Yoshie O: A family tree of vertebrate chemokine receptors for a unified nomenclature. *Dev Comp Immunol* **2011**;35:705-715
75. Horuk R: Chemokine receptors. *Cytokine Growth Factor Rev* **2001**;12:313-335
76. Zlotnik A, Yoshie O: Chemokines: a new classification system and their role in immunity. *Immunity* **2000**;12:121-127
77. Christen U, von Herrath MG: Manipulating the type 1 vs type 2 balance in type 1 diabetes. *Immunol Res* **2004**;30:309-325
78. Christen U, von Herrath MG: IP-10 and Type 1 Diabetes: A Question of Time and Location. *Autoimmunity* **2004**;37:273-282
79. Christen U, Wolfe T, Mohrle U, Hughes AC, Rodrigo E, Green EA, ... von Herrath MG: A dual role for TNF-alpha in type 1 diabetes: islet-specific expression abrogates the ongoing autoimmune process when induced late but not early during pathogenesis. *J Immunol* **2001**;166:7023-7032
80. Lohmann T, Laue S, Nietzsche U, Kapellen TM, Lehmann I, Schroeder S, ... Kiess W: Reduced expression of Th1-associated chemokine receptors on peripheral blood lymphocytes at diagnosis of type 1 diabetes. *Diabetes* **2002**;51:2474-2480

Literature

81. Shimada A, Morimoto J, Kodama K, Suzuki R, Oikawa Y, Funae O, ... Narumi S: Elevated serum IP-10 levels observed in type 1 diabetes. *Diabetes Care* **2001**;24:510-515
82. Antonelli A, Fallahi P, Ferrari SM, Pupilli C, d'Annunzio G, Lorini R, ... Ferrannini E: Serum Th1 (CXCL10) and Th2 (CCL2) chemokine levels in children with newly diagnosed Type 1 diabetes: a longitudinal study. *Diabet Med* **2008**;25:1349-1353
83. Gabbay MA, Sato MN, Duarte AJ, Dib SA: Serum titres of anti-glutamic acid decarboxylase-65 and anti-IA-2 autoantibodies are associated with different immunoregulatory milieu in newly diagnosed type 1 diabetes patients. *Clin Exp Immunol* **2012**;168:60-67
84. Clark-Lewis I, Mattioli I, Gong JH, Loetscher P: Structure-function relationship between the human chemokine receptor CXCR3 and its ligands. *J Biol Chem* **2003**;278:289-295
85. Luster AD, Unkeless JC, Ravetch JV: Gamma-interferon transcriptionally regulates an early-response gene containing homology to platelet proteins. *Nature* **1985**;315:672-676
86. Luster AD, Ravetch JV: Biochemical characterization of a gamma interferon-inducible cytokine (IP-10). *J Exp Med* **1987**;166:1084-1097
87. Kolb SA, Sporer B, Lahrtz F, Koedel U, Pfister HW, Fontana A: Identification of a T cell chemotactic factor in the cerebrospinal fluid of HIV-1-infected individuals as interferon-gamma inducible protein 10. *J Neuroimmunol* **1999**;93:172-181
88. Charles PC, Chen X, Horwitz MS, Brosnan CF: Differential chemokine induction by the mouse adenovirus type-1 in the central nervous system of susceptible and resistant strains of mice. *J Neurovirol* **1999**;5:55-64
89. Asensio VC, Campbell IL: Chemokine gene expression in the brains of mice with lymphocytic choriomeningitis. *J Virol* **1997**;71:7832-7840
90. Loetscher P, Pellegrino A, Gong JH, Mattioli I, Loetscher M, Bardi G, ... Clark-Lewis I: The ligands of CXC chemokine receptor 3, I-TAC, Mig, and IP10, are natural antagonists for CCR3. *J Biol Chem* **2001**;276:2986-2991
91. Kakimi K, Lane TE, Wieland S, Asensio VC, Campbell IL, Chisari FV, Guidotti LG: Blocking chemokine responsive to gamma-2/interferon (IFN)-gamma inducible protein and monokine induced by IFN-gamma activity in vivo reduces the pathogenetic but not the antiviral potential of hepatitis B virus-specific cytotoxic T lymphocytes. *J Exp Med* **2001**;194:1755-1766
92. Zhai Y, Shen XD, Gao F, Zhao A, Freitas MC, Lassman C, ... Kupiec-Weglinski JW: CXCL10 regulates liver innate immune response against ischemia and reperfusion injury. *Hepatology* **2008**;47:207-214

93. Frigerio S, Junt T, Lu B, Gerard C, Zumsteg U, Hollander GA, Piali L: Beta cells are responsible for CXCR3-mediated T-cell infiltration in insulinitis. *Nat Med* **2002**;8:1414-1420
94. Narumi S, Kaburaki T, Yoneyama H, Iwamura H, Kobayashi Y, Matsushima K: Neutralization of IFN-inducible protein 10/CXCL10 exacerbates experimental autoimmune encephalomyelitis. *Eur J Immunol* **2002**;32:1784-1791
95. Christen U, McGavern DB, Luster AD, von Herrath MG, Oldstone MB: Among CXCR3 chemokines, IFN-gamma-inducible protein of 10 kDa (CXC chemokine ligand (CXCL) 10) but not monokine induced by IFN-gamma (CXCL9) imprints a pattern for the subsequent development of autoimmune disease. *J Immunol* **2003**;171:6838-6845
96. Bonecchi R, Bianchi G, Bordignon PP, D'Ambrosio D, Lang R, Borsatti A, ... Sinigaglia F: Differential expression of chemokine receptors and chemotactic responsiveness of type 1 T helper cells (Th1s) and Th2s. *J Exp Med* **1998**;187:129-134
97. Loetscher M, Loetscher P, Brass N, Meese E, Moser B: Lymphocyte-specific chemokine receptor CXCR3: regulation, chemokine binding and gene localization. *Eur J Immunol* **1998**;28:3696-3705
98. Sallusto F, Lenig D, Mackay CR, Lanzavecchia A: Flexible programs of chemokine receptor expression on human polarized T helper 1 and 2 lymphocytes. *J Exp Med* **1998**;187:875-883
99. Loetscher M, Gerber B, Loetscher P, Jones SA, Piali L, Clark-Lewis I, ... Moser B: Chemokine receptor specific for IP10 and mig: structure, function, and expression in activated T-lymphocytes. *J Exp Med* **1996**;184:963-969
100. Lacotte S, Brun S, Muller S, Dumortier H: CXCR3, inflammation, and autoimmune diseases. *Ann N Y Acad Sci* **2009**;1173:310-317
101. Ehlert JE, Addison CA, Burdick MD, Kunkel SL, Strieter RM: Identification and partial characterization of a variant of human CXCR3 generated by posttranscriptional exon skipping. *J Immunol* **2004**;173:6234-6240
102. Lasagni L, Francalanci M, Annunziato F, Lazzeri E, Giannini S, Cosmi L, ... Romagnani P: An alternatively spliced variant of CXCR3 mediates the inhibition of endothelial cell growth induced by IP-10, Mig, and I-TAC, and acts as functional receptor for platelet factor 4. *J Exp Med* **2003**;197:1537-1549
103. Booth V, Keizer DW, Kamphuis MB, Clark-Lewis I, Sykes BD: The CXCR3 binding chemokine IP-10/CXCL10: structure and receptor interactions. *Biochemistry* **2002**;41:10418-10425

104. Strieter RM, Kunkel SL, Arenberg DA, Burdick MD, Polverini PJ: Interferon gamma-inducible protein 10 (IP-10), a member of the C-X-C chemokine family, is an inhibitor of angiogenesis. *Biochem Biophys Res Commun* **1995**;210:51-57
105. Angiolillo AL, Sgadari C, Taub DD, Liao F, Farber JM, Maheshwari S, ... Tosato G: Human interferon-inducible protein 10 is a potent inhibitor of angiogenesis in vivo. *J Exp Med* **1995**;182:155-162
106. Shigihara T, Oikawa Y, Kanazawa Y, Okubo Y, Narumi S, Saruta T, Shimada A: Significance of serum CXCL10/IP-10 level in type 1 diabetes. *J Autoimmun* **2006**;26:66-71
107. Cardozo AK, Proost P, Gysemans C, Chen MC, Mathieu C, Eizirik DL: IL-1beta and IFN-gamma induce the expression of diverse chemokines and IL-15 in human and rat pancreatic islet cells, and in islets from pre-diabetic NOD mice. *Diabetologia* **2003**;46:255-266
108. Christen U, Benke D, Wolfe T, Rodrigo E, Rhode A, Hughes AC, ... von Herrath MG: Cure of prediabetic mice by viral infections involves lymphocyte recruitment along an IP-10 gradient. *Journal of Clinical Investigation* **2004**;113:74-84
109. Rhode A, Pauza ME, Barral AM, Rodrigo E, Oldstone MBA, von Herrath MG, Christen U: Islet-Specific Expression of CXCL10 Causes Spontaneous Islet Infiltration and Accelerates Diabetes Development. *The Journal of Immunology* **2005**;175:3516-3524
110. Vestweber D: Adhesion and signaling molecules controlling the transmigration of leukocytes through endothelium. *Immunol Rev* **2007**;218:178-196
111. Ley K, Laudanna C, Cybulsky MI, Nourshargh S: Getting to the site of inflammation: the leukocyte adhesion cascade updated. *Nat Rev Immunol* **2007**;7:678-689
112. Garrido-Urbani S, Bradfield PF, Lee BP, Imhof BA: Vascular and epithelial junctions: a barrier for leucocyte migration. *Biochem Soc Trans* **2008**;36:203-211
113. Yang XD, Karin N, Tisch R, Steinman L, McDevitt HO: Inhibition of insulinitis and prevention of diabetes in nonobese diabetic mice by blocking L-selectin and very late antigen 4 adhesion receptors. *Proc Natl Acad Sci U S A* **1993**;90:10494-10498
114. Yang XD, Michie SA, Tisch R, Karin N, Steinman L, McDevitt HO: A predominant role of integrin alpha 4 in the spontaneous development of autoimmune diabetes in nonobese diabetic mice. *Proc Natl Acad Sci U S A* **1994**;91:12604-12608

115. Baron JL, Reich EP, Visintin I, Janeway CA, Jr.: The pathogenesis of adoptive murine autoimmune diabetes requires an interaction between alpha 4-integrins and vascular cell adhesion molecule-1. *J Clin Invest* **1994**;93:1700-1708
116. Petri B, Bixel MG: Molecular events during leukocyte diapedesis. *FEBS J* **2006**;273:4399-4407
117. Garrido-Urbani S, Bradfield PF, Imhof BA: Tight junction dynamics: the role of junctional adhesion molecules (JAMs). *Cell Tissue Res* **2014**;355:701-715
118. Mandell KJ, Parkos CA: The JAM family of proteins. *Adv Drug Deliv Rev* **2005**;57:857-867
119. Bradfield PF, Nourshargh S, Aurrand-Lions M, Imhof BA: JAM family and related proteins in leukocyte migration (Vestweber series). *Arterioscler Thromb Vasc Biol* **2007**;27:2104-2112
120. Ebnet K, Aurrand-Lions M, Kuhn A, Kiefer F, Butz S, Zander K, ... Vestweber D: The junctional adhesion molecule (JAM) family members JAM-2 and JAM-3 associate with the cell polarity protein PAR-3: a possible role for JAMs in endothelial cell polarity. *J Cell Sci* **2003**;116:3879-3891
121. Ostermann G, Weber KS, Zerneck A, Schroder A, Weber C: JAM-1 is a ligand of the beta(2) integrin LFA-1 involved in transendothelial migration of leukocytes. *Nat Immunol* **2002**;3:151-158
122. Aurrand-Lions M, Johnson-Leger C, Wong C, Du Pasquier L, Imhof BA: Heterogeneity of endothelial junctions is reflected by differential expression and specific subcellular localization of the three JAM family members. *Blood* **2001**;98:3699-3707
123. Cunningham SA, Rodriguez JM, Arrate MP, Tran TM, Brock TA: JAM2 interacts with alpha4beta1. Facilitation by JAM3. *J Biol Chem* **2002**;277:27589-27592
124. Arrate MP, Rodriguez JM, Tran TM, Brock TA, Cunningham SA: Cloning of human junctional adhesion molecule 3 (JAM3) and its identification as the JAM2 counter-receptor. *J Biol Chem* **2001**;276:45826-45832
125. Johnson-Leger CA, Aurrand-Lions M, Beltraminelli N, Fasel N, Imhof BA: Junctional adhesion molecule-2 (JAM-2) promotes lymphocyte transendothelial migration. *Blood* **2002**;100:2479-2486
126. Santoso S, Sachs UJH, Kroll H, Linder M, Ruf A, Preissner KT, Chavakis T: The Junctional Adhesion Molecule 3 (JAM-3) on Human Platelets is a Counterreceptor for the Leukocyte Integrin Mac-1. *Journal of Experimental Medicine* **2002**;196:679-691

127. Lamagna C, Meda P, Mandicourt G, Brown J, Gilbert RJ, Jones EY, ... Aurrand-Lions M: Dual interaction of JAM-C with JAM-B and alpha(M)beta2 integrin: function in junctional complexes and leukocyte adhesion. *Mol Biol Cell* **2005**;16:4992-5003
128. Aurrand-Lions M, Duncan L, Ballestrem C, Imhof BA: JAM-2, a novel immunoglobulin superfamily molecule, expressed by endothelial and lymphatic cells. *J Biol Chem* **2001**;276:2733-2741
129. Vonlaufen A, Aurrand-Lions M, Pastor CM, Lamagna C, Hadengue A, Imhof BA, Frossard JL: The role of junctional adhesion molecule C (JAM-C) in acute pancreatitis. *J Pathol* **2006**;209:540-548
130. Christen S, Coppieters K, Rose K, Holdener M, Bayer M, Pfeilschifter JM, ... Christen U: Blockade but not overexpression of the junctional adhesion molecule C influences virus-induced type 1 diabetes in mice. *PLoS One* **2013**;8:e54675
131. Bradfield PF, Scheiermann C, Nourshargh S, Ody C, Luscinskas FW, Rainger GE, ... Imhof BA: JAM-C regulates unidirectional monocyte transendothelial migration in inflammation. *Blood* **2007**;110:2545-2555
132. Rabquer BJ, Amin MA, Teegala N, Shaheen MK, Tsou PS, Ruth JH, ... Koch AE: Junctional adhesion molecule-C is a soluble mediator of angiogenesis. *J Immunol* **2010**;185:1777-1785
133. Lamagna C, Hodiola-Dilke KM, Imhof BA, Aurrand-Lions M: Antibody against junctional adhesion molecule-C inhibits angiogenesis and tumor growth. *Cancer Res* **2005**;65:5703-5710
134. Valle A, Barbagiovanni G, Jofra T, Stabilini A, Perol L, Baeyens A, ... Battaglia M: Heterogeneous CD3 expression levels in differing T cell subsets correlate with the in vivo anti-CD3-mediated T cell modulation. *J Immunol* **2015**;194:2117-2127
135. Ritzel RA, Butler AE, Rizza RA, Veldhuis JD, Butler PC: Relationship between beta-cell mass and fasting blood glucose concentration in humans. *Diabetes Care* **2006**;29:717-718
136. Thorel F, Nepote V, Avril I, Kohno K, Desgraz R, Chera S, Herrera PL: Conversion of adult pancreatic alpha-cells to beta-cells after extreme beta-cell loss. *Nature* **2010**;464:1149-1154
137. von Herrath MG, Homann D, Gairin JE, Oldstone MB: Pathogenesis and treatment of virus-induced autoimmune diabetes: novel insights gained from the RIP-LCMV transgenic mouse model. *Biochem Soc Trans* **1997**;25:630-635
138. Slifka MK, Rodriguez F, Whitton JL: Rapid on/off cycling of cytokine production by virus-specific CD8+ T cells. *Nature* **1999**;401:76-79

Literature

139. Slifka MK, Whitton JL: Activated and memory CD8+ T cells can be distinguished by their cytokine profiles and phenotypic markers. *J Immunol* **2000**;164:208-216
140. Dufour JH, Dziejman M, Liu MT, Leung JH, Lane TE, Luster AD: IFN-gamma-inducible protein 10 (IP-10; CXCL10)-deficient mice reveal a role for IP-10 in effector T cell generation and trafficking. *J Immunol* **2002**;168:3195-3204
141. Kamanaka M, Rainbow D, Schuster-Gossler K, Eynon EE, Chervonsky AV, Wicker LS, Flavell RA: Amino acid polymorphisms altering the glycosylation of IL-2 do not protect from type 1 diabetes in the NOD mouse. *Proc Natl Acad Sci U S A* **2009**;106:11236-11240
142. Yamanouchi J, Rainbow D, Serra P, Howlett S, Hunter K, Garner VE, ... Santamaria P: Interleukin-2 gene variation impairs regulatory T cell function and causes autoimmunity. *Nat Genet* **2007**;39:329-337
143. Lundholm M, Motta V, Lofgren-Burström A, Duarte N, Bergman ML, Mayans S, Holmberg D: Defective induction of CTLA-4 in the NOD mouse is controlled by the NOD allele of Idd3/IL-2 and a novel locus (Ctex) telomeric on chromosome 1. *Diabetes* **2006**;55:538-544
144. von Andrian UH, Mackay CR: T-cell function and migration. Two sides of the same coin. *N Engl J Med* **2000**;343:1020-1034
145. Müller WA: Leukocyte–endothelial-cell interactions in leukocyte transmigration and the inflammatory response. *Trends in Immunology* **2003**;24:326-333
146. Ludwig RJ, Schultz JE, Boehncke WH, Podda M, Tandi C, Krombach F, ... Zollner TM: Activated, not resting, platelets increase leukocyte rolling in murine skin utilizing a distinct set of adhesion molecules. *J Invest Dermatol* **2004**;122:830-836
147. Tsai S, Shameli A, Santamaria P: CD8+ T cells in type 1 diabetes. *Adv Immunol* **2008**;100:79-124
148. Jorns A, Akin M, Arndt T, Terbish T, Zu Vilsendorf AM, Wedekind D, ... Lenzen S: Anti-TCR therapy combined with fingolimod for reversal of diabetic hyperglycemia by beta cell regeneration in the LEW.1AR1-iddm rat model of type 1 diabetes. *J Mol Med (Berl)* **2014**;92:743-755
149. Aurrand-Lions MA, Duncan L, Du Pasquier L, Imhof BA: Cloning of JAM-2 and JAM-3: an emerging junctional adhesion molecular family? *Curr Top Microbiol Immunol* **2000**;251:91-98
150. Hirsch R, Bluestone JA, DeNenno L, Gress RE: Anti-CD3 F(ab')₂ fragments are immunosuppressive in vivo without evoking either the strong humoral response or morbidity associated with whole mAb. *Transplantation* **1990**;49:1117-1123

151. In't Veld P: Insulinitis in human type 1 diabetes: a comparison between patients and animal models. *Semin Immunopathol* **2014**;36:569-579
152. Ziegler AG, Nepom GT: Prediction and pathogenesis in type 1 diabetes. *Immunity* **2010**;32:468-478
153. Gepts W: Pathologic anatomy of the pancreas in juvenile diabetes mellitus. *Diabetes* **1965**;14:619-633
154. Faber OK, Binder C: B-cell function and blood glucose control in insulin dependent diabetics within the first month of insulin treatment. *Diabetologia* **1977**;13:263-268
155. Chatenoud L, Bluestone JA: CD3-specific antibodies: a portal to the treatment of autoimmunity. *Nat Rev Immunol* **2007**;7:622-632
156. Nishio J, Feuerer M, Wong J, Mathis D, Benoist C: Anti-CD3 therapy permits regulatory T cells to surmount T cell receptor-specified peripheral niche constraints. *J Exp Med* **2010**;207:1879-1889
157. Penaranda C, Tang Q, Bluestone JA: Anti-CD3 therapy promotes tolerance by selectively depleting pathogenic cells while preserving regulatory T cells. *J Immunol* **2011**;187:2015-2022
158. Chen G, Han G, Wang J, Wang R, Xu R, Shen B, ... Li Y: Essential roles of TGF-beta in anti-CD3 antibody therapy: reversal of diabetes in nonobese diabetic mice independent of Foxp3+CD4+ regulatory T cells. *J Leukoc Biol* **2008**;83:280-287
159. Carpenter PA, Pavlovic S, Tso JY, Press OW, Gooley T, Yu XZ, Anasetti C: Non-Fc Receptor-Binding Humanized Anti-CD3 Antibodies Induce Apoptosis of Activated Human T Cells. *The Journal of Immunology* **2000**;165:6205-6213
160. Wesselborg S, Janssen O, Kabelitz D: Induction of activation-driven death (apoptosis) in activated but not resting peripheral blood T cells. *J Immunol* **1993**;150:4338-4345
161. Goto R, You S, Zaitzu M, Chatenoud L, Wood KJ: Delayed anti-CD3 therapy results in depletion of alloreactive T cells and the dominance of Foxp3+ CD4+ graft infiltrating cells. *Am J Transplant* **2013**;13:1655-1664
162. Liu H, Rhodes M, Wiest DL, Vignali DA: On the dynamics of TCR:CD3 complex cell surface expression and downmodulation. *Immunity* **2000**;13:665-675
163. Velthuis JH, Unger WW, Abreu JR, Duinkerken G, Franken K, Peakman M, ... Roep BO: Simultaneous detection of circulating autoreactive CD8+ T-cells specific for different islet cell-associated epitopes using combinatorial MHC multimers. *Diabetes* **2010**;59:1721-1730

164. Coppieters KT, Dotta F, Amirian N, Campbell PD, Kay TW, Atkinson MA, ... von Herrath MG: Demonstration of islet-autoreactive CD8 T cells in insulinitic lesions from recent onset and long-term type 1 diabetes patients. *J Exp Med* **2012**;209:51-60
165. Sarikonda G, Pettus J, Phatak S, Sachithanatham S, Miller JF, Wesley JD, ... von Herrath M: CD8 T-cell reactivity to islet antigens is unique to type 1 while CD4 T-cell reactivity exists in both type 1 and type 2 diabetes. *J Autoimmun* **2014**;50:77-82
166. Notley CA, McCann FE, Inglis JJ, Williams RO: ANTI-CD3 therapy expands the numbers of CD4+ and CD8+ Treg cells and induces sustained amelioration of collagen-induced arthritis. *Arthritis Rheum* **2010**;62:171-178
167. Ellis SD, McGovern JL, van Maurik A, Howe D, Ehrenstein MR, Notley CA: Induced CD8+FoxP3+ Treg cells in rheumatoid arthritis are modulated by p38 phosphorylation and monocytes expressing membrane tumor necrosis factor alpha and CD86. *Arthritis Rheumatol* **2014**;66:2694-2705
168. Bisikirska B, Colgan J, Luban J, Bluestone JA, Herold KC: TCR stimulation with modified anti-CD3 mAb expands CD8+ T cell population and induces CD8+CD25+ Tregs. *J Clin Invest* **2005**;115:2904-2913
169. Liu Y, Lan Q, Lu L, Chen M, Xia Z, Ma J, ... Zheng SG: Phenotypic and functional characteristic of a newly identified CD8+ Foxp3- CD103+ regulatory T cells. *J Mol Cell Biol* **2014**;6:81-92
170. Duhon T, Duhon R, Lanzavecchia A, Sallusto F, Campbell DJ: Functionally distinct subsets of human FOXP3+ Treg cells that phenotypically mirror effector Th cells. *Blood* **2012**;119:4430-4440
171. Rhode A, Pauza ME, Barral AM, Rodrigo E, Oldstone MB, von Herrath MG, Christen U: Islet-specific expression of CXCL10 causes spontaneous islet infiltration and accelerates diabetes development. *J Immunol* **2005**;175:3516-3524
172. Alanentalo T, Hornblad A, Mayans S, Karin Nilsson A, Sharpe J, Larefalk A, ... Holmberg D: Quantification and three-dimensional imaging of the insulinitis-induced destruction of beta-cells in murine type 1 diabetes. *Diabetes* **2010**;59:1756-1764
173. Kommajosyula S, Reddy S, Nitschke K, Kanwar JR, Karanam M, Krissansen GW: Leukocytes infiltrating the pancreatic islets of nonobese diabetic mice are transformed into inactive exiles by combinational anti-cell adhesion therapy. *J Leukoc Biol* **2001**;70:510-517
174. Christen S, Holdener M, Beerli C, Thoma G, Bayer M, Pfeilschifter JM, ... Christen U: Small molecule CXCR3 antagonist NIBR2130 has only a limited impact on type 1 diabetes in a virus-induced mouse model. *Clin Exp Immunol* **2011**;165:318-328

Literature

175. Coppieters KT, Amirian N, Pagni PP, Baca Jones C, Wiberg A, Lasch S, ... von Herrath MG: Functional redundancy of CXCR3/CXCL10 signaling in the recruitment of diabetogenic cytotoxic T lymphocytes to pancreatic islets in a virally induced autoimmune diabetes model. *Diabetes* **2013**;62:2492-2499
176. Mohan K, Issekutz TB: Blockade of Chemokine Receptor CXCR3 Inhibits T Cell Recruitment to Inflamed Joints and Decreases the Severity of Adjuvant Arthritis. *The Journal of Immunology* **2007**;179:8463-8469
177. Kohler RE, Comerford I, Townley S, Haylock-Jacobs S, Clark-Lewis I, McColl SR: Antagonism of the chemokine receptors CXCR3 and CXCR4 reduces the pathology of experimental autoimmune encephalomyelitis. *Brain Pathol* **2008**;18:504-516
178. Steinmetz OM, Turner JE, Paust HJ, Lindner M, Peters A, Heiss K, ... Panzer U: CXCR3 mediates renal Th1 and Th17 immune response in murine lupus nephritis. *J Immunol* **2009**;183:4693-4704
179. Morimoto J, Yoneyama H, Shimada A, Shigihara T, Yamada S, Oikawa Y, ... Narumi S: CXC chemokine ligand 10 neutralization suppresses the occurrence of diabetes in nonobese diabetic mice through enhanced beta cell proliferation without affecting insulinitis. *J Immunol* **2004**;173:7017-7024
180. Roep BO, Kleijwegt FS, van Halteren AG, Bonato V, Boggi U, Vendrame F, ... Dotta F: Islet inflammation and CXCL10 in recent-onset type 1 diabetes. *Clin Exp Immunol* **2010**;159:338-343
181. Milicic T, Jotic A, Markovic I, Lalic K, Jeremic V, Lukic L, ... Lalic NM: High Risk First Degree Relatives of Type 1 Diabetics: An Association with Increases in CXCR3(+) T Memory Cells Reflecting an Enhanced Activity of Th1 Autoimmune Response. *Int J Endocrinol* **2014**;2014:589360
182. Biddison WE, Cruikshank WW, Center DM, Pelfrey CM, Taub DD, Turner RV: CD8+ myelin peptide-specific T cells can chemoattract CD4+ myelin peptide-specific T cells: importance of IFN-inducible protein 10. *J Immunol* **1998**;160:444-448
183. Ejrnaes M, Videbaek N, Christen U, Cooke A, Michelsen BK, von Herrath M: Different Diabetogenic Potential of Autoaggressive CD8+ Clones Associated with IFN- γ -Inducible Protein 10 (CXC Chemokine Ligand 10) Production but Not Cytokine Expression, Cytolytic Activity, or Homing Characteristics. *The Journal of Immunology* **2005**;174:2746-2755
184. Peperzak V, Veraar EA, Xiao Y, Babala N, Thiadens K, Brugmans M, Borst J: CD8+ T cells produce the chemokine CXCL10 in response to CD27/CD70 costimulation to promote generation of the CD8+ effector T cell pool. *J Immunol* **2013**;191:3025-3036

185. Mayer L, Sandborn WJ, Stepanov Y, Geboes K, Hardi R, Yellin M, ... Luo AY: Anti-IP-10 antibody (BMS-936557) for ulcerative colitis: a phase II randomised study. *Gut* **2014**;63:442-450
186. Chavakis T, Keiper T, Matz-Westphal R, Hersemeyer K, Sachs UJ, Nawroth PP, ... Santoso S: The junctional adhesion molecule-C promotes neutrophil transendothelial migration in vitro and in vivo. *J Biol Chem* **2004**;279:55602-55608
187. Rabquer BJ, Pakozdi A, Michel JE, Gujar BS, Haines GK, 3rd, Imhof BA, Koch AE: Junctional adhesion molecule C mediates leukocyte adhesion to rheumatoid arthritis synovium. *Arthritis Rheum* **2008**;58:3020-3029
188. Morris AP, Tawil A, Berkova Z, Wible L, Smith CW, Cunningham SA: Junctional Adhesion Molecules (JAMs) are differentially expressed in fibroblasts and co-localize with ZO-1 to adherens-like junctions. *Cell Commun Adhes* **2006**;13:233-247
189. Zimmerli C, Lee BP, Palmer G, Gabay C, Adams R, Aurrand-Lions M, Imhof BA: Adaptive immune response in JAM-C-deficient mice: normal initiation but reduced IgG memory. *J Immunol* **2009**;182:4728-4736
190. Cursiefen C, Schlotzer-Schrehardt U, Kuchle M, Sorokin L, Breiteneder-Geleff S, Alitalo K, Jackson D: Lymphatic vessels in vascularized human corneas: immunohistochemical investigation using LYVE-1 and podoplanin. *Invest Ophthalmol Vis Sci* **2002**;43:2127-2135
191. Ribatti D, Nico B, Cimpean AM, Raica M: Podoplanin and LYVE-1 expression in lymphatic vessels of human neuroblastoma. *J Neurooncol* **2010**;100:151-152
192. Hartwig W, Werner J, Warshaw AL, Antoniu B, Castillo CF, Gebhard MM, ... Buchler MW: Membrane-bound ICAM-1 is upregulated by trypsin and contributes to leukocyte migration in acute pancreatitis. *Am J Physiol Gastrointest Liver Physiol* **2004**;287:G1194-1199
193. Weber C, Springer TA: Interaction of very late antigen-4 with VCAM-1 supports transendothelial chemotaxis of monocytes by facilitating lateral migration. *J Immunol* **1998**;161:6825-6834
194. Chakraborty S, Hu SY, Wu SH, Karmenyan A, Chiou A: The interaction affinity between vascular cell adhesion molecule-1 (VCAM-1) and very late antigen-4 (VLA-4) analyzed by quantitative FRET. *PLoS One* **2015**;10:e0121399
195. Ludwig RJ, Zollner TM, Santoso S, Hardt K, Gille J, Baatz H, ... Podda M: Junctional adhesion molecules (JAM)-B and -C contribute to leukocyte extravasation to the skin and mediate cutaneous inflammation. *J Invest Dermatol* **2005**;125:969-976

Literature

196. Aurrand-Lions M, Lamagna C, Dangerfield JP, Wang S, Herrera P, Nourshargh S, Imhof BA: Junctional Adhesion Molecule-C Regulates the Early Influx of Leukocytes into Tissues during Inflammation. *The Journal of Immunology* **2005**;174:6406-6415
197. Scheiermann C, Colom B, Meda P, Patel NS, Voisin MB, Marrelli A, ... Nourshargh S: Junctional adhesion molecule-C mediates leukocyte infiltration in response to ischemia reperfusion injury. *Arterioscler Thromb Vasc Biol* **2009**;29:1509-1515
198. Woodfin A, Voisin MB, Beyrau M, Colom B, Caille D, Diapouli FM, ... Nourshargh S: The junctional adhesion molecule JAM-C regulates polarized transendothelial migration of neutrophils in vivo. *Nat Immunol* **2011**;12:761-769
199. Sircar M, Bradfield PF, Aurrand-Lions M, Fish RJ, Alcaide P, Yang L, ... Lusciuskas FW: Neutrophil Transmigration under Shear Flow Conditions In Vitro Is Junctional Adhesion Molecule-C Independent. *The Journal of Immunology* **2007**;178:5879-5887
200. Zen K, Babbin BA, Liu Y, Whelan JB, Nusrat A, Parkos CA: JAM-C is a component of desmosomes and a ligand for CD11b/CD18-mediated neutrophil transepithelial migration. *Mol Biol Cell* **2004**;15:3926-3937
201. Frontera V, Arcangeli ML, Zimmerli C, Bardin F, Obrados E, Audebert S, ... Aurrand-Lions M: Cutting edge: JAM-C controls homeostatic chemokine secretion in lymph node fibroblastic reticular cells expressing thrombomodulin. *J Immunol* **2011**;187:603-607
202. Leinster DA, Colom B, Whiteford JR, Ennis DP, Lockley M, McNeish IA, ... Nourshargh S: Endothelial cell junctional adhesion molecule C plays a key role in the development of tumors in a murine model of ovarian cancer. *FASEB J* **2013**;27:4244-4253
203. Kodelja V, Muller C, Tenorio S, Schebesch C, Orfanos CE, Goerdts S: Differences in angiogenic potential of classically vs alternatively activated macrophages. *Immunobiology* **1997**;197:478-493
204. Belghith M, Bluestone JA, Barriot S, Megret J, Bach JF, Chatenoud L: TGF-beta-dependent mechanisms mediate restoration of self-tolerance induced by antibodies to CD3 in overt autoimmune diabetes. *Nat Med* **2003**;9:1202-1208
205. Mamchak AA, Manenkova Y, Leconet W, Zheng Y, Chan JR, Stokes CL, ... Bresson D: Preexisting autoantibodies predict efficacy of oral insulin to cure autoimmune diabetes in combination with anti-CD3. *Diabetes* **2012**;61:1490-1499
206. Ludvigsson J: Combination therapy for preservation of beta cell function in Type 1 diabetes: new attitudes and strategies are needed! *Immunol Lett* **2014**;159:30-35

Literature

207. van Etten E, Dardenne O, Gysemans C, Overbergh L, Mathieu C: 1,25-Dihydroxyvitamin D3 alters the profile of bone marrow-derived dendritic cells of NOD mice. *Ann N Y Acad Sci* **2004**;1037:186-192
208. van Etten E, Decallonne B, Bouillon R, Mathieu C: NOD bone marrow-derived dendritic cells are modulated by analogs of 1,25-dihydroxyvitamin D3. *J Steroid Biochem Mol Biol* **2004**;89-90:457-459
209. van Halteren AG, Tysma OM, van Etten E, Mathieu C, Roep BO: 1alpha,25-dihydroxyvitamin D3 or analogue treated dendritic cells modulate human autoreactive T cells via the selective induction of apoptosis. *J Autoimmun* **2004**;23:233-239
210. Pedersen AE, Schmidt EG, Gad M, Poulsen SS, Claesson MH: Dexamethasone/1alpha-25-dihydroxyvitamin D3-treated dendritic cells suppress colitis in the SCID T-cell transfer model. *Immunology* **2009**;127:354-364
211. Suarez-Pinzon WL, Power RF, Yan Y, Wasserfall C, Atkinson M, Rabinovitch A: Combination therapy with glucagon-like peptide-1 and gastrin restores normoglycemia in diabetic NOD mice. *Diabetes* **2008**;57:3281-3288
212. Xu G, Stoffers DA, Habener JF, Bonner-Weir S: Exendin-4 stimulates both beta-cell replication and neogenesis, resulting in increased beta-cell mass and improved glucose tolerance in diabetic rats. *Diabetes* **1999**;48:2270-2276
213. Sturis J, Gotfredsen CF, Romer J, Rolin B, Ribel U, Brand CL, ... Knudsen LB: GLP-1 derivative liraglutide in rats with beta-cell deficiencies: influence of metabolic state on beta-cell mass dynamics. *Br J Pharmacol* **2003**;140:123-132
214. Garber AJ: Long-acting glucagon-like peptide 1 receptor agonists: a review of their efficacy and tolerability. *Diabetes Care* **2011**;34 Suppl 2:S279-284
215. Garber AJ: Incretin effects on beta-cell function, replication, and mass: the human perspective. *Diabetes Care* **2011**;34 Suppl 2:S258-263
216. Zinger A, Leibowitz G: Islet transplantation in type 1 diabetes: hype, hope and reality - a clinician's perspective. *Diabetes Metab Res Rev* **2014**;30:83-87
217. Oldstone MB, Nerenberg M, Southern P, Price J, Lewicki H: Virus infection triggers insulin-dependent diabetes mellitus in a transgenic model: role of anti-self (virus) immune response. *Cell* **1991**;65:319-331

13.3 Publications and Presentations

Publications

Lasch S, Mueller P, Bayer M, Pfeilschifter JM, Luster AD, Hintermann E, Christen U (2015) Anti-CD3 / anti-CXCL10 antibody combination therapy causes a persistent remission of type 1 diabetes in two mouse models. *Diabetes*. pii: db150479. [Epub ahead of print]

Lasch S, Mueller P, Bayer M, Pfeilschifter JM, Imhof B, Hintermann E, Christen U (2015) Addition of anti-JAM-C slightly improves the anti-CD3 monotherapy in T1D by reducing the neutrophil migration into the pancreas . In preparation

Coppieters KT, Amirian N, Pagni PP, Jones CB, Wiberg A, **Lasch S**, Hintermann E, Christen U, von Herrath MG (2013) Functional redundancy of CXCR3/CXCL10 signaling in the recruitment of diabetogenic CTL to pancreatic islets in a virally induced autoimmune diabetes model. *Diabetes*. 62: 2492-2499.

Presentations at conferences

Lasch S, Mueller P, Bayer M, Hintermann E, Christen U (2015) Anti-CD3 / anti-CXCL10 antibody combination therapy reverts Type 1 Diabetes in two mouse models. Poster presentation. Immunology of Diabetes Society, Munich, Germany.


Lasch S, Mueller P, Bayer M, Hintermann E, Christen U (2015) Anti-CD3 / anti-CXCL10 antibody combination therapy reverts Type 1 Diabetes by blockade of *de novo* infiltration of recovered islet-specific T cells. Poster presentation. World Immune Regulation Meeting, Davos, Switzerland

Lasch S, Mueller P, Bayer M, Hintermann E, Christen U (2014) Anti-CD3 / anti-CXCL10 antibody combination therapy reverts Type 1 Diabetes in two mouse models. Oral presentation. European Association for the Study of Diabetes, Vienna, Austria.

13.4 Declaration of academic honesty

Hereby I declare that I wrote the present thesis without any assistance from third parties and without sources than those indicated in the thesis itself.

Darmstadt, den 03.02.2016


..... (Subscription)